

UNIVERSITY OF NOVA GORICA
GRADUATE SCHOOL

**USE OF ARTIFICIAL NEURAL NETWORKS IN
THROUGH PROCESS MODELING OF ALUMINUM
FOILS**

MASTER'S THESIS

Štefan Trčko

Mentor: Prof. Dr. Božidar Šarler

Nova Gorica, 2012

Acknowledgements

My collaboration with professor Božidar Šarler began in 2007. Before that, I was employed at the Alcad company, where I worked as a system engineer for web technology. In relation to this study, I was employed at the Impol company as a researcher of artificial neural networks in through process modeling of aluminum foils. I thank professor Božidar Šarler for his support, guidance and stimulation to finish this thesis.

I would like to thank the employees at the Impol company, particularly Aleksandra Robič who helped me select important process parameters and in gathering the required data of aluminum foil production for developing artificial neural network for mechanical properties prediction.

I would also like to thank my former superior manager, Branko Hmelak, for supporting my work.

Further, I thank my parents for helping guide me through my life and work.

This work was performed in the framework of the project "Young Researcher from Industry", contract number 3211-06-000516. The author would like to acknowledge the financial support from the Slovenian Ministry of Higher Education, Science and Technology.

Use of artificial neural networks in through process modeling of aluminum foils

Abstract

Prediction of the final mechanical properties of household aluminum foil, based on the physics based numerical modeling of the whole process (Through Process Modeling - TPM), is extremely complicated due to the multi-scale and multi-phase character of the underlying physics, as well as complicated material behavior. An alternative approach to the physics based TPM, the artificial intelligence approach, based on the Artificial Neural Networks (ANNs), is proposed and described in the present master thesis.

The ANN NeuralTools program is used to build the application. For training the ANNs we use process parameters data for household aluminum foil (EN AW-8011) which is used for storage and handling foods.

The data for ANN training process were collected in Impol company. The complete process path of "cast strip - foil" production is composed of the following subsequent steps: charging preparation, melting and alloying (adjustment of chemical composition), modification, metal cleaning with Ar and Cl, hydrogen removal, casting on thin strip casting machine, coil manufacturing of thickness 6.0 mm, cold rolling, edge trimming, intermediate annealing, rolling to thickness 0.30 mm, foil rolling 1, trimming between phases, foil rolling 2, doubling, end thickness rolling, separating and final annealing. The data was collected automatically from computer data bases as well as manually in the production. 109 sets of complete history data of household foil production could be provided. The input parameters used for training ANNs are wt% of: 1 - Si, 2 - Fe, 3 - Cu, 4 - Mn, 5 - B, 6 - Zn, 7 - Pb, 8 - Bi, 9 - Mg, 10 - In, 11 - Ti, 12 - Hg, 13 - Ni, 14 - Sn, 15 - Ca, 16 - V, 17 - Cr, 18 - Sb, 19 - Ga, 20 - sum of Hg-Cd-Pb, 21 - sum of Ti-Zr, 22 - sum of Mn-Zr, 23 - sum of Mn-Cr-Ti-V, 24 - recycled aluminum, and other process parameters: 25 - width of the coil, 26 - outside diameter of the coil, 27 - annealing temperature. As the output parameters we choose the tensile strength and the elongation of the foil. These mechanical properties of the foil are measured in the laboratory. The characteristics of the trained network are quantified as the percentage of the

known answers it correctly predicts and norms between the predicted and the measured values.

For building ANNs we used multilayer feedforward with Back Propagation (BP) learning ANN architecture. This type of network is sometimes called Multilayer Perceptron (MP) because of the similarity to perceptron networks with more than one layer. This network consists of the input layer, one or more hidden layers, and the output layer. The historical cases are used to automatically adjust the weights and thresholds in order to minimize the error of the ANN.

Four ANN data sets have been used in the developed ANN TPM model. In all four networks, the configuration with one hidden layer, 6 nodes, 27 independent input variables, and 60 minutes of training time was chosen. The first and the second configuration was for predicting the tensile strength (R_m), while the third and the fourth for predicting the elongation (A). In the first case, the training data set consisted of 80 historical data rows and the testing data set consisted of 29 data rows, which were not included in the training process. The result of the testing process was 89.65 % good predictions and 10.35 % bad predictions. After elimination of several rows of training data, for which we heuristically estimated that they might not perform well in training, we ended with a second data set of only 39 rows of historical data. For training ANN we used 30 rows and for testing the remaining 9 rows. This second configuration gave us a trained ANN with 100 % good predictions and 0 % of bad predictions. We proceeded in the similar way in the third and the fourth configuration which were used for predicting elongation (A). In the third case, the training data set consisted of 80 rows of historical data and the testing data set consisted of 29 data rows, which was not included in training process. The result of the testing process was 44.83 % of good predictions and 55.17 % of bad predictions. In the same sense as in the study of the tensile strength (R_m), we eliminated some suspicious rows of training data. The fourth training data set thus consisted of only 26 rows of historical data. For training ANN we used 20 rows, and for testing the remaining 6 rows. This fourth configuration gave us a trained ANN with result of 100 % of good predictions and 0 % of bad predictions.

The ANNs training results show that proper selection of the data for training the ANN is very important. We can have the same configurations but if we do not have good historical data, the result of the trained ANN will not converge reasonably. Given the limited range of the values of input parameters on the basis of which the neural networks have been trained, the quality of the output parameters prediction is rather limited. Larger sets of historical data would lead

to a decreased error in the training of neural networks and hence a better prediction of the mechanical properties.

The results show that the increase of tensile strength is influenced most by the chemical element Cr and least by the chemical element Mn, and that the decrease of tensile strength is influenced most by the chemical element Si and least by the chemical element Ti. With regards to elongation, the results show that the increase of elongation is influenced most by the chemical element Fe and least by the chemical element Si, and that the decrease of elongation is influenced most by the chemical element Ti and least by the chemical element Mn.

With the proposed methodology and demonstration of a trained ANN TPM, the Impol company has a basis for further development of predictive models for estimation of the final product properties as a function of the process parameters of a wide variety of production paths. Respectively, much more good quality data needs to be collected in a much more systematic way in the future. This allows optimizing the production paths with respect to productivity and product quality in the perspective.

Key words

aluminum foil, alloy, foil production process path, artificial neural network, multilayer feedforward, neurons, NeuralTools

Uporaba umetnih nevronske mreže pri modeliranju skozi proces proizvodnje aluminjske folije

Povzetek

Napovedovanje mehanskih lastnosti aluminjske gospodinjske folije na podlagi fizikalno osnovanega numeričnega modeliranja celotnega procesa (modeliranje skozi proces - MSP) je izjemno zapleteno predvsem zaradi večnivojskih in večfaznih fizikalnih zasnov, kot tudi zapletenega obnašanja materiala. V tem magistrskem delu je opisano modeliranje na podlagi umetne inteligence z uporabo umetnih nevronske mreže (UNM) kot alternativni pristop k fizikalno osnovanemu MSP.

Pri izgradnji UNM aplikacije je uporabljen program NeuralTools. Za učenje UNM so uporabljeni podatki procesnih parametrov proizvodnje gospodinjskih folije (EN AW-8011), ki se uporablja za shranjevanje in ravnanje s hrano.

Podatki za učenje nevronske mreže so bili zbrani v podjetju Impol. Celotno procesno pot "liti trak - folija" sestavlja zaporedje naslednjih korakov: priprava vložka, taljenje in legiranje (prilagoditev kemijske sestave), modificiranje, čiščenje taline z Ar in Cl, odstranjevanje vodika, litje na kontinuiranem livnem stroju, izdelava kolobarja debeline 6,0 mm, hladno valjanje, stranski obrez, medfazno žarjenje, valjenje na debelino 0,3 mm, valjanje v folijo 1, obrez med fazami, valjanje v folijo 2, zdvajanje, valjanje na končno debelino, razdvajanje in končno žarjenje. Podatki so bili pridobljeni avtomatsko iz računalniških baz, kot tudi ročno med proizvodnjo. Uporabljenih je bilo možno 109 množic zgodovinskih podatkov proizvodnje gospodinjske folije. Vhodni parametri nevronske mreže so utežni deleži v %: 1 - Si, 2 - Fe, 3 - Cu, 4 - Mn, 5 - B, 6 - Zn, 7 - Pb, 8 - Bi, 9 - Mg, 10 - In, 11 - Ti, 12 - Hg, 13 - Ni, 14 - Sn, 15 - Ca, 16 - V, 17 - Cr, 18 - Sb, 19 - Ga, 20 - vsota Hg-Cd-Pb, 21 - vsota Ti-Zr, 22 - vsota Mn-Zr, 23 - vsota Mn-Cr-Ti-V, 24 - povratni aluminij in drugi procesni parametri: 25 - širina kolobarja, 26 - zunanji premer kolobarja, 27 - temperatura žarjenja. Kot izhodna parametra smo izbrali natezno trdnost in raztezek folije. Ti mehanske lastnosti folije sta merjeni v laboratoriju. Karakteristike naučene nevronske mreže se merijo kot odstotek pravilno napovedanih odgovorov in norm med napovedanimi in merjenimi vrednostmi.

Za izgradnjo UNM smo kot arhitekturo uporabili usmerjeno večnivojsko UNM s povratnim načinom učenja. Ta tip nevronske mreže se imenuje tudi večnivojski perceptron zaradi podobnosti s perceptronskimi mrežami z več kot enim

nivojem. Mreža se sestoji iz vhodnega nivoja, enega ali več skritih nivojev in izhodnega nivoja. Za zmanjšanje napak UNM so uporabljeni zgodovinski primeri, ki samodejno prilagajajo uteži in pragovne vrednosti v smislu minimizacije napake UNM.

V razvitem UNM MSP modelu smo uporabili štiri množice podatkov za UNM. V vseh štirih UNM konfiguracijah smo izbrali en skriti nivo, 6 vozlišč, 27 neodvisnih vhodnih spremenljivk in 60 minut učenja. Prva in druga konfiguracija je bila za napovedovanje natezne trdnosti (Rm), medtem ko sta bili tretja in četrta za napovedovanje raztezka (A). V prvi konfiguraciji je množica za učenje vsebovala 80 vrstic zgodovinskih podatkov in množica za testiranje 29 vrstic podatkov, ki niso bili uporabljeni v procesu učenja. Rezultat procesa testiranja je bil 89,25 % pravilnih napovedi in 10,35 % napačnih napovedi. Ko smo odstranili nekatere vrstice podatkov, za katere smo menili, da niso dobre za učenje, je ostalo 39 vrstic zgodovinskih podatkov. Za učenje smo uporabili 30 vrstic in za testiranje 9 vrstic. Naučena UNM s to konfiguracijo nam je dala 100 % pravilnih napovedi in 0 % napačnih napovedi. Po enakem postopku smo nadaljevali v tretji in četrti konfiguraciji, uporabljeni za napovedovanje raztezka (A). V tretji konfiguraciji je množica za učenje vsebovala 80 vrstic zgodovinskih podatkov in množica za testiranje 29 vrstic podatkov, ki niso bili uporabljeni v procesu učenja. Rezultat procesa testiranja je bil 44,83 % pravilnih napovedi in 55,17 % napačnih napovedi. Kot pri študiju natezne trdnosti (Rm), smo odstranili nekatere vrstice podatkov za učenje, ki so bile sumljive. Četrta množica za učenje je tako vsebovala samo 26 vrstic zgodovinskih podatkov. Za učenje smo uporabili 20 vrstic in za testiranje ostalih 6 vrstic. Naučena UNM s četrto konfiguracijo nam je dala 100 % pravilnih napovedi in 0 % napačnih napovedi.

Rezultati so pokazali, da je pravilna izbira podatkov za učenje UNM zelo pomembna. Uporabimo lahko iste konfiguracije za učenje nevronske mreže, a če nimamo dobrih zgodovinskih podatkov, naučena nevronska mreža ne bo dala dobrih rezultatov. Zaradi ozkega območja vrednosti vhodnih parametrov, na podlagi katerih so bile nevronske mreže učene, je tudi točnost napovedi izhodnih parametrov dokaj omejena. Večja množica zgodovinskih podatkov bi pomenila tudi zmanjšanje napak pri učenju nevronske mreže in s tem tudi boljšo napoved mehanskih lastnosti.

Rezultati kažejo, da na povečanje natezne trdnosti najbolj vpliva kemijski element Cr in najmanj kemijski element Mn, ter da na zmanjšanje natezne trdnosti najbolj vpliva kemijski element Si in najmanj kemijski element Ti. Za raztezek rezultati kažejo, da na povečanje najbolj vpliva kemijski element Fe in

najmanj kemijski element Si in da na zmanjšanje raztezka najbolj vpliva kemijski element Ti in najmanj kemijski element Mn.

S predstavljeno metodologijo in demonstracijo MSP z naučenimi UNM ima podjetje Impol osnovo za nadaljnji razvoj modelov napovedovanja za ocenjevanje končnih mehanskih lastnosti kot funkcijo procesnih parametrov najrazličnejših procesnih poti. Zato je v prihodnosti na sistematičen način potrebno zbrati večjo količino kvalitetnih podatkov. S tem bo v perspektivi omogočena optimizacija procesnih poti glede na produktivnost in kakovost izdelkov.

Ključne besede

aluminijska folija, zlitina, procesna pot proizvodnje folije, umetne nevronske mreže, večnivojska usmerjena nevronska mreža, nevroni, NeuralTools

Contents

List of figures	iii
List of tables	vii
List of symbols	ix
1 Introduction	1
2 Description of neural networks	7
3 Foil production process path	15
4 Preparing input data for training ANNs	27
4.1 Measurements of the tensile strength and elongation.....	27
4.2 Process parameters data.....	32
4.3 Training data quality and preprocessing.....	32
5 Results	35
5.1 Presentation and validation of the results	36
5.2 Discussion of the results	66
6 Conclusions	73
Bibliography	77
Appendix A	81
A.1 Input data for training ANN with 109 historical data (charge data) for 27 independent input variables and dependent output variable Tensile strength (R_m)	81
A.2 The new training set after heuristic elimination of rows that are not good for training ANN with 39 historical data (charge data) for 27	

independent input variables and dependent output variable Tensile strength (R_m).....	93
A.3 Input data for training ANN with 109 historical data (charge data) for 27 independent input variables and dependent output variable Elongation (A)	98
A.4 The new training set after heuristic elimination of rows that are not good for training ANN with 26 historical data (charge data) for 27 independent input variables and dependent output variable Elongation (A)	110

List of figures

2.1:	A MLF ANN with two hidden layers	8
2.2:	Polynomial curve fitting	10
2.3:	A GRN ANN for two independent numerical variables.....	12
2.4:	A PN ANN for two independent numerical variables, two dependent categories and five training cases	13
3.1:	Foil production process at the Impol company (process steps 1 – 6).....	17
3.2:	Foil production process at the Impol company (process steps 7 – 8).....	18
3.3:	Foil production process at the Impol company (process steps 9 – 10).....	19
3.4:	Foil production process at the Impol company (process steps 11 – 15)....	20
3.5:	Foil production process at the Impol company (process steps 16 – 20)....	21
3.6:	Descaling in % in foil rolling process FOIL STOCK - FOIL (ALLOY AF61) at the Impol company.....	22
4.1:	Sample before tensile strength and elongation testing (Photo author, courtesy Impol).....	29
4.2:	Testing machine for testing thin aluminum strips and foils. For measuring R_m and A (Photo author, courtesy Impol).....	30
4.3:	Testing machine with aluminum strip at the beginning of testing (Photo author, courtesy Impol).....	30
4.4:	Testing machine with aluminum strip at the end of testing (Photo author, courtesy Impol).....	31
4.5:	Sample after tensile strength and elongation testing (Photo author, courtesy Impol).....	31
5.1:	Predicted vs. real values of tensile strength for the testing data set of 29 rows	37
5.2:	Predicted vs. real values of tensile strength for testing data set of 9 rows	37
5.3:	Predicted vs. real values of elongation for the testing data set of 29 rows	38
5.4:	Predicted vs. real values of elongation for the testing data set of 6 rows..	39
5.5:	Influence of wt% Si on tensile strength and linear trend lines for tensile strength of 109 and 39 charges.....	39

5.6: Influence of wt% Fe on tensile strength and linear trend lines for tensile strength of 109 and 39 charges.....	40
5.7: Influence of wt% Mg on tensile strength and linear trend lines for tensile strength of 109 and 39 charges.....	40
5.8: Influence of annealing temperature T on tensile strength and linear trend lines for tensile strength of 109 and 39 charges	41
5.9: Influence of wt% Cu on tensile strength and linear trend lines for tensile strength of 109 and 39 charges.....	41
5.10: Influence of wt% Mn on tensile strength and linear trend lines for tensile strength of 109 and 39 charges.....	42
5.11: Influence of wt% B on tensile strength and linear trend lines for tensile strength of 109 and 39 charges	42
5.12: Influence of wt% Zn on tensile strength and linear trend lines for tensile strength of 109 and 39 charges.....	43
5.13: Influence of wt% Pb on tensile strength and linear trend lines for tensile strength of 109 and 39 charges.....	43
5.14: Influence of wt% Bi on tensile strength and linear trend lines for tensile strength of 109 and 39 charges.....	44
5.15: Influence of wt% In on tensile strength and linear trend lines for tensile strength of 109 and 39 charges.....	44
5.16: Influence of wt% Ti on tensile strength and linear trend lines for tensile strength of 109 and 39 charges.....	45
5.17: Influence of wt% Hg on tensile strength and linear trend lines for tensile strength of 109 and 39 charges.....	45
5.18: Influence of wt% Ni on tensile strength and linear trend lines for tensile strength of 109 and 39 charges.....	46
5.19: Influence of wt% Sn on tensile strength and linear trend lines for tensile strength of 109 and 39 charges.....	46
5.20: Influence of wt% Ca on tensile strength and linear trend lines for tensile strength of 109 and 39 charges.....	47
5.21: Influence of wt% V on tensile strength and linear trend lines for tensile strength of 109 and 39 charges	47
5.22: Influence of wt% Cr on tensile strength and linear trend lines for tensile strength of 109 and 39 charges.....	48
5.23: Influence of wt% Sb on tensile strength and linear trend lines for tensile strength of 109 and 39 charges.....	48
5.24: Influence of wt% Ga on tensile strength and linear trend lines for tensile strength of 109 and 39 charges.....	49
5.25: Influence of wt% sum of Hg-Cd-Pb on tensile strength and linear trend lines for tensile strength of 109 and 39 charges.....	49

5.26: Influence of wt% sum of Ti-Zr on tensile strength and linear trend lines for tensile strength of 109 and 39 charges	50
5.27: Influence of wt% sum of Mn-Zr on tensile strength and linear trend lines for tensile strength of 109 and 39 charges	50
5.28: Influence of wt% sum of Mn-Cr-Ti-V on tensile strength and linear trend lines for tensile strength of 109 and 39 charges	51
5.29: Influence of wt% Al on tensile strength and linear trend lines for tensile strength of 109 and 39 charges.....	51
5.30: Influence of width of the coil on tensile strength and linear trend lines for tensile strength of 109 and 39 charges.....	52
5.31: Influence of outside diameter of the coil on tensile strength and linear trend lines for tensile strength of 109 and 39 charges	52
5.32: Influence of wt% Si on elongation and linear trend lines for elongation of 109 and 26 charges	53
5.33: Influence of wt% Fe on elongation and linear trend lines for elongation of 109 and 26 charges.....	53
5.34: Influence of wt% Mg on elongation and linear trend lines for elongation of 109 and 26 charges	54
5.35: Influence of annealing temperature T on elongation and linear trend lines for elongation of 109 and 26 charges.....	54
5.36: Influence of wt% Cu on elongation and linear trend lines for elongation of 109 and 26 charges	55
5.37: Influence of wt% Mn on elongation and linear trend lines for elongation of 109 and 26 charges	55
5.38: Influence of wt% B on elongation and linear trend lines for elongation of 109 and 26 charges	56
5.39: Influence of wt% Zn on elongation and linear trend lines for elongation of 109 and 26 charges	56
5.40: Influence of wt% Pb on elongation and linear trend lines for elongation of 109 and 26 charges	57
5.41: Influence of wt% Bi on elongation and linear trend lines for elongation of 109 and 26 charges	57
5.42: Influence of wt% In on elongation and linear trend lines for elongation of 109 and 26 charges	58
5.43: Influence of wt% Ti on elongation and linear trend lines for elongation of 109 and 26 charges	58
5.44: Influence of wt% Hg on elongation and linear trend lines for elongation of 109 and 26 charges	59
5.45: Influence of wt% Ni on elongation and linear trend lines for elongation of 109 and 26 charges	59

5.46: Influence of wt% Sn on elongation and linear trend lines for elongation of 109 and 26 charges	60
5.47: Influence of wt% Ca on elongation and linear trend lines for elongation of 109 and 26 charges	60
5.48: Influence of wt% V on elongation and linear trend lines for elongation of 109 and 26 charges	61
5.49: Influence of wt% Cr on elongation and linear trend lines for elongation of 109 and 26 charges	61
5.50: Influence of wt% Sb on elongation and linear trend lines for elongation of 109 and 26 charges	62
5.51: Influence of wt% Ga on elongation and linear trend lines for elongation of 109 and 26 charges	62
5.52: Influence of wt% sum of Hg-Cd-Pb on elongation and linear trend lines for elongation of 109 and 26 charges	63
5.53: Influence of wt% sum of Ti-Zr on elongation and linear trend lines for elongation of 109 and 26 charges	63
5.54: Influence of wt% sum of Mn-Zr on elongation and linear trend lines for elongation of 109 and 26 charges.....	64
5.55: Influence of wt% sum of Mn-Cr-Ti-V on elongation and linear trend lines for elongation of 109 and 26 charges	64
5.56: Influence of wt% Al on elongation and linear trend lines for elongation of 109 and 26 charges	65
5.57: Influence of width of the coil on elongation and linear trend lines for elongation of 109 and 26 charges	65
5.58: Influence of outside diameter of the coil on elongation and linear trend lines for elongation of 109 and 26 charges	66

List of tables

3.1:	Table of all process parameters for alloy AF61 with minimum, maximum and average values with regard to classification	23
4.1:	Calculated average value of R_m and A of two records of historical data with the same input variable values.....	33
5.1:	Trend coefficients, which show influence of individual process parameters on tensile strength. Mn has minimum influence and Cr has maximum influence on increase of the tensile strength. Ti has minimum influence and Si has maximum influence on decrease of the tensile strength.	69
5.2:	Trend coefficients, which show influence of individual process parameters on elongation. Si has minimum influence and Fe has maximum influence on increase of the elongation. Mn has minimum influence and Ti has maximum influence on decrease of the elongation.	70
A.1:	Input data for training ANN with 109 historical data (charge data) for 27 independent input variables and dependent output variable Tensile strength (R_m) – part 1	81
A.2:	Input data for training ANN with 109 historical data (charge data) for 27 independent input variables and dependent output variable Tensile strength (R_m) – part 2	84
A.3:	Input data for training ANN with 109 historical data (charge data) for 27 independent input variables and dependent output variable Tensile strength (R_m) – part 3	87
A.4:	Input data for training ANN with 109 historical data (charge data) for 27 independent input variables and dependent output variable Tensile strength (R_m) – part 4	90
A.5:	The new training set after heuristic elimination of rows that are not good for training ANN with 39 historical data (charge data) for 27 independent input variables and dependent output variable Tensile strength (R_m) – part 1	93

A.6: The new training set after heuristic elimination of rows that are not good for training ANN with 39 historical data (charge data) for 27 independent input variables and dependent output variable Tensile strength (Rm) – part 2	94
A.7: The new training set after heuristic elimination of rows that are not good for training ANN with 39 historical data (charge data) for 27 independent input variables and dependent output variable Tensile strength (Rm) – part 3	96
A.8: The new training set after heuristic elimination of rows that are not good for training ANN with 39 historical data (charge data) for 27 independent input variables and dependent output variable Tensile strength (Rm) – part 4	97
A.9: Input data for training ANN with 109 historical data (charge data) for 27 independent input variables and dependent output variable Elongation (A) – part 1.....	98
A.10: Input data for training ANN with 109 historical data (charge data) for 27 independent input variables and dependent output variable Elongation (A) – part 2.....	101
A.11: Input data for training ANN with 109 historical data (charge data) for 27 independent input variables and dependent output variable Elongation (A) – part 3.....	104
A.12: Input data for training ANN with 109 historical data (charge data) for 27 independent input variables and dependent output variable Elongation (A) – part 4.....	107
A.13: The new training set after heuristic elimination of rows that are not good for training ANN with 26 historical data (charge data) for 27 independent input variables and dependent output variable elongation (A) – part 1	110
A.14: The new training set after heuristic elimination of rows that are not good for training ANN with 26 historical data (charge data) for 27 independent input variables and dependent output variable elongation (A) – part 2	111
A.15: The new training set after heuristic elimination of rows that are not good for training ANN with 26 historical data (charge data) for 27 independent input variables and dependent output variable elongation (A) – part 3	112
A.16: The new training set after heuristic elimination of rows that are not good for training ANN with 26 historical data (charge data) for 27 independent input variables and dependent output variable elongation (A) – part 4	113

List of symbols

Latin symbols

Rm	tensile strength
A	elongation
Fm	maximum force
K	trend coefficient
Lu	length after fracture
Lo	original gauge length
$L1$	$L1$ norm
$L2$	$L2$ norm
x_k^{ANN}	k-th element in the data set calculated by program NeuralTools
x_k^{MSR}	k-th measured element in the data set
N	number of elements in the data set
Lo	original gauge length
Lu	final gauge length after fracture
Le	extensometer gauge length

Subscripts

i, j, k	counters
-----------	----------

Acronyms

ANN	Artificial Neural Network
MLF	Multilayer Feedforward
MP	Multilayer Perceptron
GRN	Generalized Regression Network
BP	Back Propagation
PN	Probabilistic Network

CGD	Conjugate Gradient Descent
TPM	Through Process Modeling
MSP	Modeliranje Skozi Proces
min	minimum value
max	maximum value
avg	average value

1 Introduction

The present work probably for the first time shows an artificial intelligence model for the estimation of the final product properties as a function of the process parameters in aluminum industry. The model is capable of predicting the tensile strength and elongation of household foil (EN AW-8011) as a function of the process parameters. Household foil is used for storage and food handling, and is mass-produced by the Impol company [Impol, 2004]. The presented approach demonstrates an alternative to much more complicated and computationally intensive physical modeling of the situation. With the trained Artificial Neural Networks (ANNs), the Impol company can predict final mechanical properties, such as the tensile strength and elongation, based on values of chemical composition and other variables well before producing new household aluminum foil, qualities and thicknesses as well as optimizing the production of the current products. Of course, much more ANNs experience needs to be gained in the future for a reliable achievement of this goal. The presented novel methodology will allow straightforward optimization of the process path with respect to productivity and quality of other aluminum semi-products as well.

Prediction of the final mechanical properties of household aluminum foil, based on the physics based numerical modeling of the whole process (Through Process Modeling - TPM) [Quested, Crumbach, Hamerton, 2006; Crumbach, Quested, Hamerton, 2006] is extremely complicated due to the multi-scale and multi-phase character of the underlying physics as well as complicated material behavior. As an alternative approach to physical modeling, the artificial intelligence approach, based on the ANNs, is used. ANNs are computational tools, inspired by the structure and/or functional aspects of biological neural networks. They are networks of highly interconnected neural computing elements that have the ability to respond to input stimuli and to learn to adapt to the environment. ANN models offer the most promising unified approach to building truly intelligent computer systems [Bishop, 1995; Carling, 1992; Fausett, 1994; Patterson, 1996; Reed, Marks, 1998; Kriesel, 2011]. ANNs can be

effective as computational processors for various tasks, including pattern recognition (speech, visual image recognition), classification, data compression, modeling and forecasting, combinatorial problem solving, adaptive control, multisensory data fusion and noise filtering. One feature of the ANN architecture is the Multilayer Feedforward (MLF) with Back Propagation (BP) learning. This type of network is sometimes called Multilayer Perceptron (MP) because of the similarity to perceptron networks with more than one layer. This network consists of the input layer, one or more hidden layers, and the output layer. The historical cases are used to automatically adjust the weights and thresholds in order to minimize the error of the ANN [Patterson, 1995, Kocijan, 2007, Pfeifer, Damian, Fuchslin, 2010].

The process path for production of household aluminum foil in Impol company is composed of the following basic process steps: charging preparation, charging, melting and alloying, modification, metal cleaning, hydrogen removal, removal of inclusions, casting on strip casting machine, coiling with thickness of 6 mm, cold rolling, homogenization annealing, edge trimming, intermediate annealing, rolling to thickness of 0.3 mm, foil rolling, trimming between rolling passes and/or doubling, separating, end thickness rolling, final annealing, and foil packing.

27 process parameters have been identified as principal input variables for predicting the final tensile strength and elongation of the foil. They have been chosen based on discussions with the engineers at the Impol company. These parameters are chemical composition and other process parameters. The principal final measured physical properties of the foil are the tensile strength (Rm) measured in MPa and the elongation (A) measured in %. Rm is the stress at which the material breaks or permanently deforms expressed in MPa and A is the permanent elongation of the gauge length after fracture ($Lu - Lo$) expressed as a percentage of the original gauge length (Lo). Lu is length of the gauge after fracture.

In this work, we introduce an alternative approach to physical modeling, the artificial intelligence approach based on the neural networks (ANNs). The goal is to train the ANN in such a way, to be able to predict the mechanical properties of household aluminum foil.

Artificial neural networks have already been used in industry and below are some selected examples, related to the present work:

- In [Schlang, Feldkeller, Lang, Poppe, Runkler, 1999], a rolling mill process control system calculates the setup for the mill's actuators based on models of the technological process. Neural networks are applied as components of hybrid neuro/analytical process models. The application includes the calculation of the rolling force and strip temperature (hot and cold rolling), prediction of width-spread in the finishing mill, control of strip width shape, and control of the coiling temperature in a cooling train (hot rolling). The authors outline how significant benefits are achieved in the rolling mill technology by using the ANNs.
- In [Chun, Biglou, Lenard, Kim, 1999], the ability of an ANN model, using a BP learning algorithm, to predict the flow stress, roll force and roll torque obtained during the hot compression and rolling of aluminum alloys, is studied. The authors show that well-trained ANN models provide fast, accurate and consistent results, making them superior to other predictive techniques.
- In [Song, Zhang, Tseng, Zhang, 2000], the effects of deformation and solid solution time on the aging dynamics in 7175 high strength aluminum alloy have been investigated by using ANNs and a GA. The results of the study can be used to search the optimum technology adapted to this type of aluminum alloy.
- In [Song, Zhang, 2000], a systematic experimental investigation of the effect of heat-treatment technique on the mechanical properties of 7175 aluminum alloy was carried out. Particularly, an ANN and a GA were used to search for the optimum technique, adapted for 7175 aluminum alloy. The results indicated strongly that an ANN, combined with a GA, indeed offer a new effective means for the optimization of heat-treatment.
- Development of an accurate ANN material model for aluminum alloys would facilitate better process control and parameter optimization in the aircraft industry. The research in [Sen, Twomey, Ahmad, 2006] primarily attempts to design a constitutive model for aluminum 7075 alloy using MP. The BP algorithm is used to train the designed network whose performance is then validated using experimental data from a test set.
- In [Sampaio, Braga, Fujii, 2006], authors demonstrate the use of ANN in complex industrial problems by applying it to the steel temperature prediction of the ladle furnace processes. They show that the ANN used

yielded high generalization capability by obtaining a smaller mean error on the test data than the expected error specified by the steel temperature measurement instrument. Research also shows that the use of this neural thermal model results in productivity increase and energy cost reduction.

- In [Sha, Edwards, 2007], the use of ANN in materials science and engineering research is discussed. The materials science and engineering research community has and continues to take advantage from new developments in these areas with different applications regularly emerging, along with the degree of sophistication utilized. However, with the increased use, there is unfortunately a growing tendency for the misapplication of ANN methodologies, limiting their potential benefit. Central to the problem is the use of over complicated networks that are frequently mathematically indeterminate, and by using limited data for training and testing. This problem is not unique to one particular field, but has prompted the authors to bring it to the attention of the materials research community in order to elaborate the issues and hopefully prevent others and potentially new researchers from continued misuse of ANNs in the future.
- Materials workability is one of the important aspects for any process design to achieve quality products. Identifying optimum process parameters like temperature, strain rate, and strain are normally done by trial and error. In recent years, processing maps are used in choosing these parameters for hot working of materials. Identification of these parameters requires certain high-level expertise as well as detailed microstructural evidences. In [Ravia, Prasad, Sarmac, 2007], by using the available copper–aluminum alloy data, an ANN model has been developed to classify the hot-working process parameters. The results obtained, using the ANN model, are compared and validated with those obtained from the processing maps. It is further shown that even with smaller data set the development of an ANN model is possible as long as the data has some pattern in it.
- In [Hassan, Alrashdan, Hayajneh, Mayyas, 2008], the potential of using MLF with BP ANN in prediction of some physical properties and hardness of aluminum–copper/silicon carbide composites synthesized by compo casting method has been studied. Two input vectors were used in the construction of proposed network; namely weight percentage of the copper and volume fraction of the reinforced particles. Density, porosity and hardness were the three outputs developed from the proposed network. Therefore, it has been demonstrated, that, by using ANN outputs, satisfactory

results can be estimated rather than measured and hence testing time and cost can be reduced.

- In [Raj, Daniel, 2008], ANN models were developed for the simulation of compressive properties of closed-cell aluminum foam: plateau stress, Young's modulus and energy absorption capacity. The input variables for these models are relative density, average pore diameter and cell anisotropy ratio. Database of these properties are the results of the compression tests carried out on aluminum foams at a constant strain. The prediction accuracy of all the three models is found to be satisfactory. This work has shown the excellent capability of ANN approach for the simulation of the compressive properties of a closed-cell aluminum foam.
- In [Ratha, Singha, Bhaskara, Krishnaa, Santraa, Raia, Neogia, 2010], accurate prediction of roll force during hot rolling process is very important for model based automation (Level-2) of plate mills. Exit thickness of plate for each pass is calculated from roll gap, mill spring, and predicted roll force. The response of gauge control hardware strongly depends on the accuracy of prediction of roll force. Traditionally, mathematical models based on plane homogeneous plastic deformation theory are used for prediction of roll force. This method is based on many simplified assumptions which are not valid for actual industrial application. An artificial neural network (ANN)-based data driven model has been developed for prediction of roll force during plate rolling process. A very accurate data acquisition system has been installed in plate mill of Bhilai steel plant through which input and output parameters have been recorded. For a particular grade of steel, inputs to the ANN model are roll gap of previous pass, roll gap of current pass, rolling temperature, rolling speed, plate width, and pass number (6 inputs). The model output is roll force (1 output). The methodologies of development, training, and validation of ANN models have been discussed. For ANN structure, the feedforward network has been used and for network training methodology BP algorithm with variable learning rate and conjugate gradient optimization of cost function has been chosen. The model was found to be highly accurate with r-square value about 0.94.
- In [Lu, Pan, Liu, Qin, He, Cao, 2010], the behavior of the flow stress of Al-Cu-Mg-Ag heat-resistant aluminum alloys during hot compression deformation was studied by thermal simulation test. Constitutive equations and an ANN model were developed for the analysis and simulation of the flow behavior of these alloys. The inputs of the model are temperature, strain

rate and strain. The output of the model is the flow stress. A comparison between the constitutive equations and the ANN results shows that ANN model has a better prediction power than the constitutive equations.

This work is a continuation of the project where we collected process parameters data of 28 charges for 17 process parameters of "cast strip - foil" process path for alloy AF61 and we used only chemical composition parameters for strip casting alloys as input variables and not other parameters of the process. The input variables were wt% of: 1- primary aluminum, 2- aluminum quality class 1, 3 - aluminum quality class 2, 3, 4, 5, 4- Si, 5 - Fe, 6 - Cu, 7 - Mn, 8 - Mg, 9 - Cr, 10 - Zn, 11 - Ti, 12 - Pb, 13 - Pb+Cr₆+Hg+Cd, 14 - B, 15 - Li, 16 - Zr, 17 - Na. As an output variable, we had chosen tensile strength. Based on these variables we tried to train the neural network, which would be capable of predicting tensile strength while we will change the chemical composition of strip casted alloy. The trained ANN gave us 28 % bad predictions of 14 testing cases, which were the subgroup of all cases [Trčko, Šarler, 2009]. ANN trained on the data for household aluminum foil produced by Impol company predicts the tensile strength very well while we are changing the chemical composition values. However, we want to validate how this ANN predicts the tensile strength. Because the tensile strength is not just correlated with chemical composition but is also correlated to other process parameters, we chose a larger set of good input data, and more independent process parameters to gain confidence in the developed computational intelligence model.

In this work, the ANNs for predicting mechanical properties of household aluminum foils are developed as an alternative approach to the physical modeling. After the introduction in Chapter 1, Chapter 2 presents the theory, history of ANNs development and which computer software is used in the development of ANNs. Chapter 3 shows the household aluminum foil production process path used by the Impol company, as well as which parameters are important in the whole process. Preparing input data for training ANNs is presented in Chapter 4. In Chapter 5 the results of developed ANNs are presented. The results show how selection of ANN configuration and historical data influence the ANN predicting quality. Chapter 6 provides conclusions with recommendation for future research and development.

2 Description of neural networks

This chapter describes the basic concepts of ANNs, history of ANNs research and development, how they work, and which ANNs architectures are most used, followed by the characteristics of NeuralTools program [Palisade Corporation, 2005]. This program is used in the present work to build ANNs.

ANNs are computational models that are inspired by the structure and/or functional aspects of biological neural networks. They are networks of highly interconnected neural computing elements that have an ability to respond to input stimuli and to learn to adapt to the environment. Neural network models offer unified approach for building truly intelligent computer systems. ANNs can be effective as computational processors for various tasks, including pattern recognition (speech, visual image recognition), classification, data compression, modeling and forecasting, combinatorial problem solving, adaptive control, multisensory data fusion and noise filtering [Carling, 1992; Kriesel, 2011].

The earliest work in neural computing was done in the 1940's when McCulloch and Pitts introduced the first neural network computing model. In the 1950's, Rosenblatt's work resulted in a two-layer network, the perceptron, which was capable of learning certain classifications by adjusting connection weights. Although the perceptron was successful in classifying certain patterns, it had a number of limitations. The perceptron was, for instance, not able to solve the classic XOR (exclusive or) problem. Such limitations led to the decline of the field of neural networks. However, the perceptron had laid foundations for later work in neural computing. In the early 1980's, researchers showed renewed interest in neural networks. They included Boltzmann machines, Hopfield nets, competitive learning models, multilayer networks, and adaptive resonance theory models [Patterson, 1995; Tahir, 2007].

One of the more popular ANN architectures is MLF with BP learning. A general MLF ANN is illustrated in Figure 2.1. The internal layers are called "hidden", because they only receive internal inputs (inputs from other processing units)

and produce internal outputs (outputs to other processing units). They are "hidden" from the outside world. Input vectors x are presented to each of the first hidden layer units through weights. Hidden layer unit j receives input i through the weight w_{ij} , $i = 1, 2, 3, \dots, n$, and $j = 1, 2, \dots, h$. Unit j computes a function of the input signal x and the weights, and passes its output forward to all of the units in the next successive layer. The second hidden layer units are fully connected to the previous layer through weights. These units also compute a function of their inputs and their weights and pass their output on to the next layer. This process is repeated until the final computation is produced by the output units [Patterson, 1995].

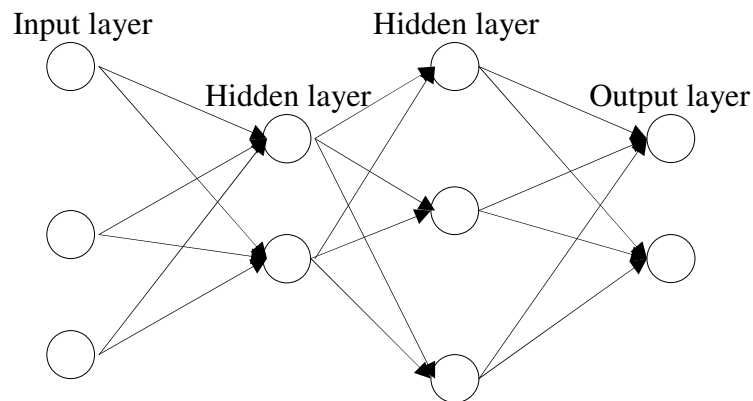


Figure 2.1: A MLF ANN with two hidden layers

The number of input and output units is defined by the problem. The number of hidden units to use is far from clear. A good starting point is to use one hidden layer, with the number of units equal to half the sum of the number of input and output units. Once the number of layers and number of units in each layer have been selected, the network's weights and thresholds must be set as to minimize the prediction error made by the network. This is the role of the training algorithms. The historical cases are used to automatically adjust the weights and thresholds in order to minimize this error. This process is equivalent to fitting the model represented by the network to the training data available. The error of a particular configuration of the network can be determined by running all the training cases through the network, comparing the actual output generated with the desired or target outputs. The differences are combined together by an error function to provide the network error. The most common error functions are the sum squared error and the cross entropy function. The sum squared error function is used for regression problems, where the individual errors of output

units on each case are squared and summed together. The cross entropy function is used for solving classification problems [Statsoft Inc., 2003].

By using the linear modeling, it is possible to algorithmically determine the model configuration that absolutely minimizes this error. The price paid for the greater non-linear modeling power of neural networks is that although we can adjust a network to lower its error, we can never be sure that the error could not be even lower. A helpful concept here is the error surface. Each of the N weights and thresholds of the network is taken to represent a dimension in space. The $N+1$ th dimension is the network error. For any possible configuration of weights the error can be plotted in the $N+1$ th dimension, forming a manifold. Following the Statsoft Inc. company we name it an error surface. The objective of network training is to find the lowest point in this surface. In a linear model with the sum squared error function, this error surface is a parabola and can therefore locate the minimum more easily [Statsoft Inc., 2003].

It is not possible to determine analytically where the global minimum of the error surface is. Neural network training process is essentially an exploration of the error surface. From an initially random configuration of weights and thresholds (i.e. a random point on the error surface), the training algorithms incrementally seeks the global minimum. Typically, a gradient or slope of an error surface is calculated at the current point, and is used to make a downhill move. Eventually, the algorithm stops in a low point, which may represent a local or even a global minimum [Reed, Marks, 1998; Statsoft Inc., 2003].

A possible choice for a neural network training algorithm is BP. This BP learning method specifies how to adjust the weights in hidden layers. In BP the gradient vector of an error surface is calculated. This vector points along the line of a steepest descent from the current point. In this way, we know that if we move along a "short" distance, we will decrease the error. The sequence of such moves will eventually find some sort of minimum. A difficult part is then to decide how large the steps should be [Fauset, 1994; Patterson, 1995; Statsoft Inc., 2003]. More recently, other nonlinear optimization methods have proved to be more efficient than BP learning method, and have come into regular use.

Large steps may converge more quickly, but may also overstep the solution or proceed in the wrong direction if the error surface is very eccentric. Very small steps may go in the correct direction, but they also require a large number of iterations. The size of a step is proportional to the slope, which is a special constant and is named the learning rate. The correct setting for the learning rate

is application-dependent, and is typically chosen by experiment. It may also vary according to time. The learning rate is getting smaller as the algorithm progresses. The algorithm therefore progresses iteratively, through a number of epochs, which is a single pass through the entire training set. In each epoch, the training cases are each submitted to the network. Target and actual outputs are compared and the error is calculated. This error, together with the error surface gradient, is used to adjust the weights. The process is repeated afterwards. The initial network configuration is random, and the training stops when a given number of epochs elapses, or when the error reaches an acceptable level [Statsoft Inc., 2003].

The most desirable property of a network is its ability to adapt to new cases. The network is trained to minimize the error of the training set, which is not the same as minimizing the error on the real error surface - the error surface of the underlying and unknown model, since we do not have a perfect and infinitely large training set. This problem is known as over-learning or over-fitting. This problem is demonstrated below by using a polynomial curve. Polynomial is an equation with terms containing only constants and powers of the variables [Statsoft Inc., 2003].

Different polynomials have different shapes with larger powers having steadily more eccentric shapes. It is possible to explain a given data set by fitting in a polynomial curve (i.e. a model). The data may be noisy and the model is not necessarily the best to pass exactly through all the given points. A low-order polynomial may not be sufficiently flexible to fit close to the points whereas a high-order polynomial is actually too flexible, fitting the data exactly by adopting a highly eccentric shape that is actually unrelated to the underlying function. An example of this is shown in Figure 2.2 [Statsoft Inc., 2003].

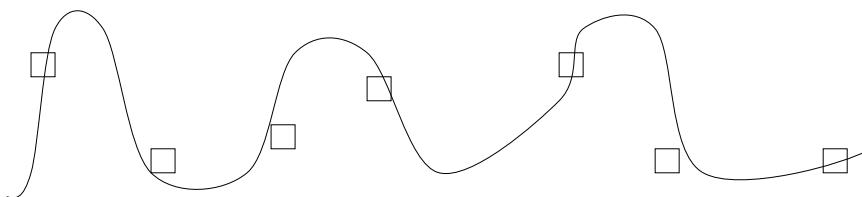


Figure 2.2: Polynomial curve fitting

ANNs have precisely the same problem. A network with more weights models a more complex function, and is therefore prone to over-fitting. A network with fewer weights may not be sufficiently powerful to model the underlying function. For example, a network with no hidden layers actually models a simple

linear function. A larger network will almost invariably achieve a lower error eventually, but this may indicate over-fitting rather than good modeling. As training progresses, the training error naturally drops, and providing training is minimizing the true error function, the selection error drops too. However, if the selection error stops dropping, or starts to rise, this indicates that the network is starting to over-fit the data, and in this case the training should cease. When over-fitting occurs during the training process, it is called over-learning. If this occurs, it is advisable to decrease the number of hidden units and/or hidden layers, as the network proves to be over-powerful for the problem at hand. If the network is not sufficiently powerful to model the underlying function, over-learning is not likely to occur, and neither training nor selection errors will drop to a satisfactory level [Statsoft Inc., 2003].

For training ANNs we used NeuralTools program, which respectively took a different approach to preventing over-learning. The approach with two distinct testing sets is often unrealistic, insofar as typically there is not enough data to split into a training set and two testing sets. Increase of error on a testing-while-training set is not a reliable indicator of over-learning. The increase could be local, and the error might continue to decrease with more training. NeuralTools program solve over-learning condition with Best Net Search function. This function starts with a network of 2 neurons, which is typically too small to result in over-learning. Using default settings, it trains networks with up to 6 neurons. If the networks with 5 and 6 neurons over-learn, that shows in the results from the single testing set; one of the networks with 2, 3 or 4 neurons have the lowest testing error [Palisade Corporation, 2005].

NeuralTools program MLF algorithm restarts itself multiple times from different initial starting weights. Therefore, the longer a network is trained the better. More times it is allowed to get restarted, more likely it is for the global minimum of the error function to be found [Palisade Corporation, 2005].

The other two types of ANNs configuration, built in the NeuralTools program are generalized regression (GRN) ANNs and probabilistic (PN) ANNs.

GRN ANNs are used for numeric prediction/function approximation, while PN ANNs are used for category prediction or classification. A GRN ANN for two independent numeric variables is structured as shown in Figure 2.3 (below). The Pattern Layer contains one node for each training case. Presenting a training case to the network consists here of presenting two independent numeric values. Each neuron in the layer computes its distance from a presented case. The value

passed to the numerator and denominator nodes are functions of the distance and the dependent value. Two nodes in the summation layer sum its inputs while the output node divides them to generate the prediction [Palisade Corporation, 2005].

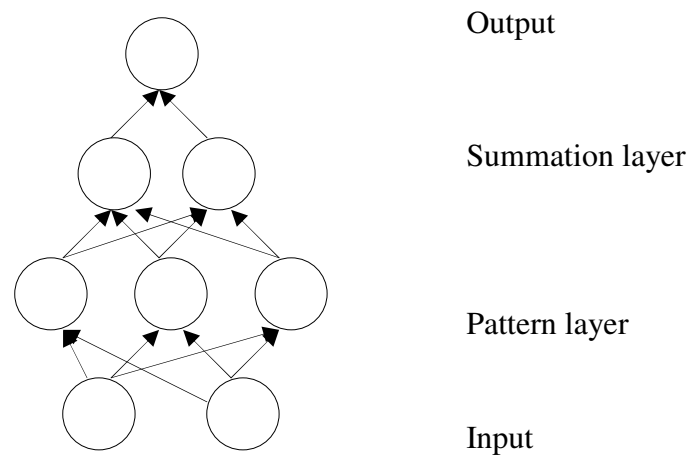


Figure 2.3: A GRN ANN for two independent numerical variables

The distance function computed in the pattern layer neurons uses "smoothing factors". Every input has its own "smoothing factor" value. With the single input, the greater the values of the smoothing factor the more significant distant training cases become for the predicted values. With 2 inputs, the smoothing factor relates to the distance along one dimension in multi-dimensional space [Palisade Corporation, 2005].

Training a GRN ANN consists of optimizing smoothing factors to minimize the error on the training set and the conjugate gradient descent (CGD) optimization method is used to accomplish that. The error measure used during training to evaluate different sets of smoothing factors is the mean squared error. When computing the squared error for a training case, that case is temporarily excluded from the pattern layer. This is because the excluded neuron would compute a zero distance, making other neurons insignificant in the computation of the prediction [Palisade Corporation, 2005].

A PN ANN is structured as shown in Figure 2.4, which assumes there are two independent numeric variables, two dependent categories and five training cases (three in one category and two in the other).

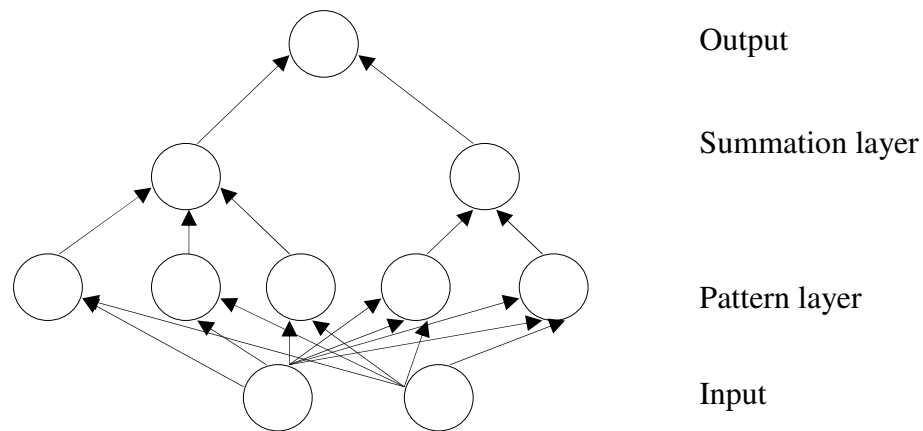


Figure 2.4: A PN ANN for two independent numerical variables, two dependent categories and five training cases

When a case is presented to the network, each neuron in the pattern layer computes the distance between the training case, represented by the neuron, and the input case. Value passed to summation layer neurons is a function of the distance and smoothing factors. As with the GRN networks, each input has its own smoothing factor. These factors determine how rapidly the significance of training cases decreases with distance. There is one neuron per dependent category in the summation layer. Each neuron sums up the output values for the neurons corresponding to the training cases in that category. Output values of the summation layer neurons can be interpreted as probability density function estimates for each class. The output neuron selects the category with the highest probability density function value as the predicted category [Palisade Corporation, 2005].

As with the GRN ANNs, training of a PN ANNs consists of optimizing smoothing factors to minimize the error on the training set and the conjugate gradient descent optimization method is used for this purpose. The error measure used during a training to evaluate different sets of smoothing factors is computed based on all the values returned by neurons in the summation layer for all the training cases. The measure takes into account not only the probability assigned to the correct category, but also distribution of probabilities assigned to incorrect categories – approximately uniform distribution of probabilities among the incorrect categories is better than some incorrect category having a large probability. When computing the error for a training case, this case is temporarily excluded from the pattern layer. This is because the excluded neuron would compute a zero distance, making other neurons insignificant in the computation [Palisade Corporation, 2005].

3 Foil production process path

This chapter describes the basic properties of foils, applications of foils and subsequent steps of process path "cast strip - foil" in the Impol company, which is also presented in a graphical form. All process parameters are represented with their minimum, maximum, and average values.

Various application fields of foils are based on excellent properties of the aluminum foil, which are: low density, high electrical conductivity, dead fold performance, corrosion-resistance, high reflectivity, light and air barrier, non-toxicity and hygiene, and the possibility of achieving very attractive effects through further processing.

The chemical compositions of alloys define their specific properties. However, the following properties are common to all aluminum alloys:

- aluminum does not react with the majority of organic substances,
- aluminum is resistant to chemical reactions,
- aluminum has good corrosion resistance,
- aluminum does not react with alimentary products,
- aluminum is opaque.

Applications of aluminum foils are:

- aluminum foils for food and beverage packaging
 - alloy: EN AW-1200, EN AW-8079
 - surface finish: doubled foil - one side matt / one side bright
 - applications: lids, bottle necks, coffee packaging, butter packaging, cheese packaging, wine capsules, confectionery, chocolate packaging

- aluminum foils for pharmaceutical use
 - alloy: EN AW–8079, EN AW–1200, EN AW-8021B
 - surface finish: doubled foil - one side matt / one side bright
 - applications: blister, coldform

- aluminum foils for technical use
 - alloy: EN AW–1200, EN AW–8079
 - surface finish: doubled foil - one side matt / one side bright
 - applications: cable wrapping, insulations

- aluminum container foils
 - alloy: EN AW–3005, EN AW–8011
 - surface finish: mill finish, degreased by annealing
 - applications: smooth–wall containers, catering containers

- aluminum household foils
 - alloy: EN AW–8011
 - surface finish: doubled foil - one side matt / one side bright
 - applications: household foil, pet–food containers, adhesive tapes

- aluminum finstock for heat exchangers
 - alloy: EN AW–1050, EN AW– 8006, EN AW–8011, EN AW 5052
 - surface finish: mill finish
 - applications: heating, ventilation and air conditioning, refrigeration systems, heat exchangers for power plants

- aluminum strips and foils for tubes
 - alloy: EN AW –1050, EN AW–8006,EN AW –8011
 - surface finish: mill finish
 - applications: multi layer pipes, flexible tubes

- aluminum strips for profiling
 - alloy: EN AW–1050, EN AW–3003; EN AW–3105
 - surface finish: mill finish
 - applications: corner beads, spacers, household appliances

The foil production process steps at the Impol company are depicted in Figures 3.1 – 3.6.

1. Charging preparation

- wt% primary aluminum
- wt% internal scrap

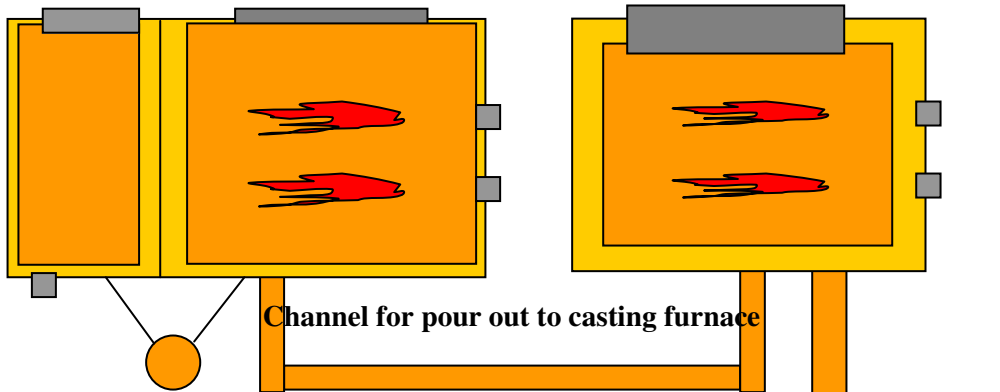


2. Charging



Two chamber melting furnace with EMP pump

Slope casting furnace



3. Melting and alloying

- chemical composition

4. Modification

- Grain refiner speed setpoint

5. Metal cleaning with Ar and Cl, hydrogen removal

- Alpur temperature

6. Removal of inclusions

- Alloy temperature

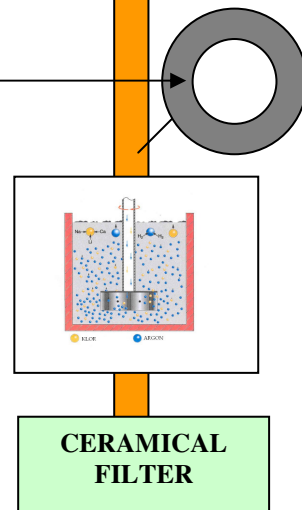
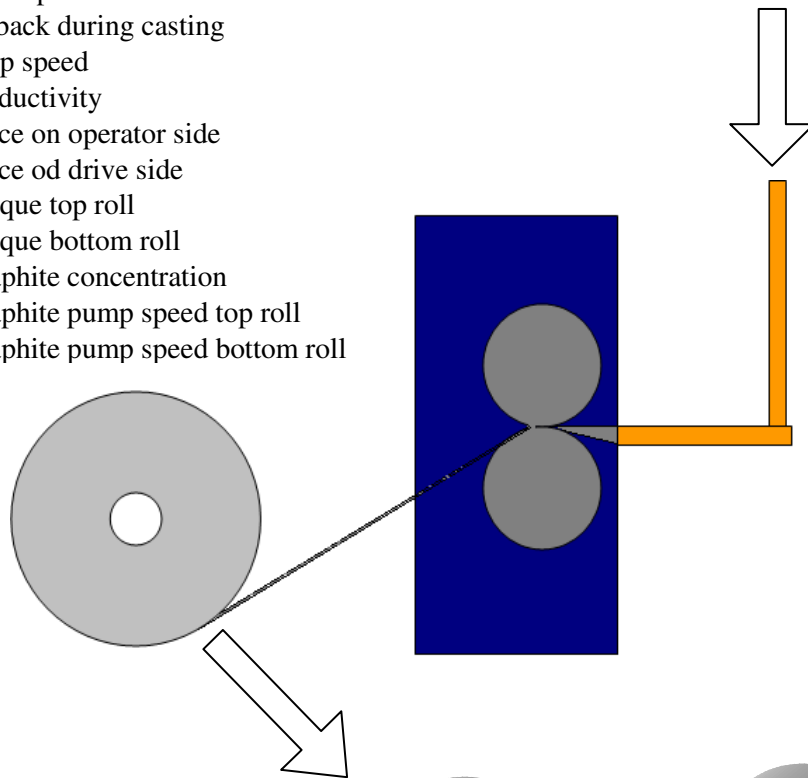


Figure 3.1: Foil production process at the Impol company (process steps 1 – 6)

7. Casting on strip casting machine

- Metal level
- Tundish temperature
- Tip center temperature
- Start-up setback
- Setback during casting
- Strip speed
- Productivity
- Force on operator side
- Force of drive side
- Torque top roll
- Torque bottom roll
- Graphite concentration
- Graphite pump speed top roll
- Graphite pump speed bottom roll

**8. Coil thickness of 6 mm**

- Profile - average
- Profile - maximum
- Tilt - average
- Tilt - maximum
- Centering - maximum

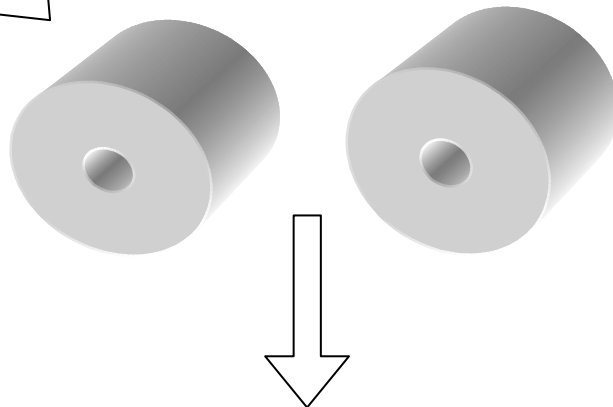
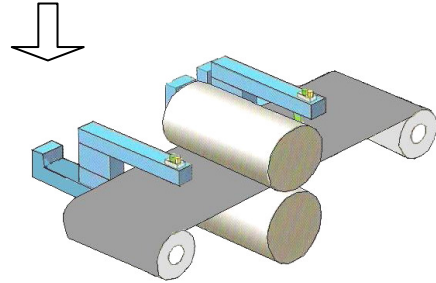


Figure 3.2: Foil production process at the Impol company (process steps 7 – 8)

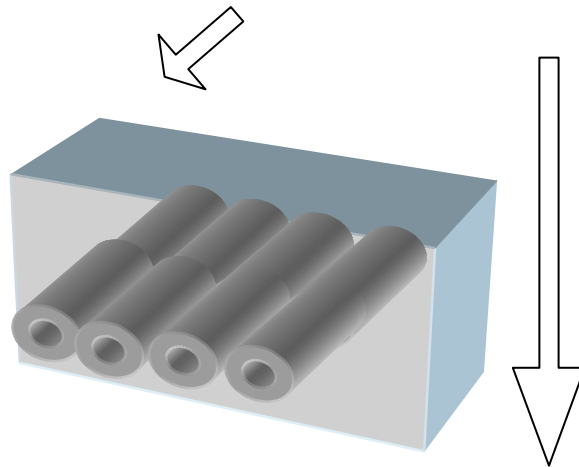
9. Cold rolling

- Input
- Output
- Force on operator side
- Force on drive side
- Sum force
- Speed
- Total deformation



10.1. Homogenization annealing

- Temperature
- Time



10.2. Cold rolling

- Force on operator side
- Force on drive side
- Speed
- Total deformation

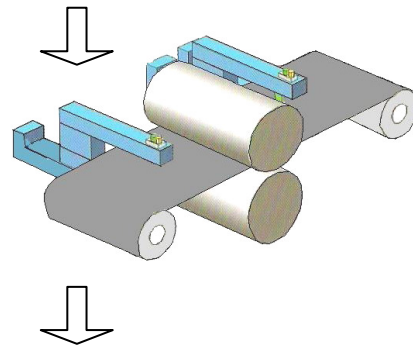


Figure 3.3: Foil production process at the Impol company (process steps 9 – 10)

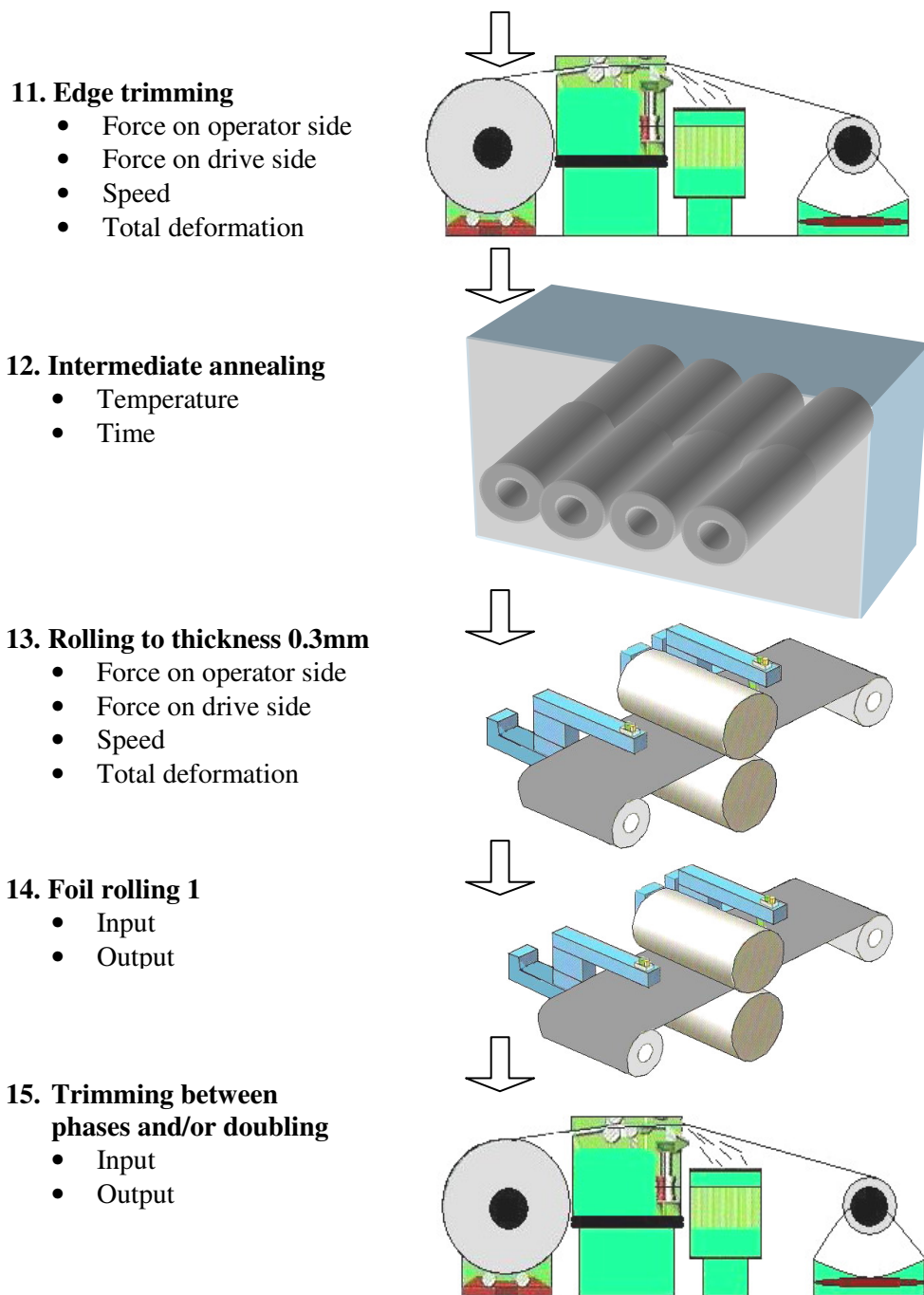


Figure 3.4: Foil production process at the Impol company (process steps 11 – 15)

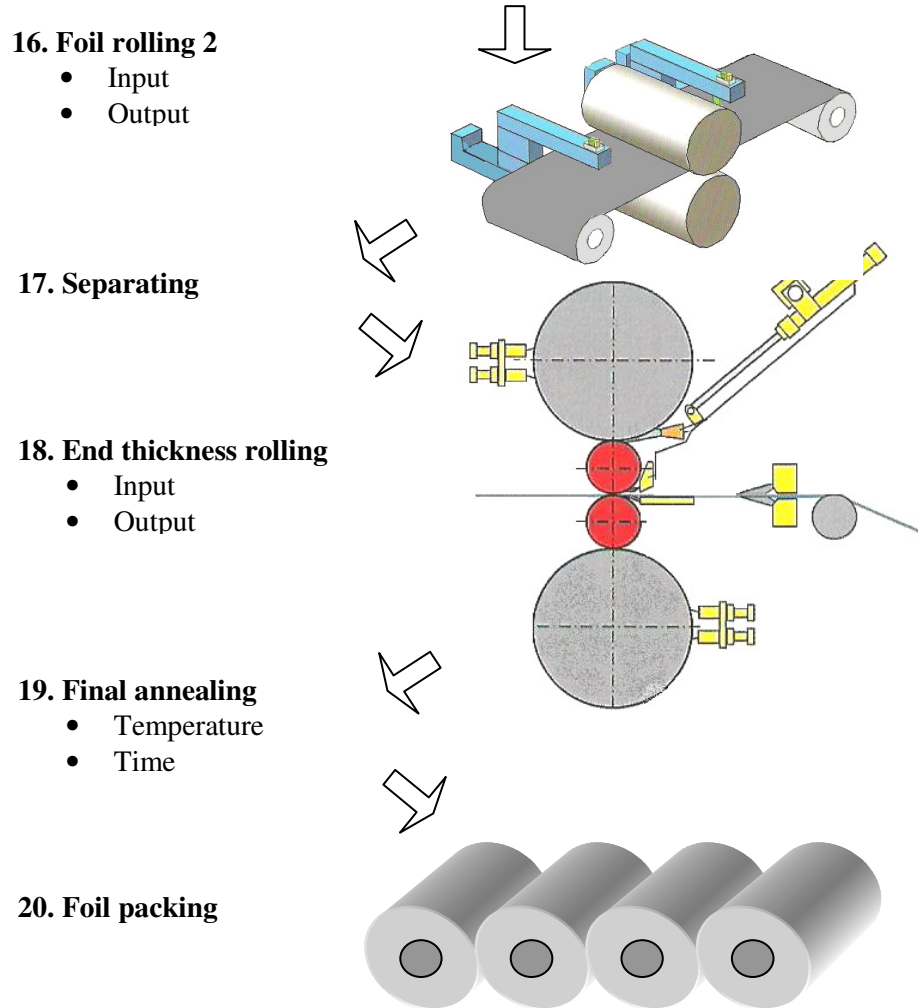


Figure 3.5: Foil production process at the Impol company (process steps 16 – 20)

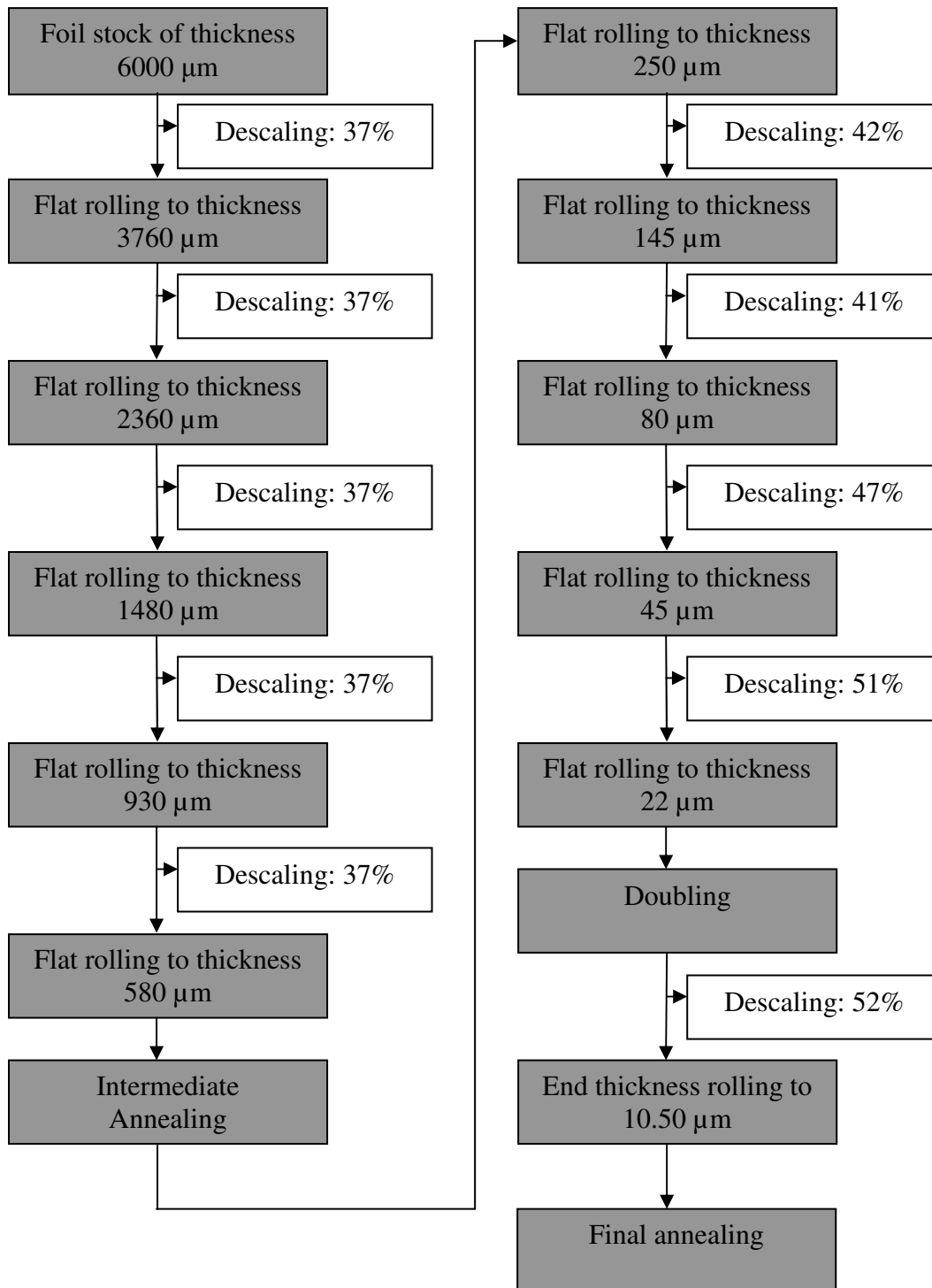


Figure 3.6: Descaling of thickness in foil rolling process FOIL STOCK - FOIL (ALLOY AF61) at the Impol company

Below is the table of all selected process parameters for alloy AF61 with their minimum, maximum and average values. These values have been selected based on suggestions from employees and process data availability at the Impol company. For training ANNs we used only 27 important process parameters as input variables (in the table below they are marked bold) from melting and alloying process (chemical composition) and annealing [Altenpohl, 1998; Trčko, Robič, Jelen, Volšak, Strnad, Skrbinek, Malenšek, Cvahte, Šarler, 2007; Trčko, Robič, Šarler, 2007; Quested, Crumbach, Hamerton, 2006; Crumbach, Quested, Hamerton, 2006]. These process parameters are described in Chapter 4. Non-bold marked process parameters are not used in ANN training process because of one or both following reasons:

- Difference between minimum and maximum value is very small
- Process parameter value is constant

Table 3.1: Table of all process parameters for alloy AF61 with minimum, maximum and average values with regard to classification

		Values				
		Input parameters	Unit	min.	max.	avg.
Charging preparation (1)		Primary aluminum	wt%	98	100	99
		Min. % of primary aluminum	wt%	30	30	30
	Internal scrap	Quality class 1	wt%	20	20	20
Melting and alloying (3)	Internal composition for strip casting alloys	Si	wt%	0.55	0.65	0.6
		Fe	wt%	0.8	0.9	0.85
		Cu	wt%	0	0.05	0.025
		Mn	wt%	0	0.022	0.011
		B	wt%	0	0.01	0.005
		Zn	wt%	0	0.05	0.025
		Pb	wt%	0	0.05	0.025
		Bi	wt%	0	0.05	0.025
		Mg	wt%	0	0.05	0.025
		Cd	wt%	0	0.05	0.025
		Zr	wt%	0	0.002	0.001
		Be	wt%	0	0.05	0.025
		In	wt%	0	0.05	0.025
		Ti	wt%	0.025	0.05	0.0375
		Hg	wt%	0	0.05	0.025
		Ni	wt%	0	0.05	0.025
		Sn	wt%	0	0.05	0.025

		Ca	wt%	0	0.002	0.001
		Na	wt%	0	0.001	0.0005
		Li	wt%	0	0.0002	0.0001
		V	wt%	0	0.05	0.025
		Sr	wt%	0	0.05	0.025
		Cr	wt%	0	0.002	0.001
		Sb	wt%	0	0.05	0.025
		Ga	wt%	0	0.05	0.025
		Sum Hg Cd Pb	wt%	0	0.15	0.075
		Sum Ti Zr	wt%	0	0.15	0.075
		Sum Mn Zr	wt%	0	0.15	0.075
		Sum Mn Cr Ti V	wt%	0	0.15	0.075
		Sum Pb Hg Cd Cr	wt%	0	0.01	0.005
Modification (4)		Grain refiner speed setpoint	cm/min	50	60	55
Metal cleaning with Ar and Cl, hydrogen removal (5)		Alpur temperature	°C	740	780	760
Casting on strip casting machine (7)		Metal level	mm	11	15	13
		Tundish temperature	°C	710	730	720
		Tip center temperature	°C	695	705	700
		Start-up setback (fix)	mm	68	68	68
		Setback during casting	mm	68	75	71.5
		Strip speed	m/min	1.15	1.25	1.2
		Productivity	t/h/m	1.10	1.22	1.16
		Force OS	t	600	650	625
		Force PS	t	600	650	625
		Torque top roll	daN.m	22000	27000	24500
		Torque bottom roll	daN.m	22000	27000	24500
		Graphite concentration	%	1.70	1.70	1.70
		Graphite pump speed top roll	%	20	30	25
		Graphite pump speed bottom roll	%	20	30	25
	Coiler tension setpoint (fix)	daN/mm ²	0.90	0.90	0.90	
Coil thickness of 6 mm (8)	Geometry properties	Profil avg.	%	0	1	
		Profil max.	%		2	
		Tilt avg.	%	0	0.5	
		Tilt max.	%		2	
		Centering max.	%		0.5	

	Width checking	Width of hot strip after trimming (fix)	mm	1.642	1.642	1.642	
		Width of cold strip after trimming (fix)	mm	1.630	1.630	1.630	
	Thickness and diameter checking	Coil width	mm	1.630	1.630	1.630	
		Thickness	mm	5.82	6.18	6.00	
		Inside diameter	mm	500	500	500	
		Outside diameter	mm	1.750	1.855	1.803	
	Cold rolling (9)	1. pass	Input	μm	6000	6000	6000
			Output	μm	3760	3760	3760
			Z force	N/mm ²	13.78	13.78	13.78
			N force	N/mm ³	22.33	22.33	22.33
Force			kN	6090	6090	6090	
Speed			m/min	149	149	149	
Esum (total deformation)				0.37	0.37	0.37	
2. pass			Input	μm	3760	3760	3760
		Output	μm	2360	2360	2360	
		Z force	N/mm ²	22.33	22.33	22.33	
		N force	N/mm ³	24.87	24.87	24.87	
		Force	kN	5371	5371	5371	
		Speed	m/min	183	183	183	
		Esum (total deformation)		0.61	0.61	0.61	
		3. pass	Input	μm	2360	2360	2360
Output			μm	1480	1480	1480	
Z force			N/mm ²	24.87	24.87	24.87	
N force			N/mm ³	26.08	26.08	26.08	
Force			kN	4461	4461	4461	
Speed			m/min	244	244	244	
Esum (total deformation)				0.75	0.75	0.75	
4. pass			Input	μm	1480	1480	1480
		Output	μm	930	930	930	
		Z force	N/mm ²	26.08	26.08	26.08	
		N force	N/mm ³	29.34	29.34	29.34	
		Force	kN	3671	3671	3671	
		Speed	m/min	320	320	320	
		Esum (total deformation)		0.85	0.85	0.85	
	Edge trimming (11)		Input	mm	1630	1630	1630
		Output	mm	1580	1580	1580	
		Input	μm	930	930	930	
		Output	μm	580	580	580	

		Z force	N/mm ²	27.10	27.10	27.10
		N force	N/mm ³	41.13	41.13	41.13
		Force	kN	2916	2916	2916
		Speed	m/min	200	200	200
		Esum (total deformation)		0.90	0.90	0.90
Intermediate annealing (12)		Temperature	°C	280	280	280
		Time	H	3	3	3
Rolling to thickness 0.3mm (13)		Input	μm	580	580	580
		Output	μm	250	250	250
		Z force	N/mm ²	13.78	13.78	13.78
		N force	N/mm ³	44.97	44.97	44.97
		Force	kN	2493	2493	2493
		Speed	m/min	495	495	495
		Esum (total deformation)		0.57	0.57	0.57
Foil rolling 1 (14)	1. pass	Input	μm	250	250	250
		Output	μm	145	145	145
	2. pass	Input	μm	145	145	145
		Output	μm	85	85	85
Trimming between phases (15)		Input	mm	1580	1580	1580
		Output	mm	1540	1540	1540
Foil rolling 2 (16)	1. pass	Input	μm	85	85	85
		Output	μm	45	45	45
	2. pass	Input	μm	45	45	45
		Output	μm	22	22	22
Doubling (15)		2 x thickness x 1540	μm	22	22	22
End thickness rolling (18)		Input (2 x thickness x 1540)	μm	22	22	22
		Output (2 x thickness x 1540)	μm	10.50	10.50	10.50
Separating (17)		Output (1 x thickness x 1540)	μm	10.50	10.50	10.50
Final annealing (19)						
Final Mechanical properties		Tensile strength R_m (thickness 10 - 24 μm)	MPa	55	115	
		Elongation A₁₀₀	%	1		

4 Preparing input data for training ANNs

This chapter provides a basic definition for measured output parameters: tensile strength and elongation. It also describes which process parameters are used to train the ANNs and how we can examine the training data quality.

Artificial neural networks (ANNs) used in this work are developed as an alternative to physical modeling for computing final mechanical properties of metal semi products. Process path of the household foil EN AW-8011 with thickness 10.5 μm in Impol aluminum industry is used as a demonstration of this new methodology. The ANN NeuralTools program, which uses neural computing elements that have the ability to respond to input stimuli and to learn to adapt the environment, is used. 27 process parameters have been identified as the most important for predicting the final tensile strength and the elongation of the foil. The selection criteria of these parameters were twofold: (I) suggestions by technologists (expert knowledge) of the Impol company and (II) process data availability at the Impol company.

4.1 Measurements of the tensile strength and elongation

The definitions of the tensile strength (R_m) and elongation (A) are described below [Slovenski standard, 2002].

- R_m - tensile strength:
 R_m is stress corresponding to the maximum force (F_m). After determination of the required yield/proof strength properties, the test rate may be increased to a static rate (or equivalent crosshead separation rate) to no greater than 0.008 s^{-1} .

If only the tensile strength of the material is required to be measured, the test rate shall not exceed 0.008 s^{-1} throughout the test.

- **A - percentage elongation after fracture:**
A is permanent elongation of the gauge length after fracture ($L_u - L_o$) expressed as a percentage of the original gauge length (L_o)
For determination of percentage elongation after fracture, two broken pieces of the test piece are carefully fitted back together so that their axes lie in a straight line. Special precautions shall be taken to ensure proper contact between the broken parts of the test piece when measuring the final gauge length. This is particularly important in the case of test pieces of small cross-section and in the case of test pieces having low elongation values. Elongation after ($L_u - L_o$) shall be determined to the nearest 0.25 mm with a measuring device with a sufficient resolution and the value of percentage elongation after fracture shall be rounded to the nearest 0.5 %. If the specified minimum percentage elongation is less than 5 %, it is recommended that special precautions are taken when determining elongation. This measurement is, in principle, valid only if the distance between the fracture and the nearest gauge mark is not less than one third of the original gauge length (L_o). However, the measurement is valid, irrespective of the position of the fracture, if the percentage elongation after fracture is equal to or greater than the specified value.

For machines, capable of measuring extension at fracture, using an extensometer, it is not necessary to mark the gauge lengths. The elongation is measured as a total extension at fracture, and it is therefore necessary to deduct the elastic extension in order to obtain the percentage elongation after the fracture. In principle, this measurement is only valid if fracture occurs within the extensometer gauge length (L_e). The measurement is valid regardless of the position of the fracture cross-section if the percentage elongation after fracture is equal to or greater than the specified value.

If elongation is measured over a given fixed length, it can be converted to proportional gauge length, using conversion formulae or tables as agreed before the commencement of testing (for example as in EN ISO 2566-1 and EN ISO 2566-2) [Slovenski standard, 2002].

A universal testing machine, also known as a materials testing machine, is a machine, which performs determination of the material properties. This machine is used to test the tensile and the compressive properties of materials. Such machines generally have two columns. Load cells and extensometers measure the key parameters of force and deformation as the sample is tested. These machines are widely used in any materials testing laboratory. A typical testing system is comprised of a materials testing machine, control and analysis software, and importantly, the test fixtures, accessories, parts and devices used to hold and support the test specimen [Slovenski standard, 2002].



Figure 4.1: Sample before tensile strength and elongation testing (Photo author, courtesy Impol)

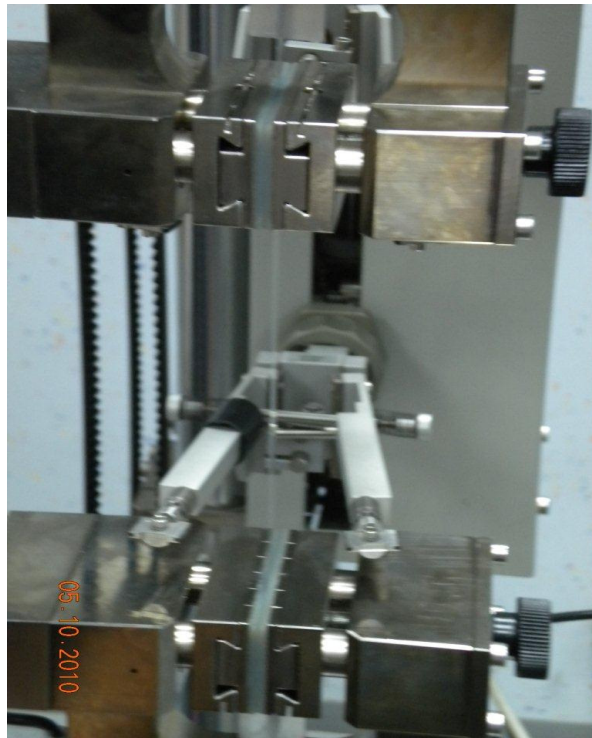


Figure 4.2: Testing machine for testing thin aluminum strips and foils. For measuring R_m and A (Photo author, courtesy Impol)

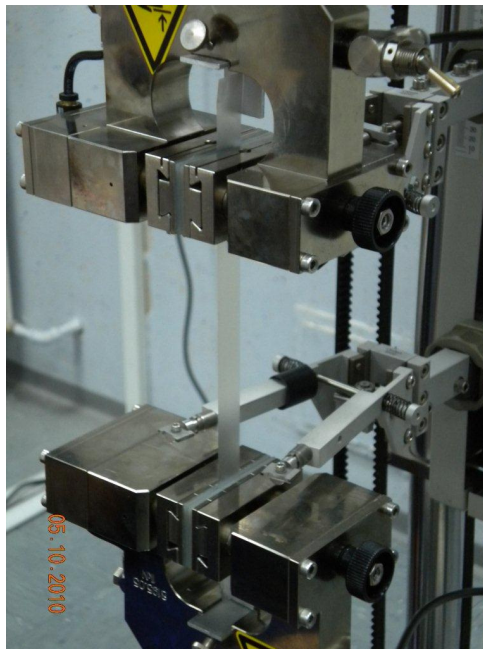


Figure 4.3: Testing machine with aluminum strip at the beginning of testing (Photo author, courtesy Impol)

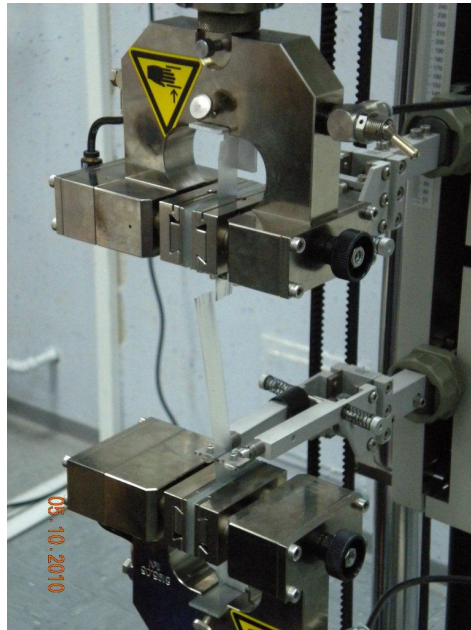


Figure 4.4: Testing machine with aluminum strip at the end of testing (Photo author, courtesy Impol)



Figure 4.5: Sample after tensile strength and elongation testing (Photo author, courtesy Impol)

4.2 Process parameters data

We train the ANN with data from industry for household aluminum foils (EN AW-8011) with thickness 10.5 μm , produced at the Impol company. 109 sets of complete history data (time-independent process data) of foil production were collected. The ANN maps functional relation between selected inputs and outputs. This functional relation described static characteristic of the modeled system without any dynamics considered. All 109 sets were used for training ANNs to predict tensile strength and elongation. After ANNs are trained, they are capable of predicting tensile strength and elongation while we change the values of input variables. The input variables are wt% of: 1 - Si, 2 - Fe, 3 - Cu, 4 - Mn, 5 - B, 6 - Zn, 7 - Pb, 8 - Bi, 9 - Mg, 10 - In, 11 - Ti, 12 - Hg, 13 - Ni, 14 - Sn, 15 - Ca, 16 - V, 17 - Cr, 18 - Sb, 19 - Ga, 20 - sum of Hg-Cd-Pb, 21 - sum of Ti-Zr, 22 - sum of Mn-Zr, 23 - sum of Mn-Cr-Ti-V, 24 - recycled aluminum, and other process parameters: 25 - width of the coil, 26 - outside diameter of the coil, 27 - annealing temperature. We choose tensile strength and elongation as our output variables. One row of values of these input and output variables comprises one set for training ANNs, which are then developed in four steps: data preparation, training, testing calculated known output values, and prediction of unknown output values based on different combination of input chemical composition and other process parameters [Trčko, Šarler, 2009].

4.3 Training data quality and preprocessing

Data for the ANN training process were collected at the company Impol over the period of three months from December 2008 to March 2009. For some process parameters, data were collected automatically with other computer systems and some parameter values were collected manually. After we checked the collected data, we noticed some errors in this data. For example the same values of input variables have different values of output variables (tensile strength - R_m and elongation - A). These errors mostly occur when data are collected manually. Because the result of the ANN training process with this kind of erroneous data could not be satisfactory, we calculated average output values for records, which had the same input variable values and different values of output variables. This is shown in table 4.1. This approach enables a reasonable accounting of all the available data. The averaging in this case is justifiable, since the difference between the output data for the same input data is small.

Table 4.1: Calculated average value of Rm and A of two records of historical data with the same input variable values.

	Historical data record 1	Historical data record 2	Data record with average values (Rm and A)
Charge	92926	92926	92926
Alloy	AF61	AF61	AF61
Width (mm)	290.0	290.0	290.0
Outside diameter (mm)	900.0	900.0	900.0
Al (wt%)	98.489	98.489	98.489
Si (wt%)	0.587	0.587	0.587
Fe (wt%)	0.847	0.847	0.847
Cu (wt%)	0.001	0.001	0.001
Mn (wt%)	0.005	0.005	0.005
B (wt%)	0.002	0.002	0.002
Zn (wt%)	0.004	0.004	0.004
Pb (wt%)	0.001	0.001	0.001
Bi (wt%)	0	0	0
Mg (wt%)	0.002	0.002	0.002
Cd (wt%)	0	0	0
Zr (wt%)	0.001	0.001	0.001
Be (wt%)	0	0	0
In (wt%)	0	0	0
Ti (wt%)	0.03	0.03	0.03
Hg (wt%)	0.002	0.002	0.002
Ni (wt%)	0.002	0.002	0.002
Sn (wt%)	0.001	0.001	0.001
Ca (wt%)	0.001	0.001	0.001
Na (wt%)	0	0	0
Li (wt%)	0	0	0
V (wt%)	0.006	0.006	0.006
Sr (wt%)	0	0	0
Cr (wt%)	0.002	0.002	0.002
Sb (wt%)	0.005	0.005	0.005
Ga (wt%)	0.011	0.011	0.011
Sum of Hg-Cd-Pb (wt%)	0.003	0.003	0.003
Sum of Ti-Zr (wt%)	0.03	0.03	0.03
Sum of Mn-Zr (wt%)	0.007	0.007	0.007
Sum of Mn-Cr-Ti-V (wt%)	0.043	0.043	0.043
Sum of Pb-Hg-Cd-Cr (wt%)	0	0	0

Temp. (°C)	290	290	290
Rm (Mpa)	105.62	108.82	107.22
A (%)	2.80	2.52	2.66

The process of finding erroneous data and calculating average values can possibly be automated by using an appropriate artificial intelligence method.

5 Results

The ANN is trained from a data set comprised of cases with known output values. These data consists of historical cases for which we know the values of output or dependent variables. 109 sets of complete history data of foil production were used. After training, ANN is tested to see how well it does at predicting known output values. The data used for testing is usually a subset of historical data. This subset is not used in training the network. After testing, the performance of the network is measured by statistics such as the percentage of the known answers it correctly predicts. To measure the error between the real and the predicted output data, we calculate norms $L1$ and $L2$,

$$L1: \frac{1}{N} \sum_{k=1}^N |x_k^{ANN} - x_k^{MSR}| \quad (1)$$

$$L2: \frac{1}{N} \sqrt{\sum_{k=1}^N |x_k^{ANN} - x_k^{MSR}|^2} \quad (2)$$

where N represent the number of elements in the data set, x_k^{ANN} represent k-th calculated value by ANN and x_k^{MSR} represent k-th measured value.

Four ANN MLF configurations have been tested in this work. In all neural network configurations, we chose one hidden layer with 6 nodes, 27 independent input variables and 60 minutes of training time as suggested by the NeuralTools program Best Net Search option.

The first and the second configuration are used for predicting the tensile strength (Rm) while the third and the fourth are employed for predicting the elongation (A).

For validating trained ANNs we used the cross-validation method. Cross-validation is a statistical method of evaluating and comparing learning algorithms by dividing data into two subsets. One subset is used to train the ANN and the other used to validate the ANN. In typical cross-validation, the training and validation sets must cross-over in successive rounds such that each data point has a chance of being validated against. The basic form of cross-validation is k-fold cross-validation [Refaeilzadeh, Tang, Liu, 2009].

In k-fold cross-validation the data is first partitioned into k equally or nearly equally sized segments or folds. Subsequently k iterations of training and validation are performed such that within each iteration a different fold of the data is held-out for validation while the remaining k - 1 folds are used for learning. 10-fold cross-validation is commonly used [Refaeilzadeh, Tang, Liu, 2009].

Leave-one-out cross-validation is a special case of k-fold cross-validation where all the data except for a single observation are used for training and the model is tested on that single observation. Leave-one-out cross-validation is computationally expensive because it requires many repetitions of training [Refaeilzadeh, Tang, Liu, 2009].

5.1 Presentation and validation of the results

Since our history data set was big enough for separating it into two subsets, we decided not to use k-fold or leave-one-out cross-validations. Instead of this we divide history data set into two subsets with approximately 75 % of rows for training ANNs and 25 % of rows for testing the trained ANNs.

ANN for tensile strength, Step 1: In the first configuration, the MLF ANN training data set consisted of 80 historical data rows (charge data) with 27 independent input variables and the testing data set consisted of 29 data rows, which was not included in the training process. The result of the testing process was 89.65 % good predictions and 10.35 % bad predictions. Good prediction means that the ANN predicted value does not differ more than 5 % from the real testing value. The performance of the tested MLF ANN for process parameter tensile strength (Rm) is shown in Fig. 5.1, where predicted versus real (collected) values for tensile strength are shown. The value of $L1$ was 1.888 and the value of $L2$ was 0.655.

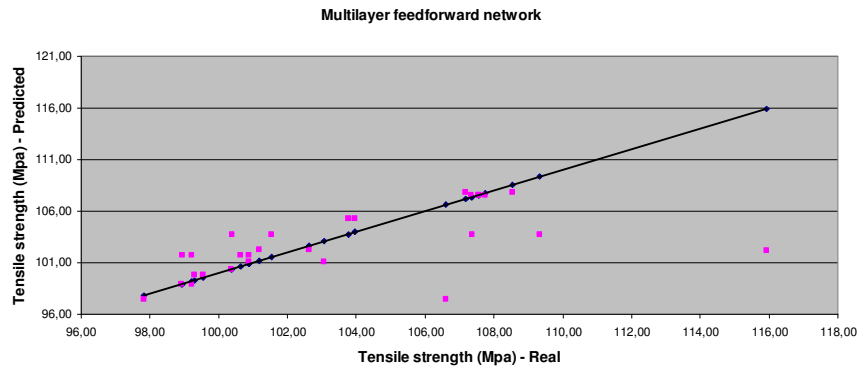


Figure 5.1: Predicted vs. real values of tensile strength for the testing data set of 29 rows

Step 2: Afterwards we eliminated several rows of training data for which we heuristically estimated (engineering judgment) that they might not perform well in training. Elimination means that we calculated average values of tensile strength for rows that have the same values of input variables and different values for output variable tensile strength. The new training data set consisted of only 39 rows of historical data. For training ANN we used 30 rows and for testing the remaining 9 rows. This second configuration gave us a tested ANN with result of 100 % good predictions and 0 % of bad predictions. The performance of the MLF ANN for variable tensile strength (R_m) is shown in Fig. 5.2, where the predicted versus collected values for tensile strength are shown. The value of $L1$ was 0.855 and the value of $L2$ was 0.318.

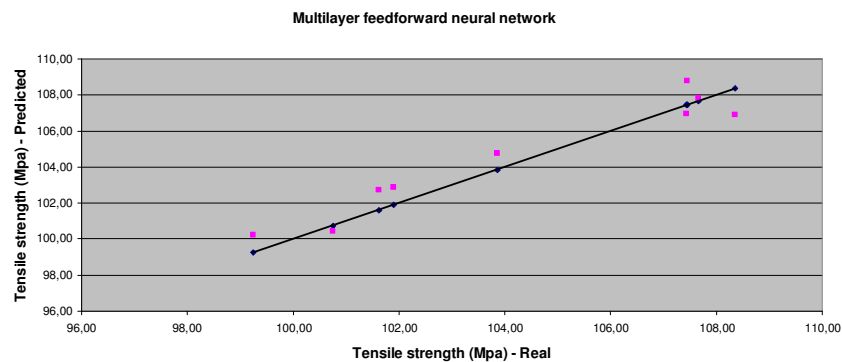


Figure 5.2: Predicted vs. real values of tensile strength for testing data set of 9 rows

ANN for elongation, Step 1: The third and the fourth configuration of ANNs was used for predicting material property elongation (A). The training data set

consisted of 80 rows of historical data with 27 independent input variables and the testing data set consisted of 29 data rows, which was not included in training process. The result of the testing process was 44.83 % of good predictions and 55.17 % of bad predictions. The performance of the MLF ANN for variable elongation (A) is shown in Fig. 5.3, where the predicted versus real values for elongation are shown. The value of $L1$ was 0.290 and the value of $L2$ was 0.080.

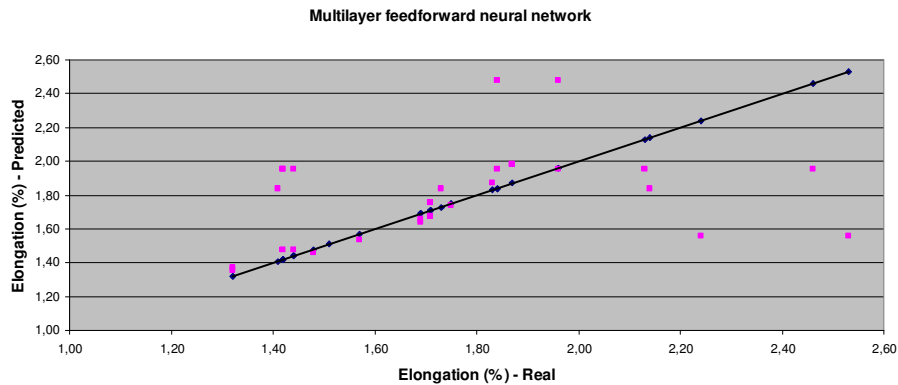


Figure 5.3: Predicted vs. real values of elongation for the testing data set of 29 rows

Step 2: In the same sense as in the study of the tensile strength, we eliminated some suspicious rows of training data. The new training data set consisted of only 26 rows of historical data with 27 independent input variables. For training ANN we used 20 rows, and for testing the remaining 6 rows. This fourth configuration gave us a tested ANN with result of 100 % of good predictions and 0 % of bad predictions. The performance of the MLF ANN for variable elongation (A) is shown in Fig. 5.4, where the predicted versus real values for elongation are shown. The value of $L1$ was 0.023 and the value of $L2$ was 0.006.

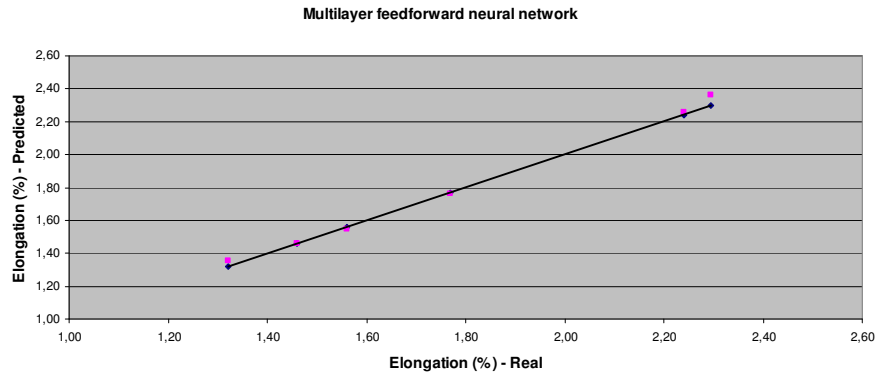


Figure 5.4: Predicted vs. real values of elongation for the testing data set of 6 rows

The following graphs show how specific process parameters influence tensile strength and elongation. They represent tensile strength and elongation dependencies upon chemical elements Si, Fe, Mg, Cu, Mn, B, Zn, Pb, Bi, In, Ti, Hg, Ni, Sn, Ca, V, Cr, Sb, Ga, sum of Hg-Cd-Pb, sum of Ti-Zr, sum of Mn-Zr, sum of Mn-Cr-Ti-V, width of the coil, outside diameter of the coil and annealing temperature T. Every graph has a trend line, which shows a trend of tensile strength and elongation (Fig. 5.5 – 5.58).

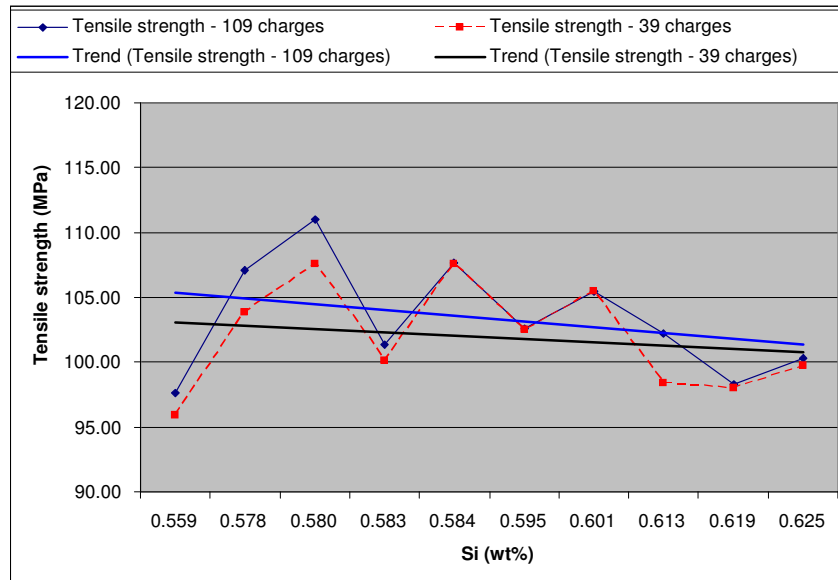


Figure 5.5: Influence of wt% Si on tensile strength and linear trend lines for tensile strength of 109 and 39 charges

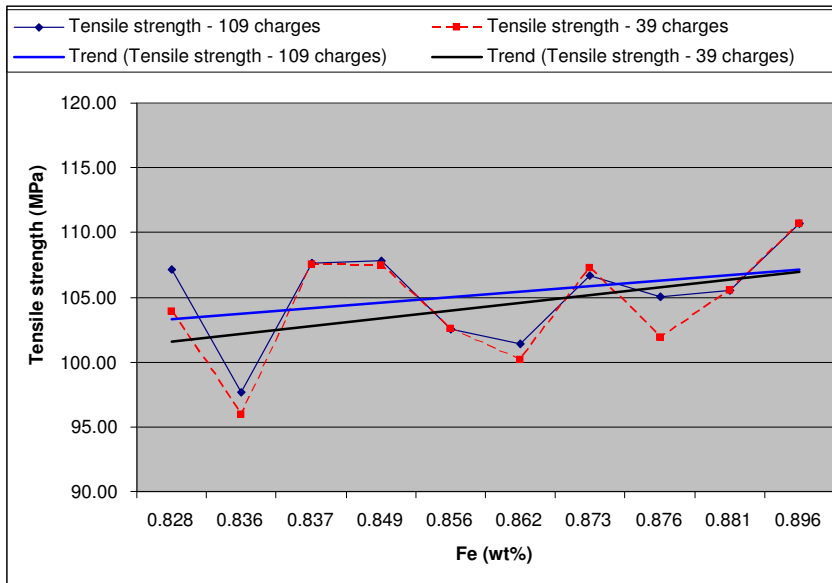


Figure 5.6: Influence of wt% Fe on tensile strength and linear trend lines for tensile strength of 109 and 39 charges

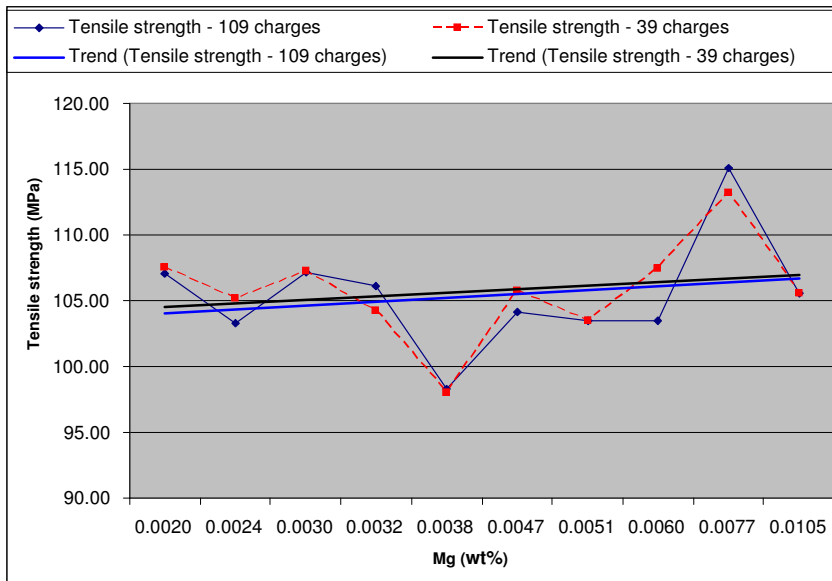


Figure 5.7: Influence of wt% Mg on tensile strength and linear trend lines for tensile strength of 109 and 39 charges

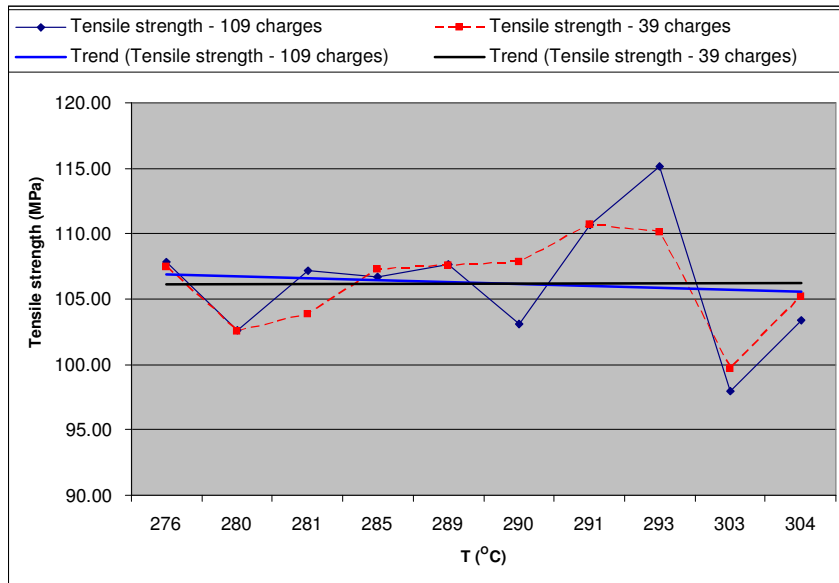


Figure 5.8: Influence of annealing temperature T on tensile strength and linear trend lines for tensile strength of 109 and 39 charges

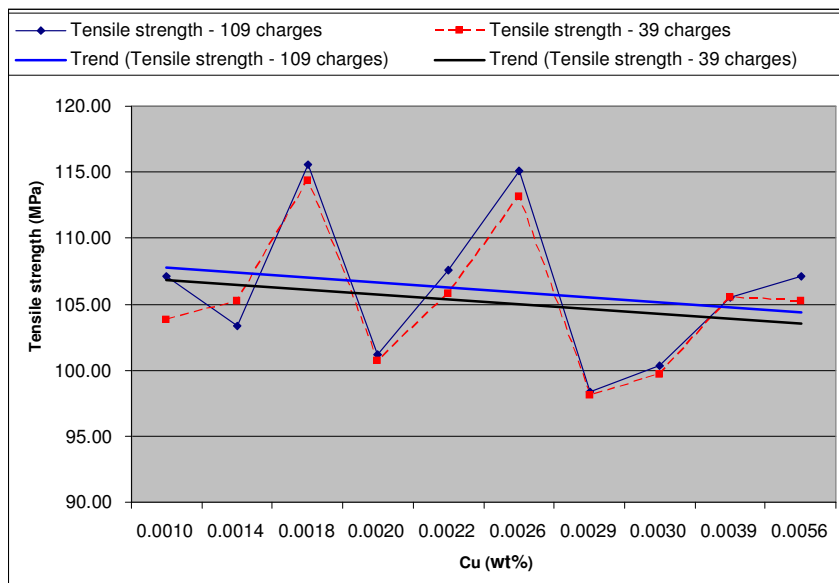


Figure 5.9: Influence of wt% Cu on tensile strength and linear trend lines for tensile strength of 109 and 39 charges

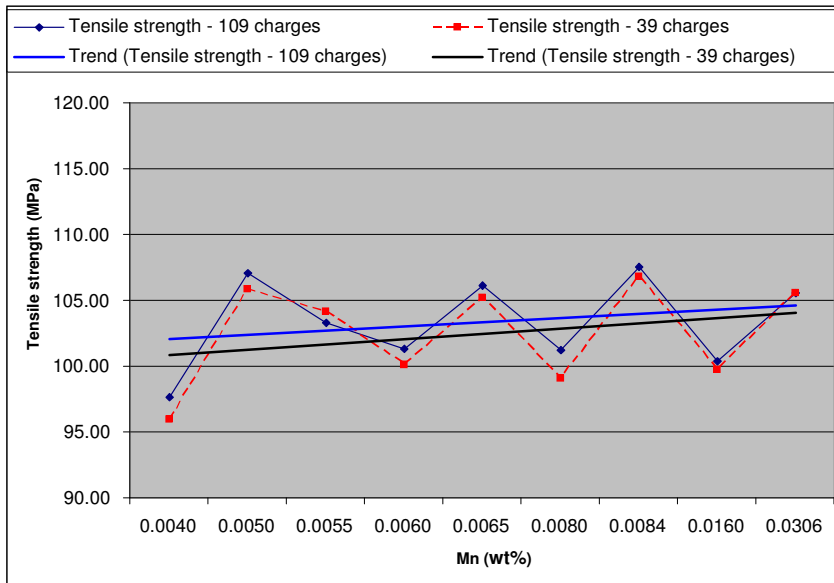


Figure 5.10: Influence of wt% Mn on tensile strength and linear trend lines for tensile strength of 109 and 39 charges

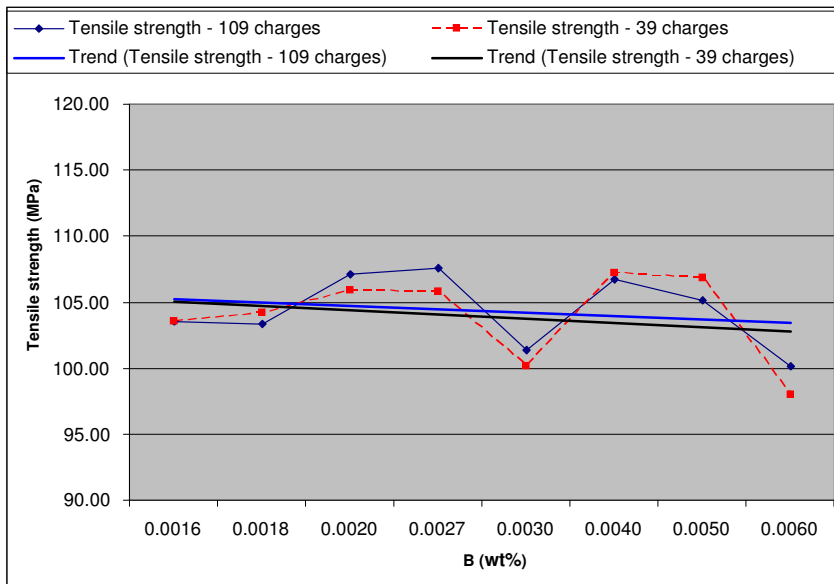


Figure 5.11: Influence of wt% B on tensile strength and linear trend lines for tensile strength of 109 and 39 charges

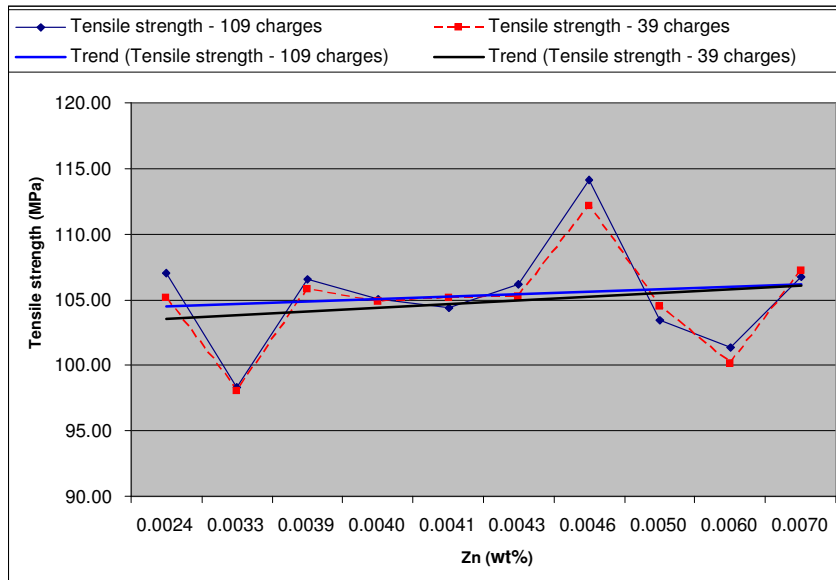


Figure 5.12: Influence of wt% Zn on tensile strength and linear trend lines for tensile strength of 109 and 39 charges

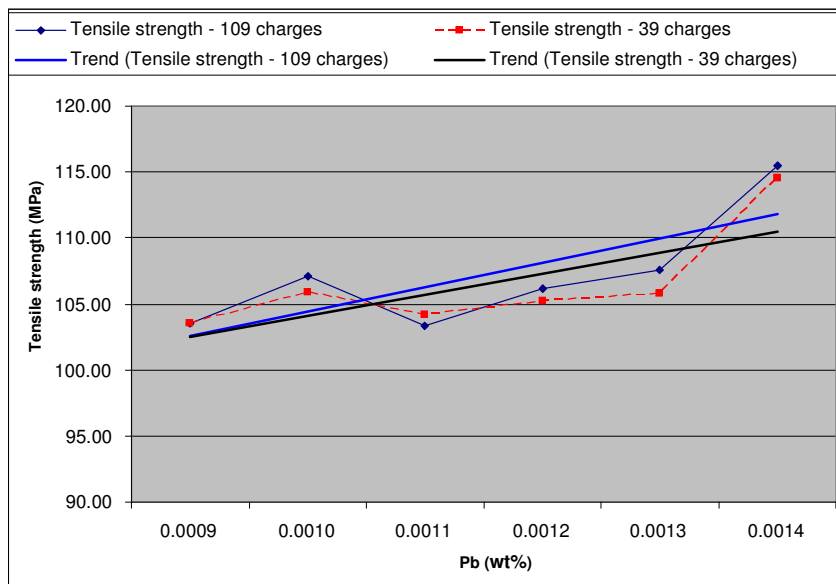


Figure 5.13: Influence of wt% Pb on tensile strength and linear trend lines for tensile strength of 109 and 39 charges

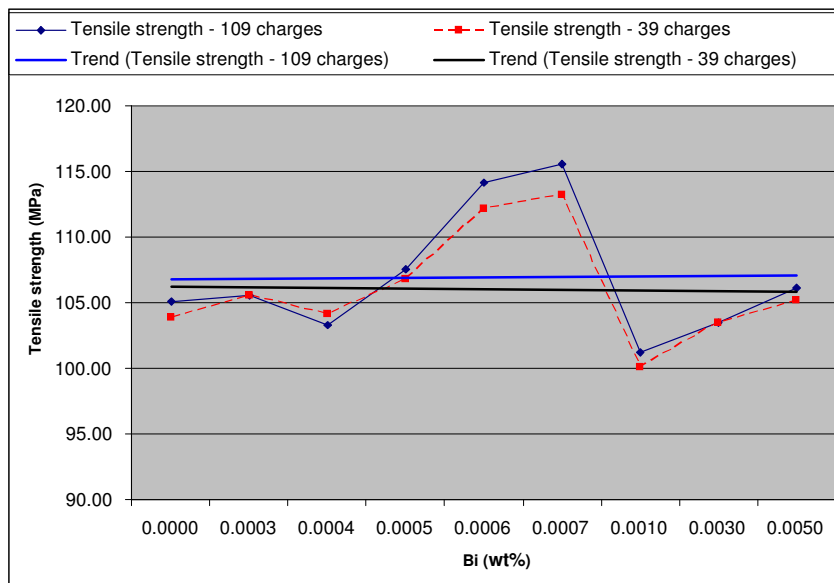


Figure 5.14: Influence of wt% Bi on tensile strength and linear trend lines for tensile strength of 109 and 39 charges

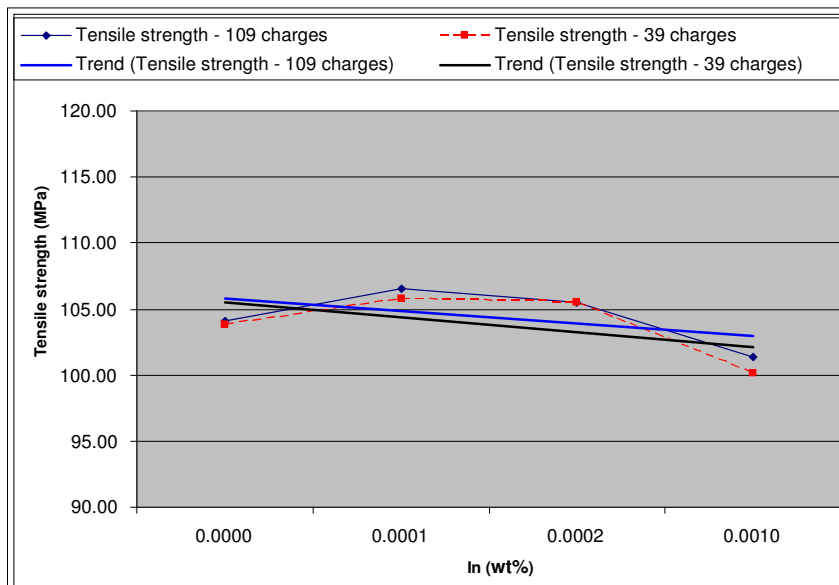


Figure 5.15: Influence of wt% In on tensile strength and linear trend lines for tensile strength of 109 and 39 charges

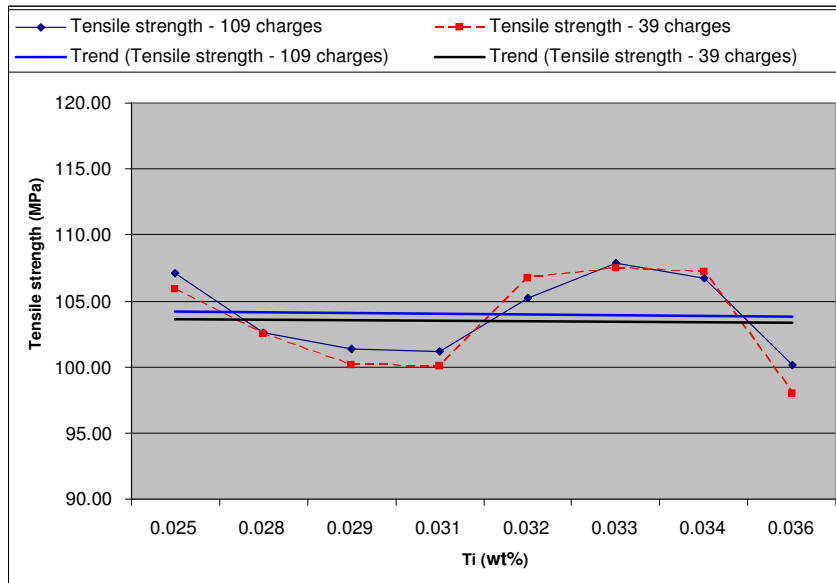


Figure 5.16: Influence of wt% Ti on tensile strength and linear trend lines for tensile strength of 109 and 39 charges

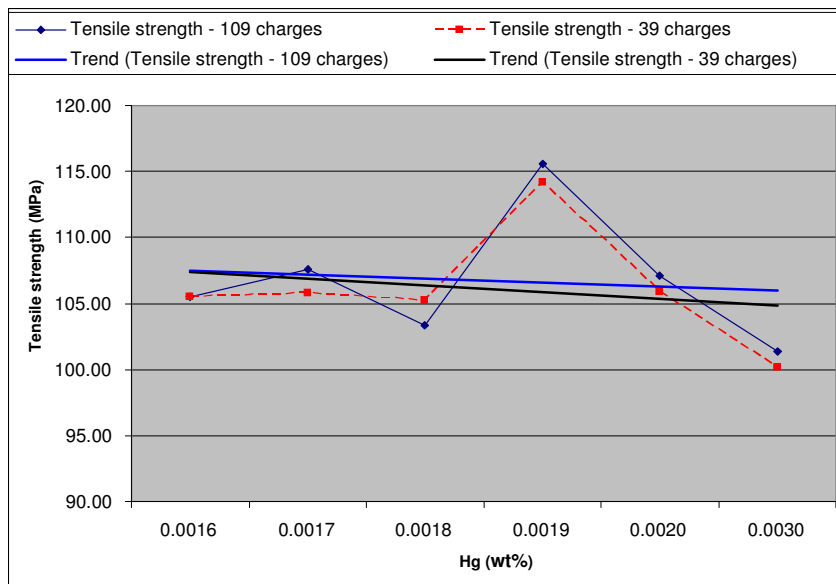


Figure 5.17: Influence of wt% Hg on tensile strength and linear trend lines for tensile strength of 109 and 39 charges

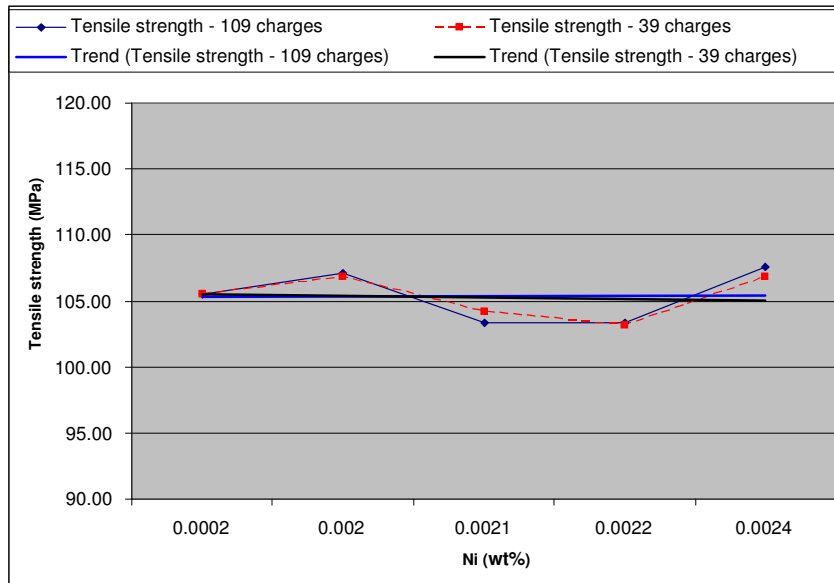


Figure 5.18: Influence of wt% Ni on tensile strength and linear trend lines for tensile strength of 109 and 39 charges

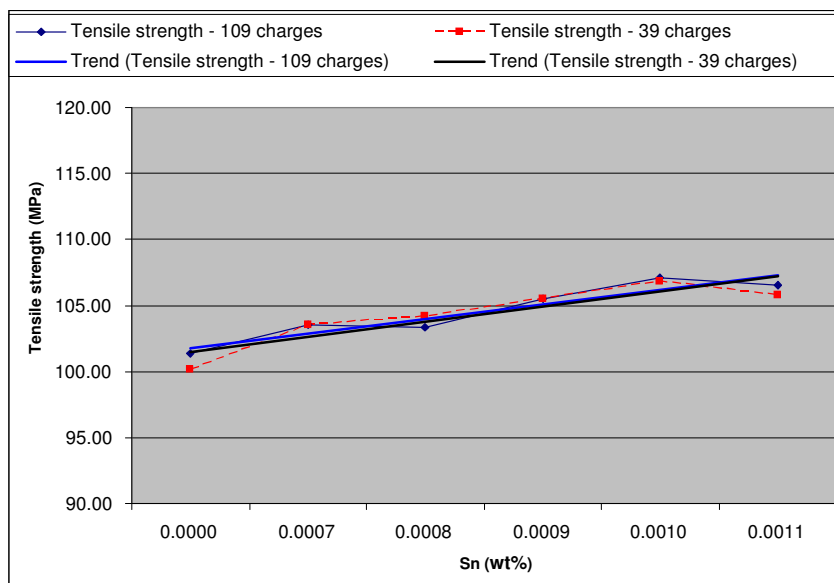


Figure 5.19: Influence of wt% Sn on tensile strength and linear trend lines for tensile strength of 109 and 39 charges

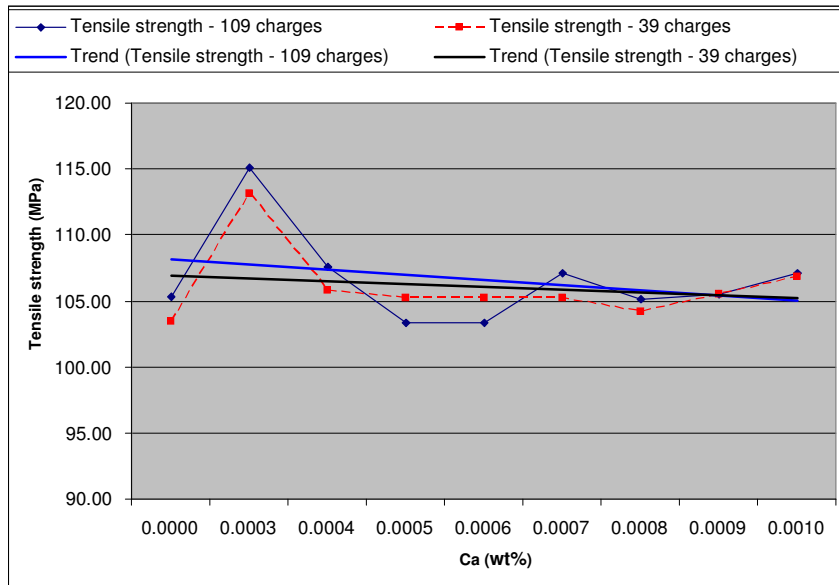


Figure 5.20: Influence of wt% Ca on tensile strength and linear trend lines for tensile strength of 109 and 39 charges

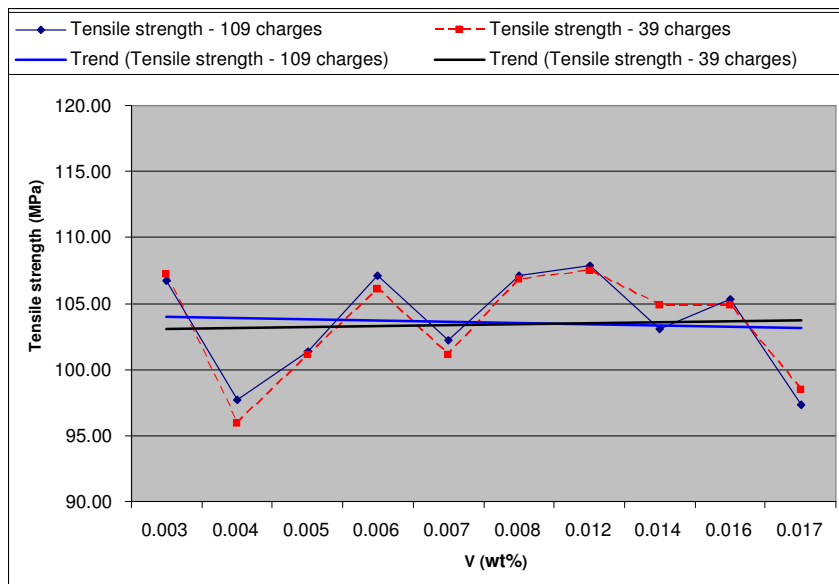


Figure 5.21: Influence of wt% V on tensile strength and linear trend lines for tensile strength of 109 and 39 charges

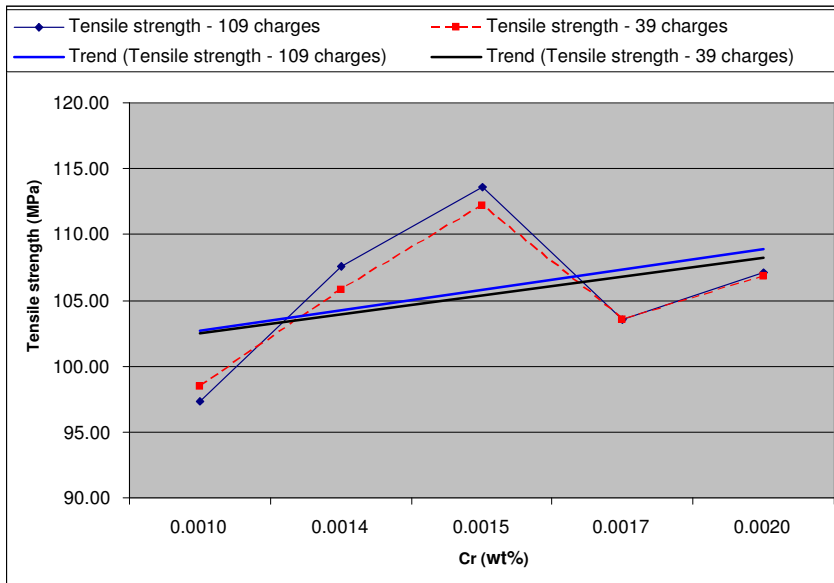


Figure 5.22: Influence of wt% Cr on tensile strength and linear trend lines for tensile strength of 109 and 39 charges

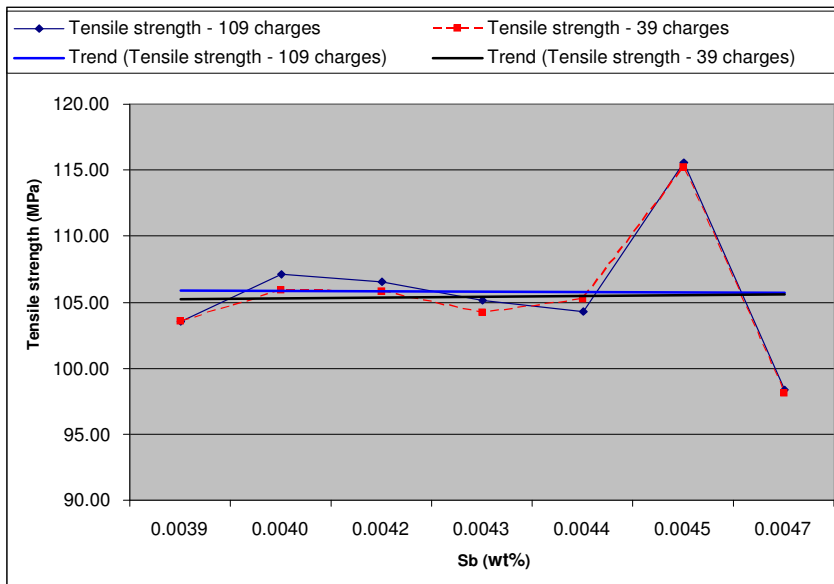


Figure 5.23: Influence of wt% Sb on tensile strength and linear trend lines for tensile strength of 109 and 39 charges

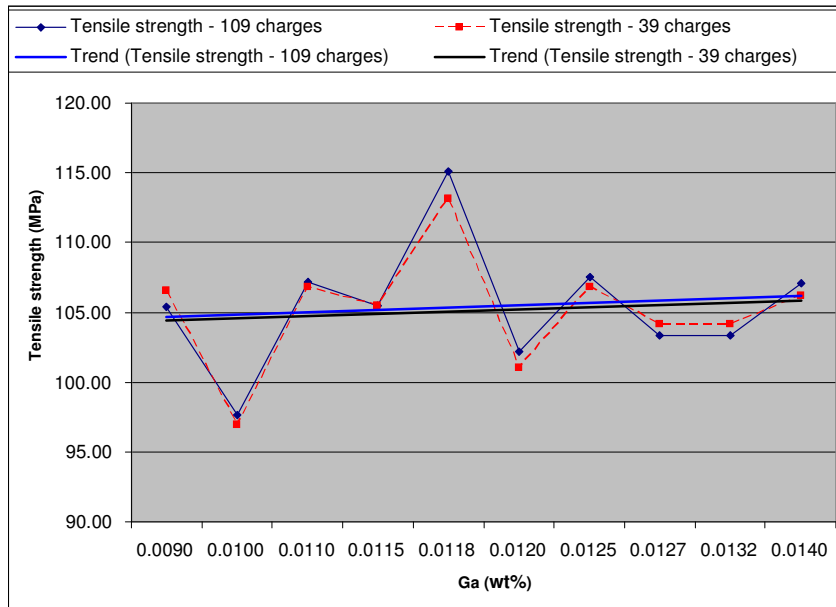


Figure 5.24: Influence of wt% Ga on tensile strength and linear trend lines for tensile strength of 109 and 39 charges

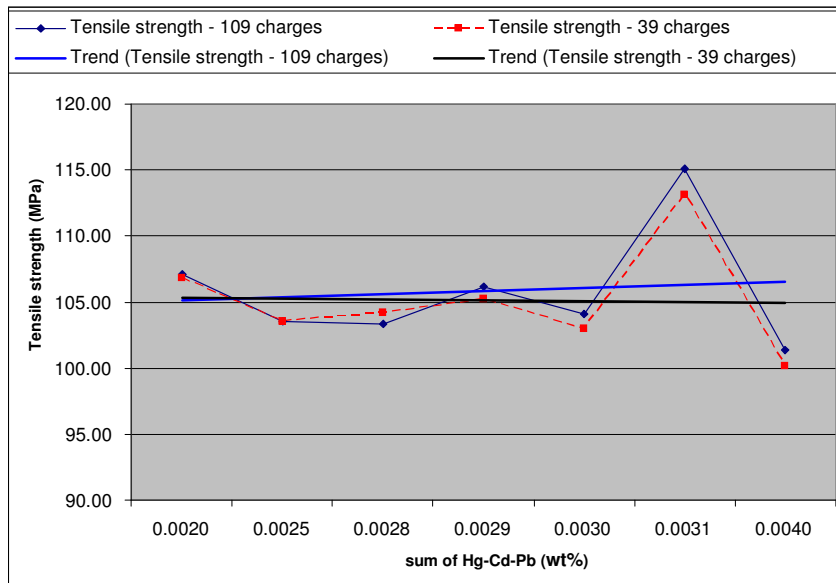


Figure 5.25: Influence of wt% sum of Hg-Cd-Pb on tensile strength and linear trend lines for tensile strength of 109 and 39 charges

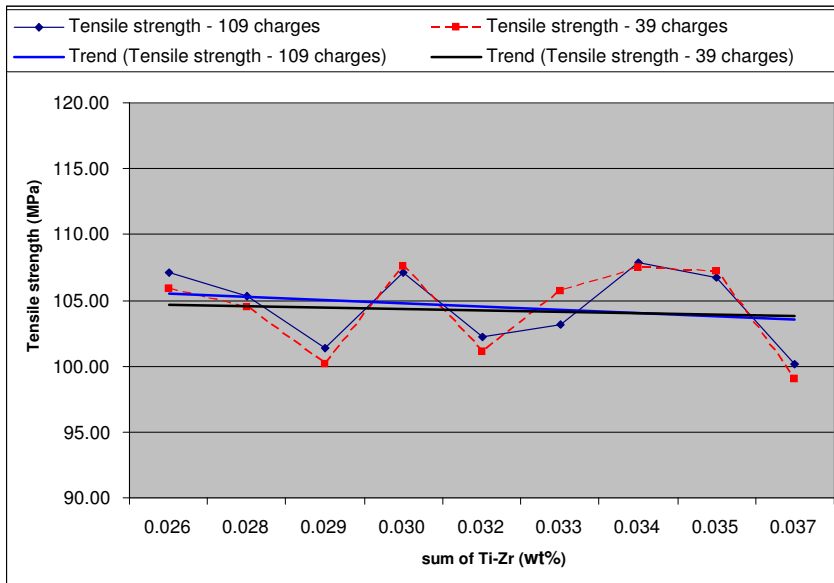


Figure 5.26: Influence of wt% sum of Ti-Zr on tensile strength and linear trend lines for tensile strength of 109 and 39 charges

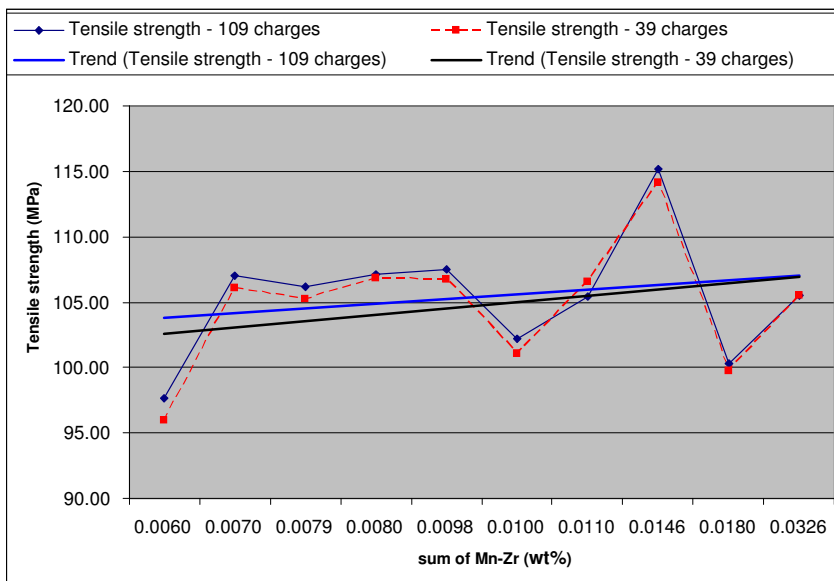


Figure 5.27: Influence of wt% sum of Mn-Zr on tensile strength and linear trend lines for tensile strength of 109 and 39 charges

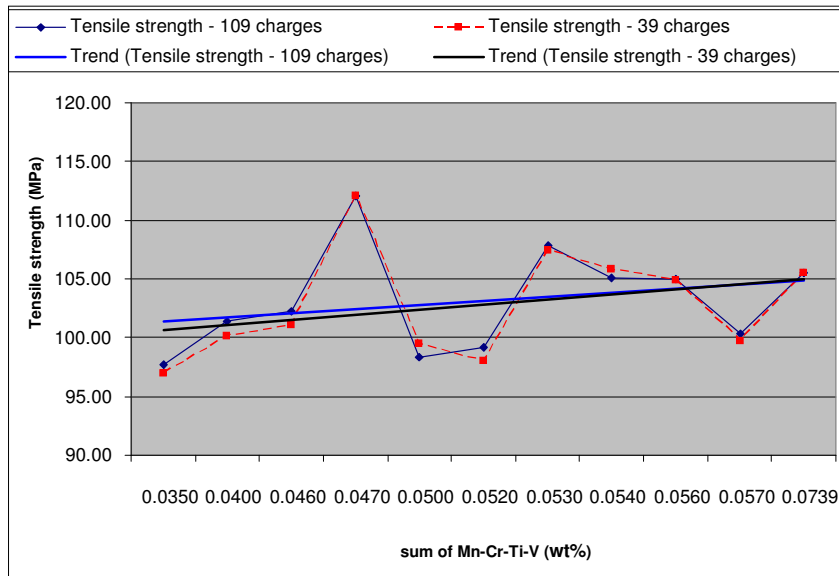


Figure 5.28: Influence of wt% sum of Mn-Cr-Ti-V on tensile strength and linear trend lines for tensile strength of 109 and 39 charges

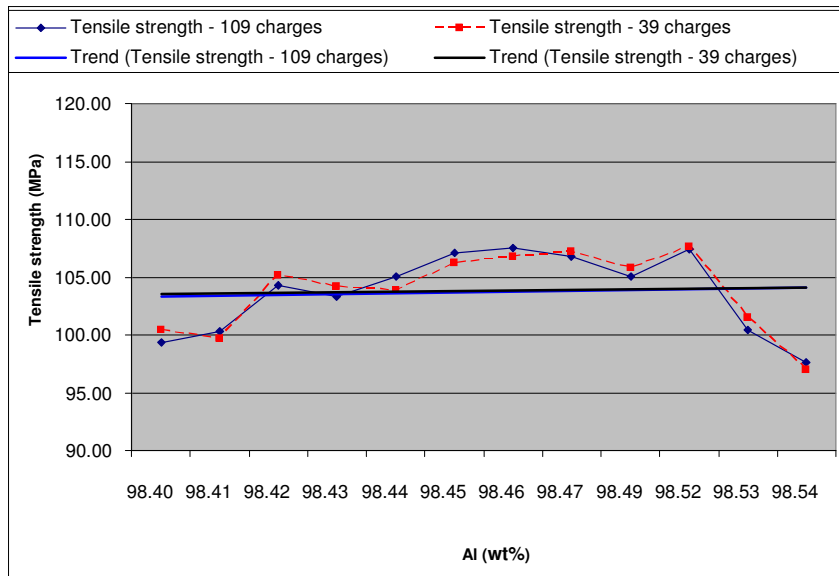


Figure 5.29: Influence of wt% Al on tensile strength and linear trend lines for tensile strength of 109 and 39 charges

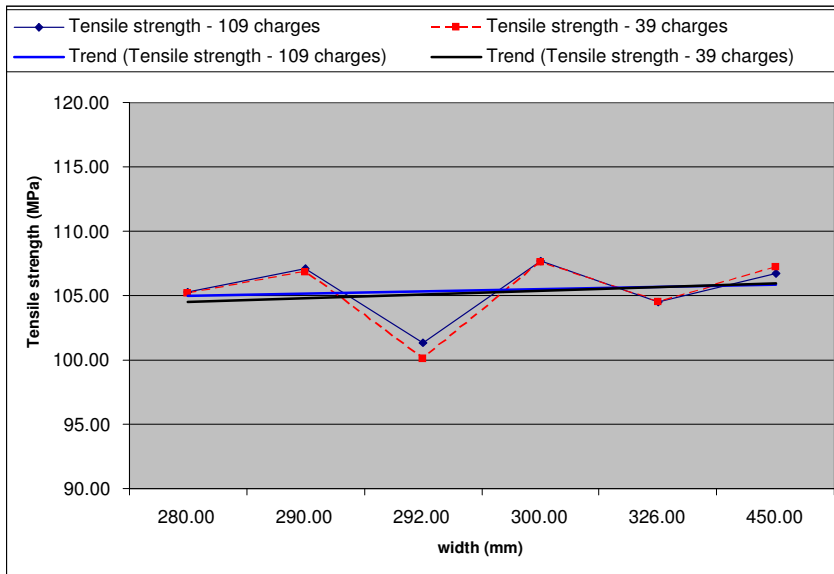


Figure 5.30: Influence of width of the coil on tensile strength and linear trend lines for tensile strength of 109 and 39 charges

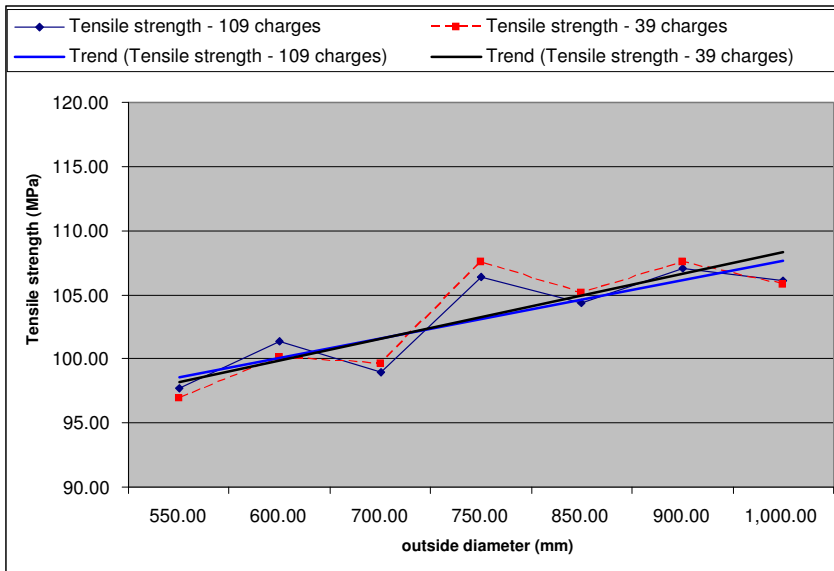


Figure 5.31: Influence of outside diameter of the coil on tensile strength and linear trend lines for tensile strength of 109 and 39 charges

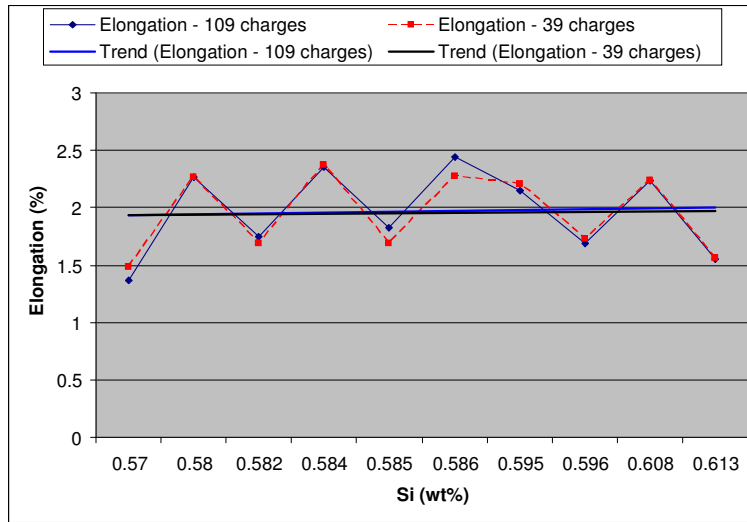


Figure 5.32: Influence of wt% Si on elongation and linear trend lines for elongation of 109 and 26 charges

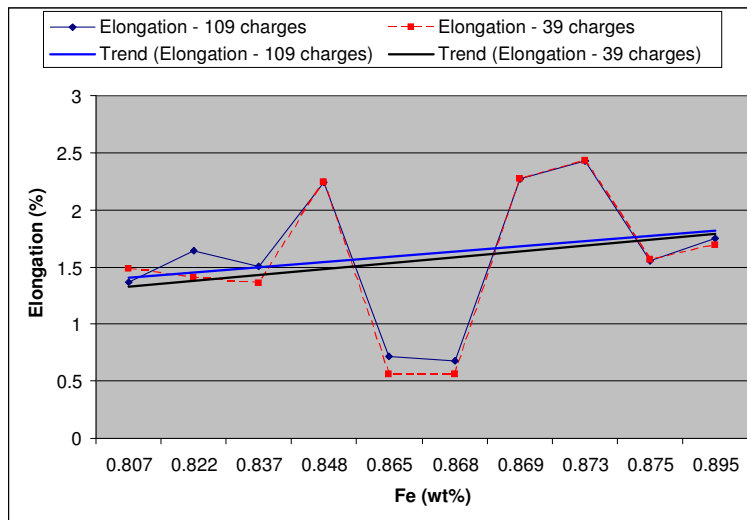


Figure 5.33: Influence of wt% Fe on elongation and linear trend lines for elongation of 109 and 26 charges

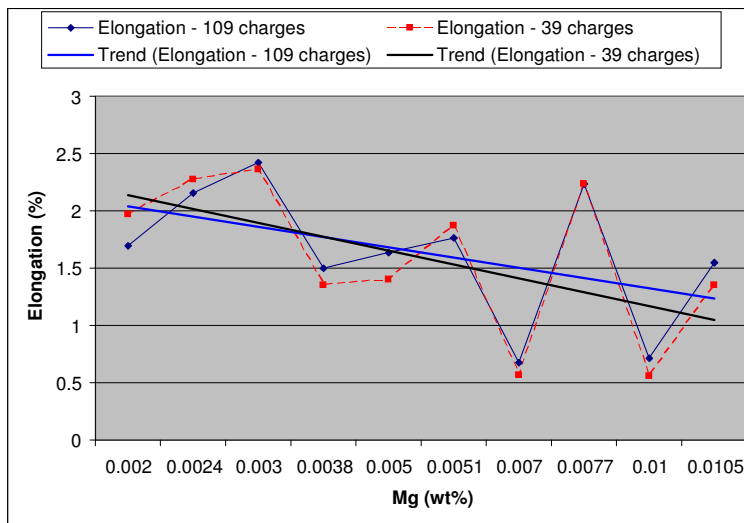


Figure 5.34: Influence of wt% Mg on elongation and linear trend lines for elongation of 109 and 26 charges

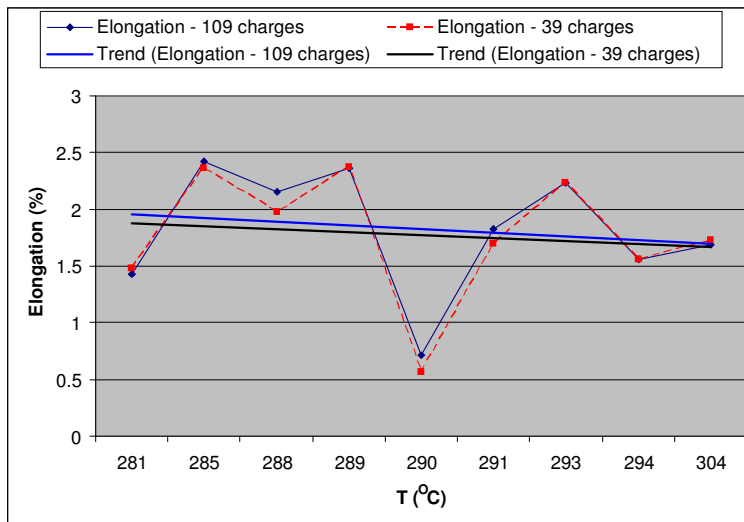


Figure 5.35: Influence of annealing temperature T on elongation and linear trend lines for elongation of 109 and 26 charges

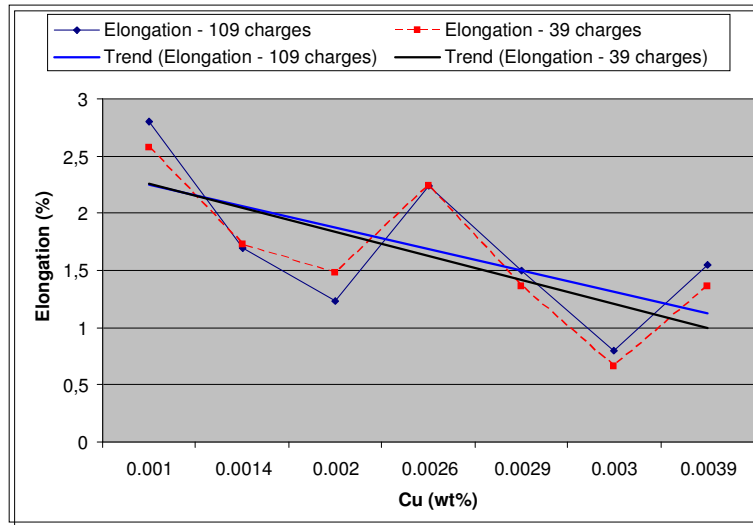


Figure 5.36: Influence of wt% Cu on elongation and linear trend lines for elongation of 109 and 26 charges

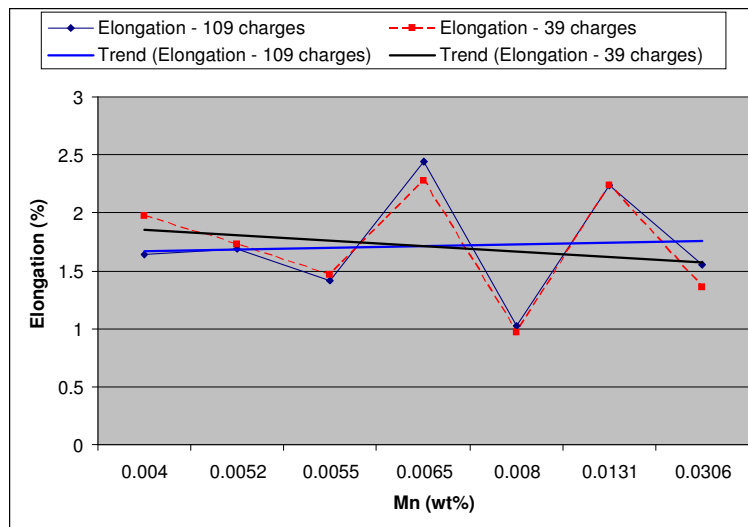


Figure 5.37: Influence of wt% Mn on elongation and linear trend lines for elongation of 109 and 26 charges

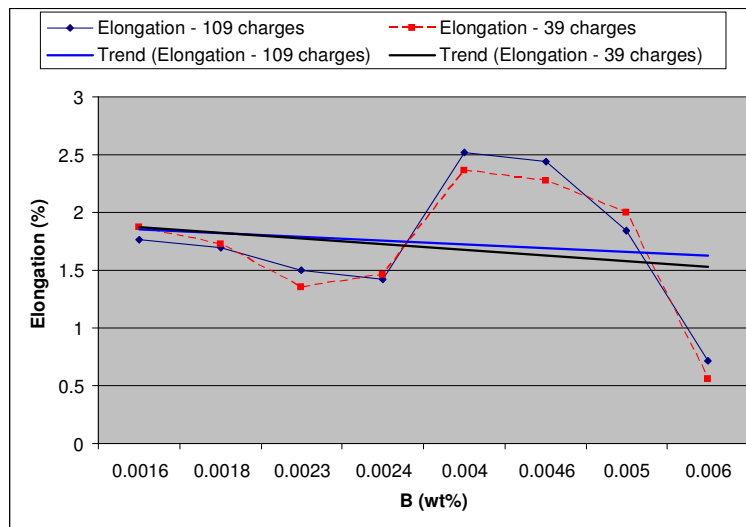


Figure 5.38: Influence of wt% B on elongation and linear trend lines for elongation of 109 and 39 charges

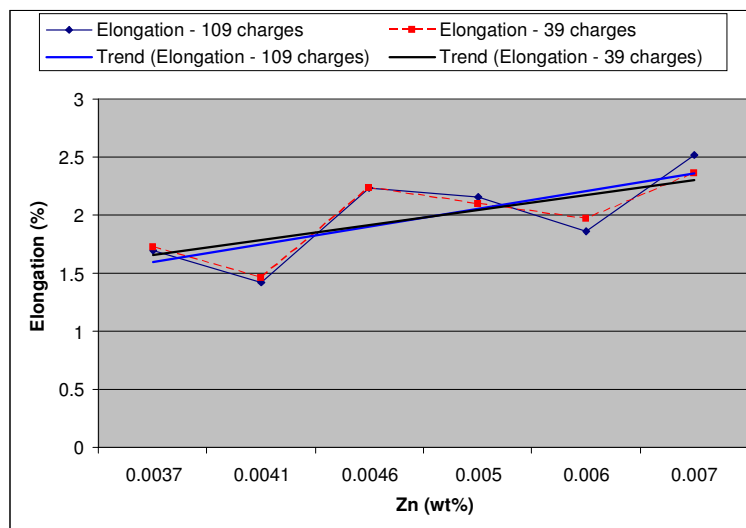


Figure 5.39: Influence of wt% Zn on elongation and linear trend lines for elongation of 109 and 39 charges

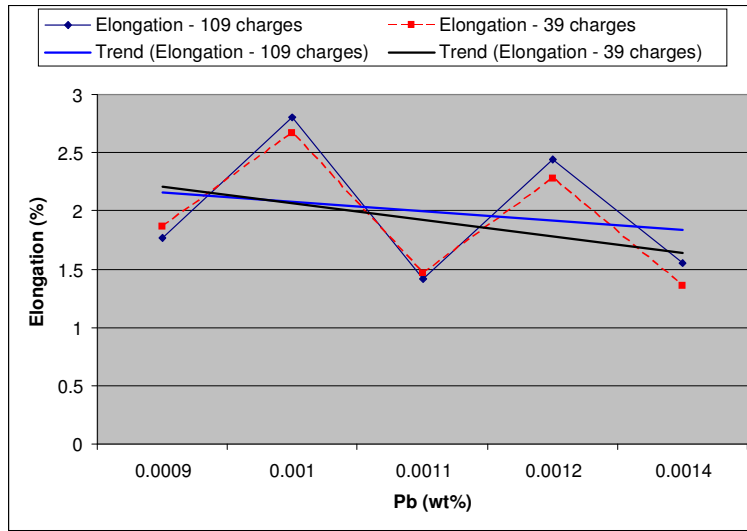


Figure 5.40: Influence of wt% Pb on elongation and linear trend lines for elongation of 109 and 26 charges

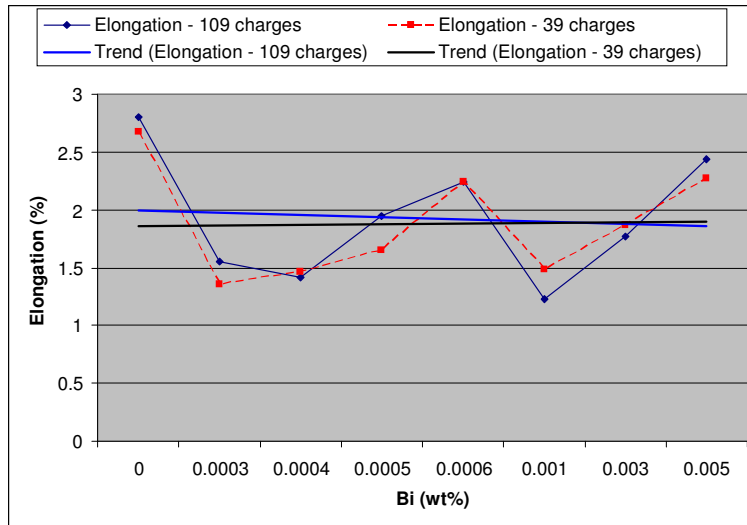


Figure 5.41: Influence of wt% Bi on elongation and linear trend lines for elongation of 109 and 26 charges

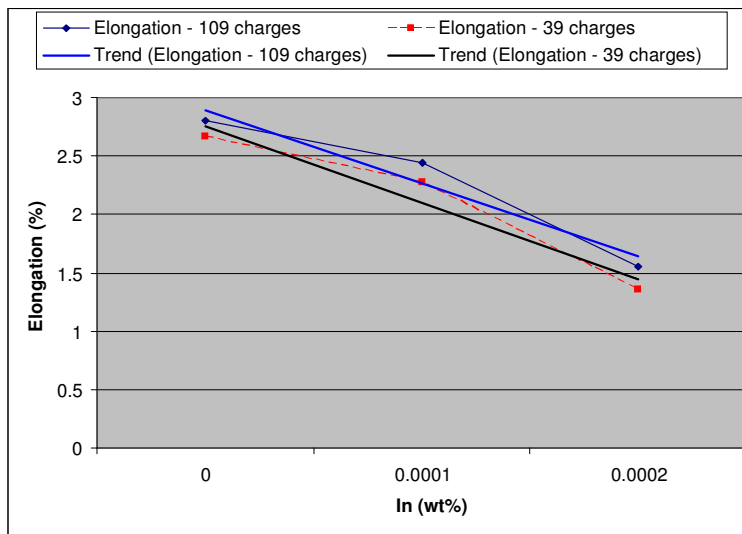


Figure 5.42: Influence of wt% In on elongation and linear trend lines for elongation of 109 and 39 charges

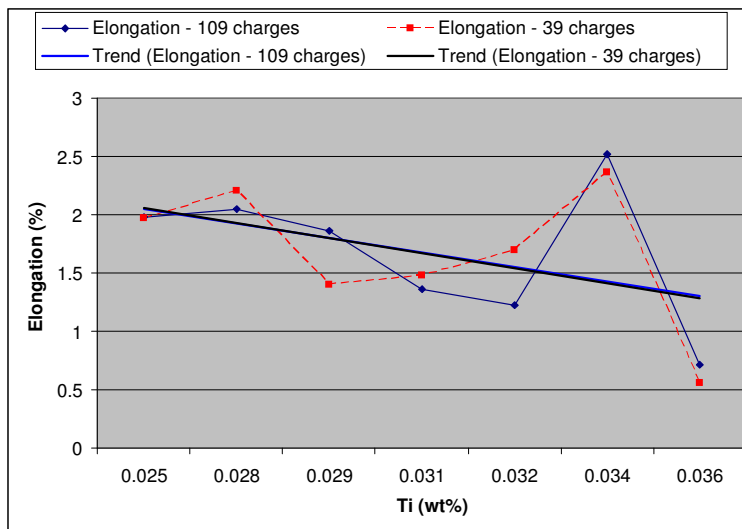


Figure 5.43: Influence of wt% Ti on elongation and linear trend lines for elongation of 109 and 39 charges

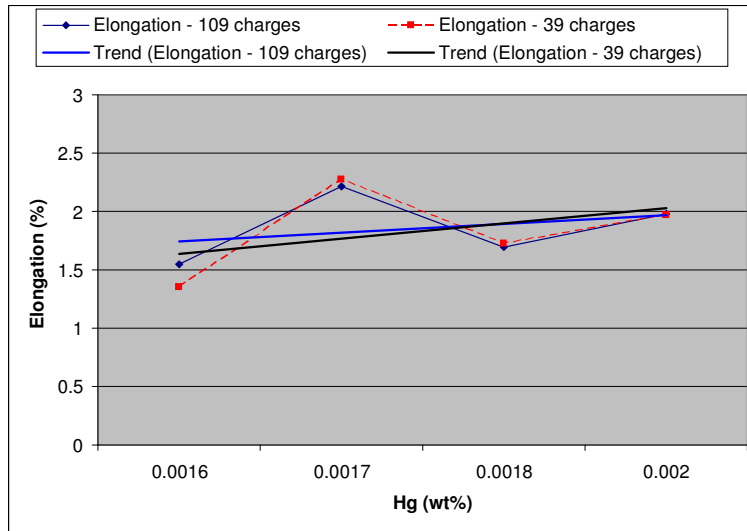


Figure 5.44: Influence of wt% Hg on elongation and linear trend lines for elongation of 109 and 26 charges

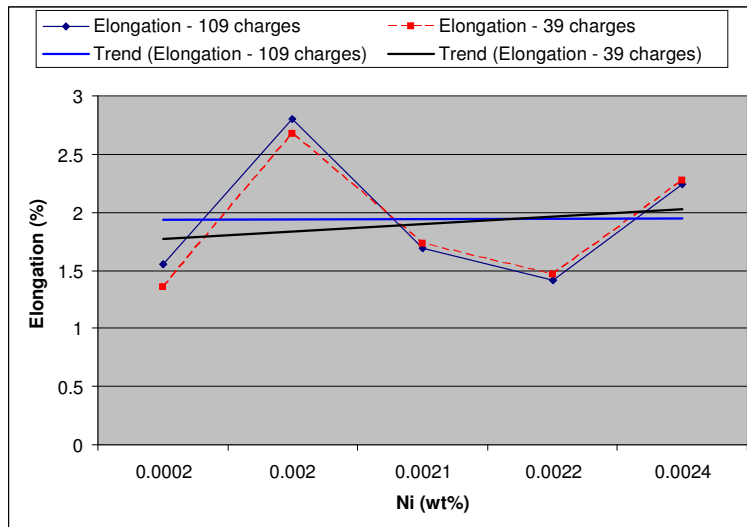


Figure 5.45: Influence of wt% Ni on elongation and linear trend lines for elongation of 109 and 26 charges

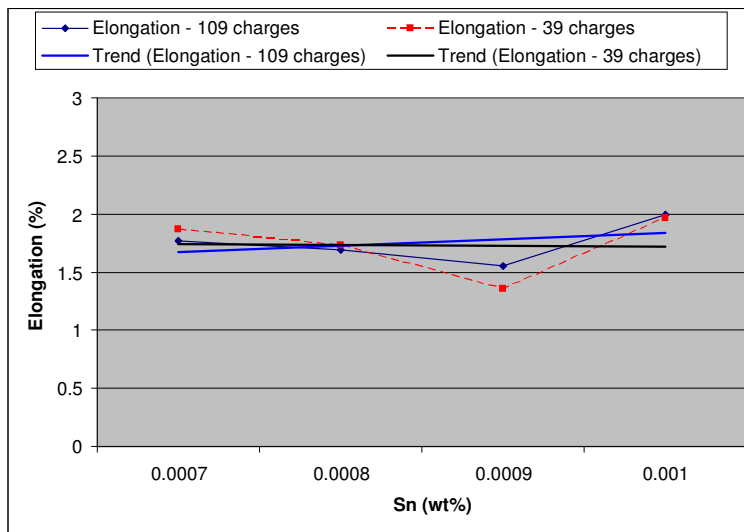


Figure 5.46: Influence of wt% Sn on elongation and linear trend lines for elongation of 109 and 39 charges

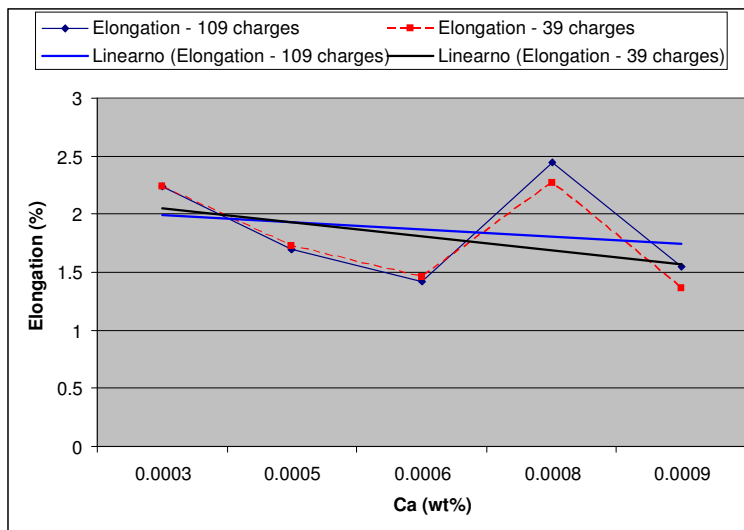


Figure 5.47: Influence of wt% Ca on elongation and linear trend lines for elongation of 109 and 39 charges

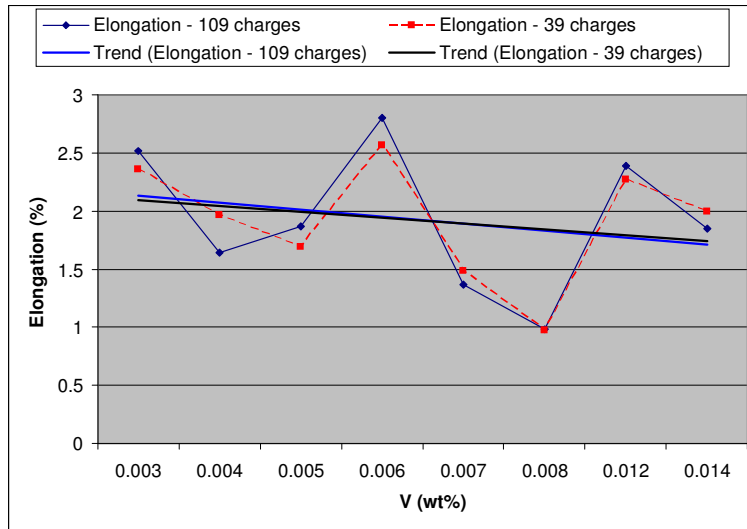


Figure 5.48: Influence of wt% V on elongation and linear trend lines for elongation of 109 and 26 charges

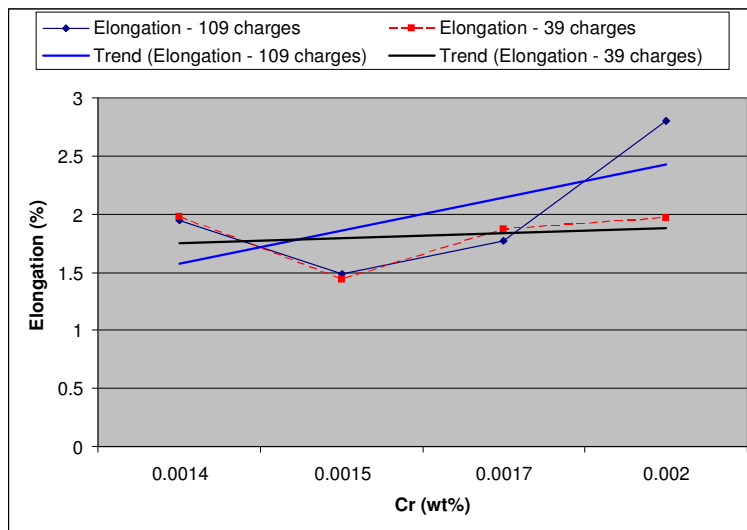


Figure 5.49: Influence of wt% Cr on elongation and linear trend lines for elongation of 109 and 26 charges

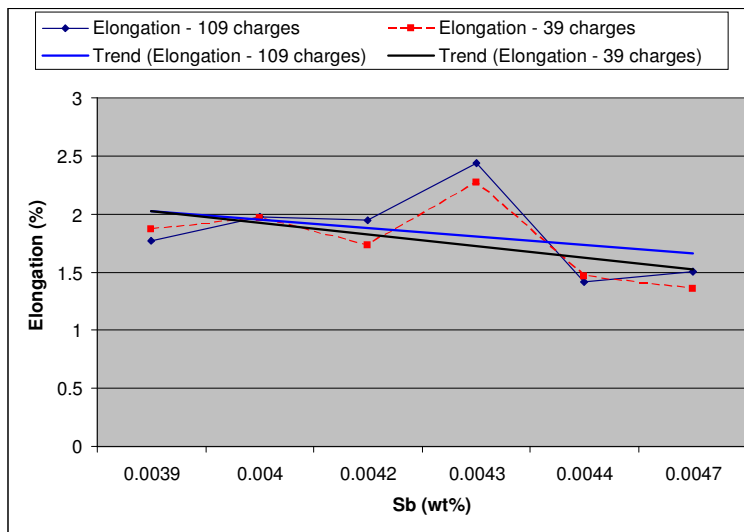


Figure 5.50: Influence of wt% Sb on elongation and linear trend lines for elongation of 109 and 39 charges

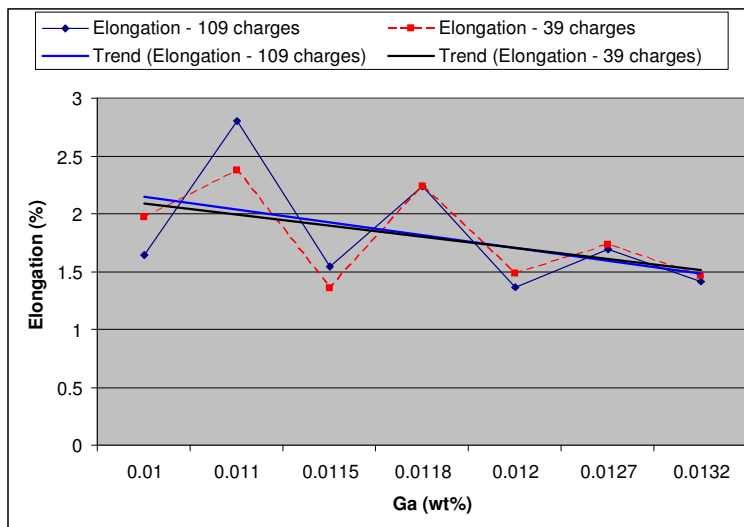


Figure 5.51: Influence of wt% Ga on elongation and linear trend lines for elongation of 109 and 39 charges

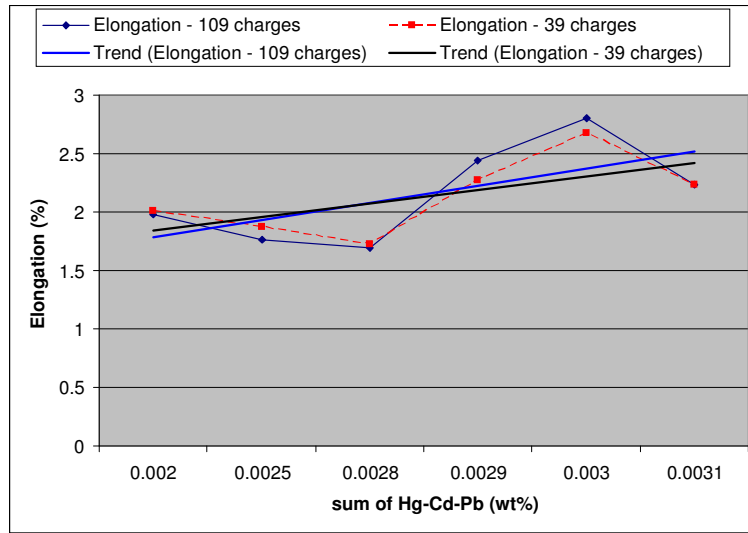


Figure 5.52: Influence of wt% sum of Hg-Cd-Pb on elongation and linear trend lines for elongation of 109 and 26 charges

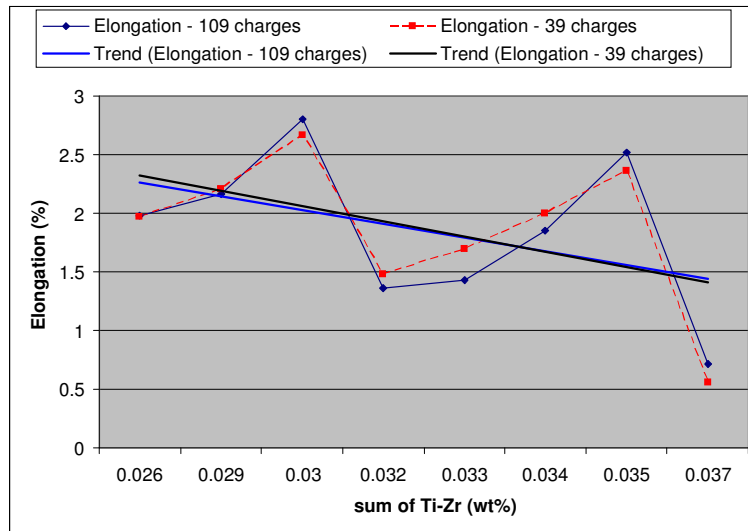


Figure 5.53: Influence of wt% sum of Ti-Zr on elongation and linear trend lines for elongation of 109 and 26 charges

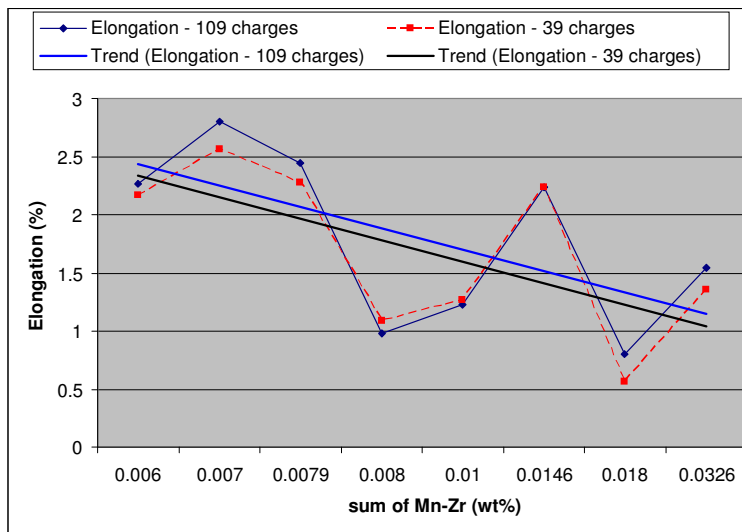


Figure 5.54: Influence of wt% sum of Mn-Zr on elongation and linear trend lines for elongation of 109 and 26 charges

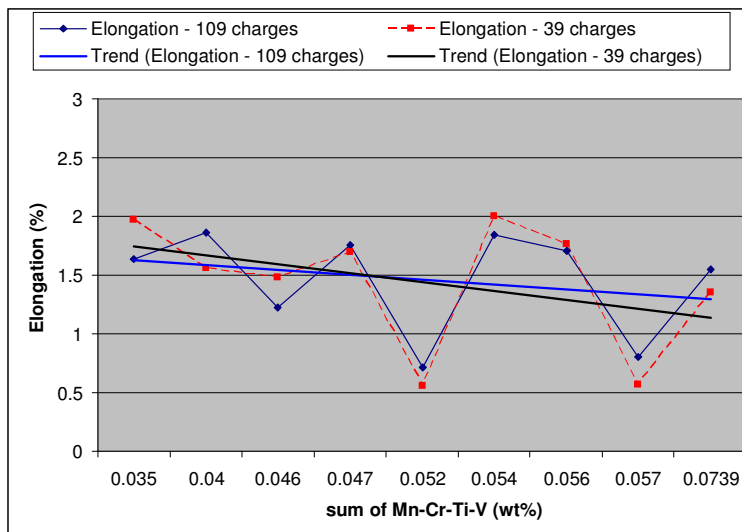


Figure 5.55: Influence of wt% sum of Mn-Cr-Ti-V on elongation and linear trend lines for elongation of 109 and 26 charges

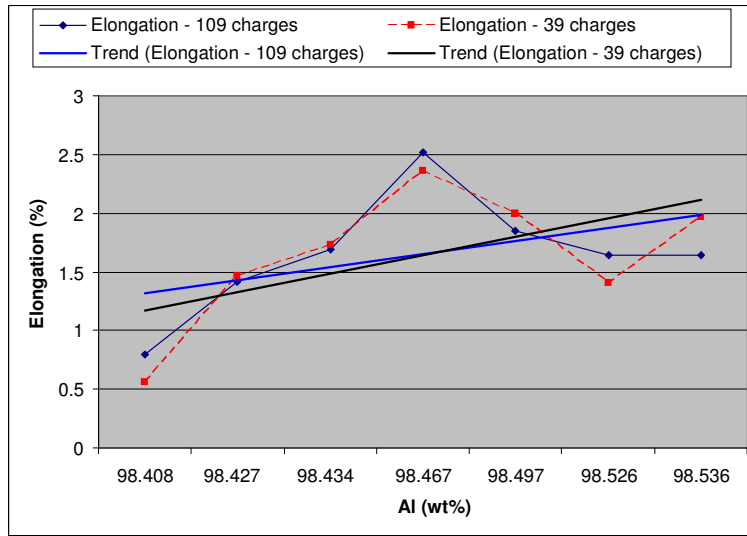


Figure 5.56: Influence of wt% Al on elongation and linear trend lines for elongation of 109 and 26 charges

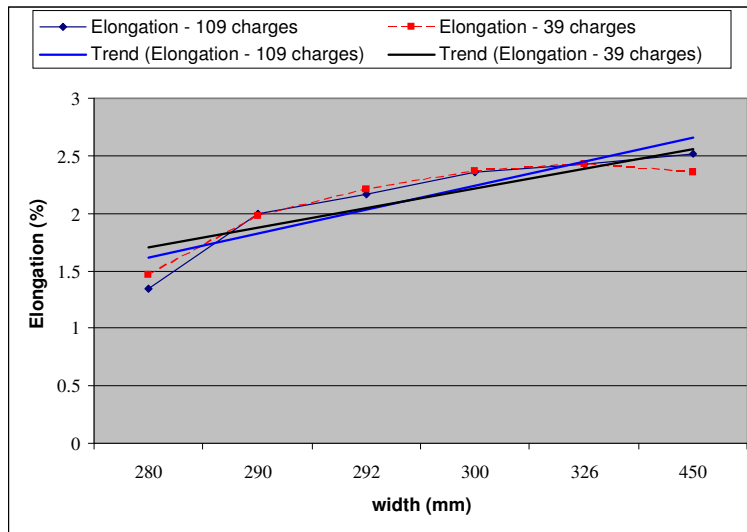


Figure 5.57: Influence of width of the coil on elongation and linear trend lines for elongation of 109 and 26 charges

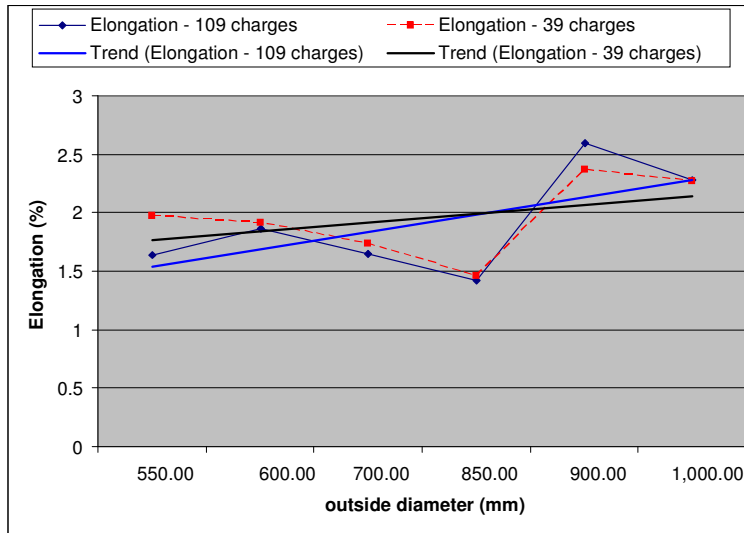


Figure 5.58: Influence of outside diameter of the coil on elongation and linear trend lines for elongation of 109 and 26 charges

5.2 Discussion of the results

Figure 5.5 depicts a slight drop of tensile strength with increase of the wt% Si.

Figure 5.6 depicts a slight increase of tensile strength with increase of the wt% Fe.

Figure 5.7 depicts insensitivity of the tensile strength with wt% Mg on the observed range of Mg variation.

Figure 5.8 depicts insensitivity of the tensile strength with annealing temperature in the range from 276 - 304 °C.

Figure 5.9 depicts decrease of the tensile strength with increase of wt% Cu.

Figure 5.10 depicts increase of the tensile strength with increase of the wt% Mn.

Figure 5.11 depicts decrease of the tensile strength with increase of wt% B.

Figure 5.12 depicts insensitivity of the tensile strength with wt% Zn on the observed range of Zn variation.

Figure 5.13 depicts increase of the tensile strength with increase of wt% Pb.

Figure 5.14 depicts insensitivity of the tensile strength with increase of the wt% Bi on the observed range of Bi variation.

Figure 5.15 depicts decrease of the tensile strength with increase of the wt% In.

Figure 5.16 depicts insensitivity of the tensile strength with increase of the wt% Ti on the observed range of Ti variation.

Figure 5.17 depicts insensitivity of the tensile strength with increase of the wt% Hg on the observed range of Hg variation.

Figure 5.18 depicts insensitivity of the tensile strength with increase of the wt% Ni on the observed range of Ni variation.

Figure 5.19 depicts increase of the tensile strength with increase of the wt% Sn.

Figure 5.20 depicts decrease of the tensile strength with increase of the wt% Ca.

Figure 5.21 depicts insensitivity of the results with increase of wt% V on the observed range of V variation.

Figure 5.22 depicts increase of the tensile strength with increase of the wt% Cr.

Figure 5.23 depicts insensitivity of the tensile strength with increase of the wt% Sb on the observed range of Sb variation.

Figure 5.24 depicts insensitivity of the tensile strength with increase of the wt% Ga on the observed range of Ga variation.

Figure 5.25 depicts insensitivity of the tensile strength with the increase of the wt% sum of Hg-Cd-Pb.

Figure 5.26 depicts decrease of the tensile strength with the increase of the wt% sum of Ti-Zr.

Figure 5.27 depicts increase of the tensile strength with the increase of the wt% sum of Mn-Zr.

Figure 5.28 depicts increase of the tensile strength with the increase of the wt% sum of Mn-Cr-Ti-V.

Figure 5.29 depicts insensitivity of the tensile strength with the increase of the wt% Al on the observed range of Al variation.

Figure 5.30 depicts insensitivity of the tensile strength with the increase of the coil width on the observed coil width variation.

Figure 5.31 depicts increase of the tensile strength with increase of the diameter of the coil.

Figure 5.32 depicts insensitivity of elongation with increase of the wt% Si on the observed range of the Si variation.

Figure 5.33 depicts a slight increase of the elongation with increase of the wt% Fe.

Figure 5.34 depicts decrease of elongation with increase of wt% Mg.

Figure 5.35 depicts slight decrease of the elongation with annealing temperature in the range from 281 - 304 °C.

Figure 5.36 depicts decrease of the elongation with increase of wt% Cu.

Figure 5.37 depicts insensitivity of the elongation with increase of the wt% Mn in the range of the Mn variation.

Figure 5.38 depicts decrease of the elongation with increase of wt% B.

Figure 5.39 depicts increase of the elongation with wt% Zn.

Figure 5.40 depicts decrease of the elongation with increase of wt% Pb.

Figure 5.41 depicts insensitivity of the elongation with increase of the wt% Bi on the observed range of Bi variation.

Figure 5.42 depicts decrease of the elongation with increase of the wt% In.

Figure 5.43 depicts decrease of the elongation with increase of the wt% Ti.

Figure 5.44 depicts increase of the elongation with increase of the wt% Hg.

Figure 5.45 depicts insensitivity of the elongation with increase of the wt% Ni on the observed range of Ni variation.

Figure 5.46 depicts insensitivity of the elongation with increase of the wt% Sn on the observed range of Sn variation.

Figure 5.47 depicts decrease of the elongation with increase of the wt% Ca.

Figure 5.48 depicts decrease of the elongation with increase of wt% V.

Figure 5.49 depicts increase of the elongation with increase of the wt% Cr.

Figure 5.50 depicts decrease of the elongation with decrease of the wt% Sb.

Figure 5.51 depicts decrease of the elongation with increase of the wt% Ga.

Figure 5.52 depicts increase of the elongation with increase of the wt% sum of Hg-Cd-Pb.

Figure 5.53 depicts decrease of the elongation with the increase of the wt% sum of Ti-Zr.

Figure 5.54 depicts decrease of the elongation with the increase of the wt% sum of Mn-Zr.

Figure 5.55 depicts decrease of the elongation with the increase of the wt% sum of Mn-Cr-Ti-V.

Figure 5.56 depicts increase of the elongation with the increase of the wt% Al.

Figure 5.57 depicts increase of the elongation with the increase of the coil width.

Figure 5.58 depicts increase of the elongation with increase of the diameter of the coil.

In Table 5.1, we summarize the trend coefficients (K), which show influence of individual process parameters on the tensile strength. Trend coefficients are calculated for all process parameters Si, Fe, Mg, Cu, Mn, B, Zn, Pb, Bi, In, Ti, Hg, Ni, Sn, Ca, V, Cr, Sb, Ga, sum of Hg-Cd-Pb, sum of Ti-Zr, sum of Mn-Zr, sum of Mn-Cr-Ti-V, width of the coil, outside diameter of the coil and annealing temperature T .

The "Coverage" column represents the ratio between the difference of the maximum and the minimum process parameters found in the history data and the respective bounds, prescribed by the internal standard of the Impol company. It can be seen that in the case of tensile strength, the most covered historical data are with respect to Mn, and the least are with respect to Pb (Table 5.1) and that in the case of elongation the most covered historical data are with respect to Mn, and the least are with respect to In (Table 5.2).

Table 5.1: Trend coefficients, which show influence of individual process parameters on tensile strength. Mn has **minimum influence** and Cr has **maximum influence** on increase of the tensile strength. Ti has **minimum influence** and Si has **maximum influence** on decrease of the tensile strength.

Process parameter	Min. (ANN training values)	Max. (ANN training values)	Coverage (%)	L1 Norm (Mpa)	L2 Norm (Mpa)	K	
Al (wt%)	98.40	98.54	6.80	2.7534	0.9383	0.0460	Mpa/%
Si (wt%)	0.5590	0.6250	66.00	3.4819	1.2329	-0.2523	Mpa/%
Fe (wt%)	0.8280	0.8960	68.00	3.4105	1.2956	0.5891	Mpa/%
Mg (wt%)	0.0020	0.0105	17.00	2.4722	1.1420	0.2679	Mpa/%
Cu (wt%)	0.0010	0.0056	9.20	3.6504	1.5827	-0.3620	Mpa/%
Mn (wt%)	0.0040	0.0306	120.91	3.3618	1.2033	0.3994	Mpa/%
B (wt%)	0.0016	0.0060	44.00	2.5432	1.0896	-0.3174	Mpa/%
Zn (wt%)	0.0024	0.0070	9.20	2.3725	1.1369	0.2911	Mpa/%
Pb (wt%)	0.0009	0.0014	1.00	2.6692	1.5018	1.5958	Mpa/%
Bi (wt%)	0.0000	0.0050	10.00	3.1063	1.3164	-0.0417	Mpa/%
In (wt%)	0.0000	0.0010	2.00	1.8539	1.1322	-1.1516	Mpa/%
Ti (wt%)	0.0250	0.0360	44.00	3.3122	1.2457	-0.0305	Mpa/%
Hg (wt%)	0.0016	0.0030	2.80	2.6926	1.6880	-0.5091	Mpa/%
Ni (wt%)	0.0002	0.0024	4.40	1.2973	0.6452	-0.1133	Mpa/%
Sn (wt%)	0.0000	0.0011	2.20	1.7269	0.8887	1.1364	Mpa/%
Ca (wt%)	0.0000	0.0010	50.00	1.7551	0.8882	-0.2094	Mpa/%
V (wt%)	0.0030	0.0170	28.00	3.3911	1.2027	0.0753	Mpa/%
Cr (wt%)	0.0010	0.0020	50.00	3.4945	1.9957	1.4492	Mpa/%
Sb (wt%)	0.0039	0.0047	1.60	3.0412	1.7800	0.0596	Mpa/%
Ga (wt%)	0.0090	0.0140	10.00	2.8415	1.2604	0.1538	Mpa/%
Hg-Cd-Pb (wt%)	0.0020	0.0040	1.33	2.8014	1.4356	-0.0775	Mpa/%
Ti-Zr (wt%)	0.0260	0.0370	7.33	2.8015	1.0489	-0.1036	Mpa/%
Mn-Zr (wt%)	0.0060	0.0326	17.73	3.5357	1.4826	0.4822	Mpa/%
Mn-Cr-Ti-V (wt%)	0.0350	0.0739	25.93	3.9283	1.3357	0.4386	Mpa/%
T (°C)	276.0	304.0	280.00	2.7268	1.0292	0.0113	Mpa/°C
width (mm)	280.00	450.00	100.00	1.9784	1.0384	0.2997	Mpa/mm
Outside diameter (mm)	550.0	1000.0	100.00	3.7423	1.5006	1.6835	Mpa/mm

The increase of tensile strength is mostly influenced by the chemical element Cr, and it is least influenced by the chemical element Mn. The decrease of tensile strength with respect to alloy composition is mostly influenced by the chemical element Si, and it is least influenced by the chemical element Ti.

In Table 5.2, we summarize the trend coefficients, which show influence of individual process parameters on elongation. The trend coefficients are calculated for all process parameters Si, Fe, Mg, Cu, Mn, B, Zn, Pb, Bi, In, Ti,

Hg, Ni, Sn, Ca, V, Cr, Sb, Ga, sum of Hg-Cd-Pb, sum of Ti-Zr, sum of Mn-Zr, sum of Mn-Cr-Ti-V, width of the coil, outside diameter of the coil and annealing temperature T.

Table 5.2: Trend coefficients, which show influence of individual process parameters on elongation. Si has **minimum influence** and Fe has **maximum influence** on increase of the elongation. Mn has **minimum influence** and Ti has **maximum influence** on decrease of the elongation.

Process parameter	Min. (ANN training values)	Max. (ANN training values)	Coverage (%)	L1 Norm (Mpa)	L2 Norm (Mpa)	K	
Al (wt%)	98.41	98.54	6.40	0.4267	0.2025	0.1564	%/%
Si (wt%)	0.5700	0.6130	43.00	0.3200	0.1041	0.0045	%/%
Fe (wt%)	0.8070	0.8950	88.00	0.4813	0.1946	0.0509	%/%
Mg (wt%)	0.0020	0.0105	17.00	0.5464	0.1988	-0.1212	%/%
Cu (wt%)	0.0010	0.0039	5.80	0.4725	0.2199	-0.2107	%/%
Mn (wt%)	0.0040	0.0306	120.91	0.3882	0.1696	-0.0472	%/%
B (wt%)	0.0016	0.0060	44.00	0.4308	0.1916	-0.0495	%/%
Zn (wt%)	0.0037	0.0070	6.60	0.2561	0.1244	0.1298	%/%
Pb (wt%)	0.0009	0.0014	1.00	0.4363	0.2207	-0.1425	%/%
Bi (wt%)	0.0000	0.0050	10.00	0.3883	0.1563	0.0050	%/%
In (wt%)	0.0000	0.0002	0.40	0.4955	0.3177	-0.6573	%/%
Ti (wt%)	0.0250	0.0360	44.00	0.4448	0.2114	-0.1299	%/%
Hg (wt%)	0.0016	0.0020	0.80	0.2892	0.1676	0.1301	%/%
Ni (wt%)	0.0002	0.0024	4.40	0.4587	0.2235	0.0621	%/%
Sn (wt%)	0.0007	0.0010	0.60	0.1887	0.1165	-0.0067	%/%
Ca (wt%)	0.0003	0.0009	30.00	0.3550	0.1710	-0.1223	%/%
V (wt%)	0.0030	0.0140	22.00	0.3985	0.1715	-0.0509	%/%
Cr (wt%)	0.0014	0.0020	30.00	0.1868	0.1098	0.0428	%/%
Sb (wt%)	0.0039	0.0047	1.60	0.2608	0.1258	-0.1014	%/%
Ga (wt%)	0.0100	0.0132	6.40	0.3359	0.1403	-0.0959	%/%
Hg-Cd-Pb (wt%)	0.0020	0.0031	0.73	0.2624	0.1256	0.1171	%/%
Ti-Zr (wt%)	0.0260	0.0370	7.33	0.4666	0.2134	-0.1299	%/%
Mn-Zr (wt%)	0.0060	0.0326	17.73	0.6219	0.2358	-0.1857	%/%
Mn-Cr-Ti-V (wt%)	0.0350	0.0739	25.93	0.4074	0.1693	-0.0764	%/%
T (°C)	280.0	304.0	240.00	0.4122	0.1653	-0.0260	%/°C
width (mm)	280.0	450.0	100.00	0.2776	0.1370	0.1718	%/mm
outside diameter (mm)	550.0	1000.0	100.00	0.2501	0.1251	0.0742	%/mm

The increase of elongation is mostly influenced by the chemical element Fe, and it is least influenced by the chemical element Si. The decrease of elongation is mostly influenced by the chemical element Ti, and it is least influenced by the chemical element Mn.

For tensile strength and elongation, the following expert knowledge rules are in use at the Impol company:

- larger concentration of chemical element Fe enlarges tensile strength
- elongation is inversely proportional to tensile strength; greater tensile strength means lower elongation

We verified how the obtained data on the basis of learned neural networks complies with these rules. The results are as follows:

For tensile strength R_m (MPa)

- Trend coefficient for process parameter Fe is 0.5891 MPa/%, which means that tensile strength increases when increasing the concentration of chemical element Fe. This is in accordance with the expert knowledge.

For elongation A (%)

- Trend coefficient for process parameter Fe is 0.0509 %/%, which means that, based on the data, elongation slowly increases by increasing the concentration of chemical element Fe. This finding is not in line with the common expert perception of the behavior.

The tensile strength and elongation depend on many parameters. It is therefore difficult to give an engineering estimate about reasonability of all of the calculated trend coefficients.

The tool was first of all used to demonstrate the methodology. A lot of initially collected data, used in the training, have been found to be inconsistent. This pointed out to deficiencies in the data acquisition. Respectively, this resulted in a subsequent more careful and extensive collecting of the process data at the Impol company, not only in the foil production path. The automatic and reliable data collection will allow much easier future use of the developed methodology.

6 Conclusions

An ANN for TPM of aluminum foils, based on the data available and collected from the Impol company, is developed in the present master thesis. The process path for production of household aluminum foil is composed of the following basic process steps: charging preparation, charging, melting and alloying, modification, metal cleaning, hydrogen removal, removal of inclusions, casting on strip casting machine, coiling with thickness of 6.0 mm, cold rolling, homogenization annealing, edge trimming, intermediate annealing, rolling to thickness of 0.3 mm, foil rolling, trimming between rolling passes and/or doubling, separating, end thickness rolling, final annealing, and foil packing. The principal final measured physical properties of the foil are the tensile strength and elongation.

Prediction of the final mechanical properties of the household aluminum foil, based on the physics based numerical modeling of the whole process (TPM), is extremely complicated due to the multi-scale and multi-phase character of the underlying physics as well as complicated material behavior. Respectively, an alternative approach to the physical modeling, the artificial intelligence approach, based on the ANNs, is developed and described in this work.

ANNs are networks of highly interconnected neural computing elements that have the ability to respond to input stimuli and to learn to adapt the environment. For ANNs, the NeuralTools program is used in the present work to build the application. We trained ANNs with process data for household aluminum foils (EN AW-8011) which are afterwards capable of predicting tensile strength and elongation while we change values of input variables. The performance of the trained network is measured by statistics such as the percentage of the known answers it correctly predicts and norms between predicted and the actual values.

Four ANN data sets have been used in the developed ANN TPM model. In all four networks, the configuration with one hidden layer, 6 nodes, 27 independent

input variables, and 60 minutes of training time was chosen. The first and the second configuration is for predicting the tensile strength (R_m), while the third and the fourth for predicting the elongation (A). In the first case, the training data set consisted of 80 historical data rows and the testing data set consisted of 29 data rows, which were not included in the training process. The result of the testing process was 89.65 % good predictions and 10.35 % bad predictions. After elimination of several rows of training data, for which we heuristically estimated that they might not perform well in training, we ended with a second data set of only 39 rows of historical data. For training ANN we used 30 rows and for testing the remaining 9 rows. This second configuration gave us a trained ANN with 100 % good predictions and 0 % of bad predictions. We proceeded in the similar way in the third and the fourth configuration which were used for predicting elongation (A). In the third case, the training data set consisted of 80 rows of historical data and the testing data set consisted of 29 data rows, which was not included in training process. The result of the testing process was 44.83 % of good predictions and 55.17 % of bad predictions. In the same sense as in the study of the tensile strength (R_m), we eliminated some suspicious rows of training data. The fourth training data set thus consisted of only 26 rows of historical data. For training ANN we used 20 rows, and for testing the remaining 6 rows. This fourth configuration gave us a trained ANN with result of 100 % of good predictions and 0 % of bad predictions.

The results show that proper selection of the data for training the ANN is very important. If we do not have good historical data, the result of trained ANN will not converge reasonably. Given the limited range of values of input variables for learning ANNs, the quality of the output variables prediction is rather limited. A larger set of historical data than the available one would lead to smaller errors in the learning of neural networks and hence a better prediction of mechanical properties.

The results show that the increase of tensile strength is mostly influenced by the chemical element Cr, and least influenced by the chemical element Mn, and that the decrease of tensile strength is mostly influenced by the chemical element Si, and least influenced by the chemical element Ti. For elongation, the ANN results show that the increase of elongation is mostly influenced by the chemical element Fe, and least influenced by the chemical element Si, and that the decrease of elongation is mostly influenced by the chemical element Ti, and least influenced by the chemical element Mn.

The presented work will be enhanced and upgraded with more extensive (in range and in values of historical data rows) and reliable training data in the future. In order to be industrially relevant and effective, ANN modeling should always be used with great care and with sufficient data. Physical models [Šarler, Vertnik, 2006; Šarler, Kosec, Lorbiecka, Vertnik, 2010] should also be developed in parallel and used wherever possible, to supplement and validate the ANN models [Sha, Edwards, 2007]. This would allow also better and more versatile validation and interpretation of the results.

With the presented trained artificial intelligence TPM, the Impol company obtained a basic model and particularly a new state-of-the-art methodology for estimation of the final product properties as a function of process parameters. The developed methodology is particularly important, since its main ideas can be readily applied to other product process paths than the foil production, such as for example the extrusion of aluminum rods. This allows the optimization of the whole production with respect to the productivity, quality, use of resources and environmental impact in the perspective.

Bibliography

Altenpohl, D. G. (1998). *Aluminum: Technology, Applications, and Environment: A profile of a Modern Metal*. Aluminum Association & TMS, Washington D.C., Pennsylvania.

Bishop, C. (1995). *Neural Networks for Pattern Recognition*. Clarendon Press, Oxford, United Kingdom.

Carling, A. (1992). *Introducing Neural Networks*. Sigma Press, Wilmslow, United Kingdom.

Chun, M. S., Biglou, J., Lenard, J. G., Kim, J. G. (1998). Using neural networks to predict parameters in the hot working of aluminum alloys. *Journal of Materials Processing Technology*, Vol. 86, Issues 1-3, pp. 245-251.

Crumbach, M., Quested, T., Hamerton, R. (2006). Industrial application of through-process modeling II: Microstructural models and descriptors required for thermo-mechanical processing. *Materials Science Forum*, Vol. 519-521, pp. 1511-1518.

Fausett, L. (1994). *Fundamentals of Neural Networks*. Prentice Hall, Florida.

Hassan, A., Alrashdan, A., Hayajneh, M., Mayyas, A. (2009). Prediction of density, porosity and hardness in aluminum–copper-based composite materials using artificial neural network. *Journal of Materials Processing Technology*, Vol. 209, pp. 894-899.

Impol (2004). Foils. *Technical Report for Foils*, Retrieved from <http://www.impol.com/products/>.

Kocijan, J. (2007). *Modeliranje dinamičnih sistemov z umetnimi nevronskimi mrežami in sorodnimi metodami*, Založba Univerze v Novi Gorici, Nova Gorica.

Kriesel, D. (2011). *A Brief Introduction to Neural Networks*, Retrieved from <http://www.dkriesel.com>.

Lu, Z., Pan, Q., Liu, X., Qin, Y., He, Y., Cao, S. (2010). Artificial neural network prediction to the hot compressive deformation behavior of Al-Cu-Mg-Ag heat-resistant aluminum alloy. *Mechanics Research Communications*, Vol. 38, pp. 192-197.

Palisade Corporation (2005). *NeuralTools. User guide*, Retrieved from <http://www.palisade.com>.

Patterson, W. (1995). *Artificial Neural Networks - Theory and Applications*. Prentice Hall, Singapore.

Pfeifer, R., Damian, D., Fuchslin, R. (2010). *Neural Networks*. University of Zurich, Switzerland.

Quested, T., Crumbach, M., Hamerton, R. (2006). Industrial application of through-process modeling I: Microstructural descriptors required from the casting model for downstream process stages. *Materials Science Forum*, Vol. 519-521, pp. 1783-1788.

Raj, R., Daniel, B. (2008). Prediction of compressive properties of closed-cell aluminum foam using artificial neural network. *Computational Materials Science*, Vol. 43, pp. 767-773.

Ratha, S., Singha, A., Bhaskara, U., Krishnaa, B., Santraa, B., Raia, D., Neogia, N. (2010). Artificial neural network modeling for prediction of roll force during plate rolling process. *Materials and Manufacturing Processes*, Vol. 25, pp. 149-153.

Ravia, R., Prasadb, Y., Sarmac, V. (2007). An Artificial Neural Network (ANN) model for predicting instability regimes in copper-aluminum alloys. *Materials and Manufacturing Processes*, Vol. 22, pp. 846-850.

Reed, R., Marks, R. (1998). *Neural Smithing: Supervised Learning in Feedforward Artificial Neural Networks*. Massachusetts Institute of Technology Press, United States of America.

Refaeilzadeh, P., Tang, L., Liu, H. (2009). *Cross-Validation*. Arizona State University, United States of America.

Sampaio, P., Braga, A., Fujii, T. (2006). *Neural Network Thermal Model of a Ladle Furnace*. Retrieved from <http://citeseerx.ist.psu.edu>, Technical report.

Schlang, M., Feldkeller, B., Lang, B., Poppe, T., Runkler, T. (1999). *Neural Computation in Steel Industry*. Retrieved from <http://citeseerx.ist.psu.edu>, Technical report.

Sen, S., Twomey, J., Ahmad, J. (2006). *Development of an Artificial Neural Network Constitutive Model for Aluminum 7075 Alloy*. Retrieved from <http://citeseerx.ist.psu.edu>, Technical report.

Sha, W., Edwards, K. (2007). The use of artificial neural networks in materials science based research. *Materials & Design*, Vol. 28, pp. 1747-1752.

Slovenski standard (2002). *Kovinski materiali- Natezni preskus – 1.del: Metoda preskušanja pri temperature okolice*. Slovenski inštitut za standardizacijo.

Song, R., Zhang, Q. (2001). Heat treatment technique optimization for 7175 aluminum alloy by an artificial neural network and a genetic algorithm. *Journal of Materials Processing Technology*, Vol. 117, pp. 84-88.

Song, R., Zhang, Q., Tseng, M., Zhang, B. (1995). The application of artificial neural networks to the investigation of aging dynamics in 7175 aluminum alloys. *Materials Science and Engineering*, Vol. 3C, pp. 39-41.

Statsoft Inc. (2003). *Neural Networks*. Retrieved from <http://www.statsoft.com>, Electronic textbook.

Šarler, B., Vertnik, R. (2006). Mesh-free simulation of transport phenomena in continuous casting of aluminum alloys. *Materials Science Forum*, Vol. 508, pp. 497-502.

Šarler, B., Kosec, G., Lorbiecka, A. Z., Vertnik, R. (2010). A meshless approach in solution of multiscale solidification modeling. *Materials Science Forum*, Vol. 649, pp. 211-216.

Tahir, M. (2007). *Java Implementation of Neural Networks*. Booksurge Publishing, United States of America.

Trčko, Š., Robič, A., Jelen, M., Volšak, D., Strnad, V., Skrbinek, R., Malenšek, M., Cvahte, P., Šarler, B. (2007). *Tehnološke sheme procesov v podjetju Impol d.d. z naborom procesnih parametrov: revizija 0*. Univerza v Novi Gorici, Laboratorij za večfazne procese, Nova Gorica, Technical report.

Trčko, Š., Robič, A., Šarler, B. (2007). *Razlaga in prevod pomembnih izrazov aluminijske tehnologije: revizija 0*. Univerza v Novi Gorici, Laboratorij za večfazne procese, Nova Gorica, Technical report.

Trčko, Š., Šarler B. (2009). Use of artificial neural networks in predicting properties of household foil in Impol d.d. company, *Slovenska konferenca o materialih in tehnologijah za trajnostni razvoj*. In: Valant, M., Pirnat, U., editors, Založba Univerze v Novi Gorici, Ajdovščina, pp. 126-130.

Trčko, Š., Šarler, B. (2012). Use of artificial neural networks in through process modeling of aluminum foils. *Materials and Manufacturing Processes*, (submitted).

Appendix A

A.1 Input data for training ANN with 109 historical data (charge data) for 27 independent input variables and dependent output variable Tensile strength (R_m)

Table A.1: Input data for training ANN with 109 historical data (charge data) for 27 independent input variables and dependent output variable Tensile strength (R_m) – part 1

Charge	Width (mm)	Outside diameter (mm)	Al (wt%)	Si (wt%)	Fe (wt%)	Cu (wt%)	Mn (wt%)
92929	290.0	900.0	98.489	0.587	0.847	0.001	0.005
92929	290.0	900.0	98.489	0.587	0.847	0.001	0.005
92926	290.0	1,000.0	98.52	0.578	0.828	0.001	0.005
92926	290.0	1,000.0	98.52	0.578	0.828	0.001	0.005
92926	290.0	1,000.0	98.52	0.578	0.828	0.001	0.005
92926	290.0	1,000.0	98.52	0.578	0.828	0.001	0.005
93321	292.0	600.0	98.479	0.583	0.862	0.001	0.006
93321	292.0	600.0	98.479	0.583	0.862	0.001	0.006
93327	290.0	550.0	98.536	0.559	0.836	0.001	0.004
93327	290.0	550.0	98.536	0.559	0.836	0.001	0.004
93323	290.0	1,000.0	98.429	0.626	0.875	0.001	0.005
93323	290.0	1,000.0	98.429	0.626	0.875	0.001	0.005
93323	290.0	1,000.0	98.429	0.626	0.875	0.001	0.005
93323	290.0	1,000.0	98.429	0.626	0.875	0.001	0.005
93328	290.0	1,000.0	98.482	0.58	0.869	0.001	0.004
93328	290.0	1,000.0	98.482	0.58	0.869	0.001	0.004
93326	290.0	600.0	98.472	0.595	0.844	0.001	0.004
93326	290.0	600.0	98.472	0.595	0.844	0.001	0.004
93326	290.0	600.0	98.472	0.595	0.844	0.001	0.004

93326	290.0	600.0	98.472	0.595	0.844	0.001	0.004
93325	290.0	600.0	98.51	0.595	0.828	0.001	0.004
93325	290.0	600.0	98.51	0.595	0.828	0.001	0.004
93339	450.0	550.0	98.467	0.58	0.873	0.001	0.005
93339	450.0	550.0	98.467	0.58	0.873	0.001	0.005
93339	326.0	550.0	98.467	0.58	0.873	0.001	0.005
93339	326.0	550.0	98.467	0.58	0.873	0.001	0.005
93336	290.0	1,000.0	98.448	0.577	0.889	0.002	0.008
93336	290.0	1,000.0	98.448	0.577	0.889	0.002	0.008
93336	290.0	1,000.0	98.448	0.577	0.889	0.002	0.008
93336	290.0	1,000.0	98.448	0.577	0.889	0.002	0.008
93347	292.0	600.0	98.474	0.595	0.856	0.001	0.006
93347	292.0	600.0	98.474	0.595	0.856	0.001	0.006
93761	450.0	550.0	98.534	0.57	0.807	0.002	0.006
93761	450.0	550.0	98.534	0.57	0.807	0.002	0.006
93761	326.0	550.0	98.534	0.57	0.807	0.002	0.006
93761	326.0	550.0	98.534	0.57	0.807	0.002	0.006
93762	290.0	600.0	98.484	0.593	0.836	0.002	0.006
93762	290.0	600.0	98.484	0.593	0.836	0.002	0.006
93762	290.0	600.0	98.484	0.593	0.836	0.002	0.006
93762	290.0	600.0	98.484	0.593	0.836	0.002	0.006
93765	295.0	600.0	98.471	0.592	0.852	0.001	0.005
93765	295.0	600.0	98.471	0.592	0.852	0.001	0.005
93763	300.0	900.0	98.493	0.584	0.837	0.002	0.005
93763	300.0	900.0	98.493	0.584	0.837	0.002	0.005
93763	300.0	900.0	98.493	0.584	0.837	0.002	0.005
93763	300.0	900.0	98.493	0.584	0.837	0.002	0.005
93982	300.0	600.0	98.446	0.613	0.849	0.002	0.006
93982	300.0	600.0	98.446	0.613	0.849	0.002	0.006
93982	450.0	600.0	98.446	0.613	0.849	0.002	0.006
93982	450.0	600.0	98.446	0.613	0.849	0.002	0.006
94237	280.0	530.0	98.472	0.564	0.88	0.002	0.004
94237	280.0	530.0	98.472	0.564	0.88	0.002	0.004
94289	290.0	900.0	98.497	0.576	0.836	0.002	0.005
94289	290.0	900.0	98.497	0.576	0.836	0.002	0.005
94289	290.0	900.0	98.497	0.576	0.836	0.002	0.005
94289	290.0	900.0	98.497	0.576	0.836	0.002	0.005
94298	290.0	1,000.0	98.437	0.59	0.876	0.002	0.006
94298	290.0	1,000.0	98.437	0.59	0.876	0.002	0.006

94299	290.0	1,000.0	98.4	0.642	0.874	0.001	0.005
94299	290.0	1,000.0	98.4	0.642	0.874	0.001	0.005
94337	290.0	550.0	98.466	0.57	0.865	0.002	0.008
94337	290.0	550.0	98.466	0.57	0.865	0.002	0.008
94337	290.0	550.0	98.466	0.57	0.865	0.002	0.008
94337	290.0	550.0	98.466	0.57	0.865	0.002	0.008
94337	450.0	550.0	98.466	0.57	0.865	0.002	0.008
94337	450.0	550.0	98.466	0.57	0.865	0.002	0.008
94334	450.0	550.0	98.408	0.625	0.868	0.003	0.016
94334	450.0	550.0	98.408	0.625	0.868	0.003	0.016
94334	290.0	550.0	98.408	0.625	0.868	0.003	0.016
94334	290.0	550.0	98.408	0.625	0.868	0.003	0.016
94337	450.0	550.0	98.466	0.57	0.865	0.002	0.008
94337	450.0	550.0	98.466	0.57	0.865	0.002	0.008
94338	290.0	1,000.0	98.434	0.582	0.895	0.002	0.006
94338	290.0	1,000.0	98.434	0.582	0.895	0.002	0.006
94482	290.0	1,000.0	98.435	0.613	0.875	0.002	0.005
94482	290.0	1,000.0	98.435	0.613	0.875	0.002	0.005
94482	290.0	1,000.0	98.435	0.613	0.875	0.002	0.005
94482	290.0	1,000.0	98.435	0.613	0.875	0.002	0.005
94483	290.0	1,000.0	98.526	0.575	0.822	0.002	0.005
94483	290.0	1,000.0	98.526	0.575	0.822	0.002	0.005
94481	290.0	550.0	98.434	0.585	0.896	0.003	0.006
94481	290.0	550.0	98.434	0.585	0.896	0.003	0.006
94603	290.0	700.0	98.467	0.612	0.84	0.003	0.008
94603	290.0	700.0	98.467	0.612	0.84	0.003	0.008
94984	450.0	550.0	98.3962	0.601	0.881	0.0039	0.0306
94755	292.0	750.0	98.523	0.572	0.828	0.003	0.008
94755	292.0	750.0	98.523	0.572	0.828	0.003	0.008
94984	450.0	550.0	98.3962	0.601	0.881	0.0039	0.0306
94984	290.0	550.0	98.3962	0.601	0.881	0.0039	0.0306
94984	290.0	550.0	98.3962	0.601	0.881	0.0039	0.0306
94984	326.0	550.0	98.3962	0.601	0.881	0.0039	0.0306
94984	326.0	550.0	98.3962	0.601	0.881	0.0039	0.0306
94990	326.0	550.0	98.4548	0.609	0.851	0.0022	0.0084
94990	326.0	550.0	98.4548	0.609	0.851	0.0022	0.0084
94990	450.0	550.0	98.4548	0.609	0.851	0.0022	0.0084
94990	450.0	550.0	98.4548	0.609	0.851	0.0022	0.0084
94994	290.0	550.0	98.4313	0.613	0.8655	0.0018	0.0061

94994	290.0	550.0	98.4313	0.613	0.8655	0.0018	0.0061
94995	300.0	600.0	98.479	0.586	0.837	0.002	0.0065
94995	300.0	600.0	98.479	0.586	0.837	0.002	0.0065
94997	290.0	700.0	98.4456	0.608	0.848	0.0026	0.0131
95334	300.0	600.0	98.4341	0.596	0.89	0.0014	0.0052
95334	290.0	900.0	98.4341	0.596	0.89	0.0014	0.0052
95335	280.0	850.0	98.4264	0.612	0.876	0.0014	0.0055
95337	300.0	600.0	98.451	0.605	0.8545	0.0056	0.0054
95337	294.0	800.0	98.451	0.605	0.8545	0.0056	0.0054
95343	300.0	600.0	98.4729	0.602	0.8397	0.003	0.0065
95345	280.0	600.0	98.4651	0.619	0.837	0.0029	0.0059
95680	280.0	600.0	98.512	0.586	0.821	0.001	0.007

Table A.2: Input data for training ANN with 109 historical data (charge data) for 27 independent input variables and dependent output variable Tensile strength (R_m) – part 2

B (wt%)	Zn (wt%)	Pb (wt%)	Bi (wt%)	Mg (wt%)	In (wt%)	Ti (wt%)	Hg (wt%)	Ni (wt%)
0.002	0.004	0.001	0	0.002	0	0.03	0.002	0.002
0.002	0.004	0.001	0	0.002	0	0.03	0.002	0.002
0.002	0.004	0.001	0	0.003	0	0.025	0.002	0.002
0.002	0.004	0.001	0	0.003	0	0.025	0.002	0.002
0.002	0.004	0.001	0	0.003	0	0.025	0.002	0.002
0.002	0.004	0.001	0	0.003	0	0.025	0.002	0.002
0.003	0.006	0.001	0	0.002	0.001	0.029	0.003	0.002
0.003	0.006	0.001	0	0.002	0.001	0.029	0.003	0.002
0.003	0.006	0.001	0	0.002	0	0.025	0.002	0.002
0.003	0.006	0.001	0	0.002	0	0.025	0.002	0.002
0.002	0.006	0.001	0	0.002	0	0.026	0.002	0.002
0.002	0.006	0.001	0	0.002	0	0.026	0.002	0.002
0.002	0.006	0.001	0	0.002	0	0.026	0.002	0.002
0.002	0.006	0.001	0	0.002	0	0.026	0.002	0.002
0.003	0.006	0.001	0	0.002	0	0.025	0.002	0.002
0.003	0.006	0.001	0	0.002	0	0.025	0.002	0.002
0.009	0.005	0.001	0	0.002	0	0.038	0.002	0.002
0.009	0.005	0.001	0	0.002	0	0.038	0.002	0.002
0.009	0.005	0.001	0	0.002	0	0.038	0.002	0.002
0.009	0.005	0.001	0	0.002	0	0.038	0.002	0.002
0.002	0.005	0.001	0	0.001	0	0.025	0.002	0.002

0.006	0.006	0.001	0.001	0.01	0	0.036	0.002	0.002
0.006	0.006	0.001	0.001	0.01	0	0.036	0.002	0.002
0.006	0.006	0.001	0.001	0.01	0	0.036	0.002	0.002
0.006	0.006	0.001	0.001	0.01	0	0.036	0.002	0.002
0.006	0.006	0.001	0.001	0.01	0	0.036	0.002	0.002
0.006	0.006	0.001	0.001	0.01	0	0.036	0.002	0.002
0.003	0.005	0.001	0.001	0.007	0	0.031	0.002	0.002
0.003	0.005	0.001	0.001	0.007	0	0.031	0.002	0.002
0.003	0.005	0.001	0.001	0.007	0	0.031	0.002	0.002
0.003	0.005	0.001	0.001	0.007	0	0.031	0.002	0.002
0.006	0.006	0.001	0.001	0.01	0	0.036	0.002	0.002
0.006	0.006	0.001	0.001	0.01	0	0.036	0.002	0.002
0.005	0.005	0.001	0	0.007	0	0.034	0.002	0.002
0.005	0.005	0.001	0	0.007	0	0.034	0.002	0.002
0.002	0.005	0.001	0	0.005	0	0.028	0.002	0.002
0.002	0.005	0.001	0	0.005	0	0.028	0.002	0.002
0.002	0.005	0.001	0	0.005	0	0.028	0.002	0.002
0.002	0.005	0.001	0	0.005	0	0.028	0.002	0.002
0.002	0.005	0.001	0	0.005	0	0.029	0.002	0.002
0.002	0.005	0.001	0	0.005	0	0.029	0.002	0.002
0.003	0.005	0.001	0	0.005	0	0.032	0.002	0.002
0.003	0.005	0.001	0	0.005	0	0.032	0.002	0.002
0.002	0.004	0.001	0.001	0.007	0	0.028	0.002	0.002
0.002	0.004	0.001	0.001	0.007	0	0.028	0.002	0.002
0.0061	0.005	0.001	0.0003	0.011	0.0002	0.036	0.002	0.0002
0.002	0.005	0.001	0	0.005	0	0.025	0.002	0.002
0.002	0.005	0.001	0	0.005	0	0.025	0.002	0.002
0.0061	0.005	0.001	0.0003	0.011	0.0002	0.036	0.002	0.0002
0.0061	0.005	0.001	0.0003	0.011	0.0002	0.036	0.002	0.0002
0.0061	0.005	0.001	0.0003	0.011	0.0002	0.036	0.002	0.0002
0.0061	0.005	0.001	0.0003	0.011	0.0002	0.036	0.002	0.0002
0.0061	0.005	0.001	0.0003	0.011	0.0002	0.036	0.002	0.0002
0.0027	0.0039	0.001	0.0005	0.005	0.0001	0.027	0.002	0.002
0.0027	0.0039	0.001	0.0005	0.005	0.0001	0.027	0.002	0.002
0.0027	0.0039	0.001	0.0005	0.005	0.0001	0.027	0.002	0.002
0.0027	0.0039	0.001	0.0005	0.005	0.0001	0.027	0.002	0.002
0.0039	0.0044	0.001	0.0007	0.003	0.0002	0.03	0.002	0.003
0.0039	0.0044	0.001	0.0007	0.003	0.0002	0.03	0.002	0.003
0.0046	0.0043	0.001	0.005	0.003	0.0001	0.035	0.002	0.002

0.0046	0.0043	0.001	0.005	0.003	0.0001	0.035	0.002	0.002
0.0027	0.0046	0.001	0.0006	0.008	0.0001	0.029	0.002	0.002
0.0018	0.0037	0.001	0.0003	0.002	0	0.032	0.002	0.002
0.0018	0.0037	0.001	0.0003	0.002	0	0.032	0.002	0.002
0.0024	0.0041	0.001	0.0004	0.003	0.0001	0.034	0.002	0.002
0.002	0.0024	0.001	0.0007	0.003	0.0002	0.034	0.002	0.002
0.002	0.0024	0.001	0.0007	0.003	0.0002	0.034	0.002	0.002
0.0016	0.0046	0.0009	0.003	0.005	0	0.031	0.002	0.002
0.0023	0.0033	0.001	0.0005	0.004	0.0001	0.028	0.002	0.002
0.002	0.005	0.001	0	0.003	0	0.026	0.002	0.002

Table A.3: Input data for training ANN with 109 historical data (charge data) for 27 independent input variables and dependent output variable Tensile strength (R_m) – part 3

Sn (wt%)	Ca (wt%)	V (wt%)	Cr (wt%)	Sb (wt%)	Ga (wt%)	Sum Hg Cd Pb (wt%)	Sum Ti Zr (wt%)
0.001	0.001	0.006	0.002	0.005	0.011	0.003	0.03
0.001	0.001	0.006	0.002	0.005	0.011	0.003	0.03
0.001	0.001	0.008	0.002	0.004	0.011	0.002	0.026
0.001	0.001	0.008	0.002	0.004	0.011	0.002	0.026
0.001	0.001	0.008	0.002	0.004	0.011	0.002	0.026
0	0.001	0.005	0.002	0.004	0.011	0.004	0.029
0	0.001	0.005	0.002	0.004	0.011	0.004	0.029
0.001	0.001	0.004	0.002	0.004	0.01	0.003	0.026
0.001	0.001	0.004	0.002	0.004	0.01	0.003	0.026
0.001	0.001	0.004	0.002	0.004	0.011	0.003	0.026
0.001	0.001	0.004	0.002	0.004	0.011	0.003	0.026
0.001	0.001	0.004	0.002	0.004	0.011	0.003	0.026
0.001	0.001	0.004	0.002	0.004	0.01	0.003	0.026
0.001	0.001	0.004	0.002	0.004	0.01	0.003	0.026
0.001	0.001	0.004	0.002	0.004	0.011	0.003	0.026
0.001	0.001	0.004	0.002	0.004	0.011	0.003	0.026
0.001	0.001	0.004	0.002	0.004	0.01	0.003	0.026
0.001	0.001	0.005	0.002	0.004	0.011	0.003	0.039
0.001	0.001	0.005	0.002	0.004	0.011	0.003	0.039
0.001	0.001	0.005	0.002	0.004	0.011	0.003	0.039
0.001	0.001	0.005	0.002	0.004	0.011	0.003	0.039
0.001	0.001	0.004	0.002	0.004	0.011	0.003	0.026
0.001	0.001	0.004	0.002	0.004	0.011	0.003	0.026
0.001	0.001	0.003	0.002	0.004	0.01	0.003	0.035

0.001	0.001	0.006	0.002	0.004	0.011	0.003	0.037
0.001	0.001	0.006	0.002	0.004	0.011	0.003	0.037
0.001	0.001	0.006	0.002	0.004	0.011	0.003	0.037
0.001	0.001	0.006	0.002	0.004	0.011	0.003	0.037
0.001	0.001	0.008	0.002	0.004	0.011	0.003	0.032
0.001	0.001	0.008	0.002	0.004	0.011	0.003	0.032
0.001	0.001	0.008	0.002	0.004	0.011	0.003	0.032
0.001	0.001	0.008	0.002	0.004	0.011	0.003	0.032
0.001	0.001	0.006	0.002	0.004	0.011	0.003	0.037
0.001	0.001	0.006	0.002	0.004	0.011	0.003	0.037
0.001	0.001	0.005	0.002	0.004	0.01	0.003	0.035
0.001	0.001	0.005	0.002	0.004	0.01	0.003	0.035
0.001	0.001	0.005	0.002	0.004	0.011	0.003	0.029
0.001	0.001	0.005	0.002	0.004	0.011	0.003	0.029
0.001	0.001	0.005	0.002	0.004	0.011	0.003	0.029
0.001	0.001	0.005	0.002	0.004	0.01	0.002	0.03
0.001	0.001	0.005	0.002	0.004	0.01	0.002	0.03
0.001	0.001	0.006	0.002	0.004	0.011	0.003	0.033
0.001	0.001	0.006	0.002	0.004	0.011	0.003	0.033
0.001	0	0.004	0.002	0.004	0.01	0.003	0.029
0.001	0	0.004	0.002	0.004	0.01	0.003	0.029
0.0009	0.0009	0.006	0.002	0.004	0.012	0.003	0.037
0.001	0.001	0.004	0.002	0.004	0.009	0.003	0.026
0.001	0.001	0.004	0.002	0.004	0.009	0.003	0.026
0.0009	0.0009	0.006	0.002	0.004	0.012	0.003	0.037
0.0009	0.0009	0.006	0.002	0.004	0.012	0.003	0.037
0.0009	0.0009	0.006	0.002	0.004	0.012	0.003	0.037
0.0009	0.0009	0.006	0.002	0.004	0.012	0.003	0.037
0.0011	0.0004	0.01	0.001	0.004	0.013	0.003	0.0282
0.0011	0.0004	0.01	0.001	0.004	0.013	0.003	0.0282
0.0011	0.0004	0.01	0.001	0.004	0.013	0.003	0.0282
0.0011	0.0004	0.01	0.001	0.004	0.013	0.003	0.0282
0.0012	0.0009	0.012	0.002	0.005	0.013	0.0032	0.0314
0.0012	0.0009	0.012	0.002	0.005	0.013	0.0032	0.0314
0.001	0.0008	0.012	0.001	0.004	0.012	0.0029	0.0354
0.001	0.0008	0.012	0.001	0.004	0.012	0.0029	0.0354
0.001	0.0003	0.013	0.002	0.004	0.012	0.0031	0.0299

0.0008	0.0005	0.008	0.001	0.004	0.013	0.0028	0.0327
0.0008	0.0005	0.008	0.001	0.004	0.013	0.0028	0.0327
0.001	0.0006	0.008	0.002	0.004	0.013	0.0029	0.0352
0.001	0.0007	0.008	0.001	0.005	0.014	0.003	0.0352
0.001	0.0007	0.008	0.001	0.005	0.014	0.003	0.0352
0.0007	0.0009	0.007	0.002	0.004	0.011	0.0025	0.0316
0.0009	0.0009	0.006	0.002	0.005	0.012	0.0028	0.0292
0.001	0.001	0.012	0.002	0.004	0.012	0.003	0.027

Table A.4: Input data for training ANN with 109 historical data (charge data) for 27 independent input variables and dependent output variable Tensile strength (R_m) – part 4

Sum Mn Zr (wt%)	Sum Mn Cr Ti V (wt%)	T (°C)	Rm (Mpa)
0.007	0.043	290	105.62
0.007	0.043	290	108.82
0.008	0.041	281	104.29
0.008	0.041	281	111.09
0.008	0.041	281	106.05
0.008	0.041	281	112.98
0.007	0.04	288	100.13
0.007	0.04	288	100.10
0.006	0.035	288	97.13
0.006	0.035	288	94.78
0.007	0.036	288	92.21
0.007	0.036	288	97.66
0.007	0.036	288	108.87
0.007	0.036	288	107.34
0.006	0.035	288	111.84
0.006	0.035	288	110.27
0.006	0.049	288	105.79
0.006	0.049	288	109.78
0.006	0.049	288	97.12
0.006	0.049	288	96.99
0.006	0.035	288	105.23
0.006	0.035	288	109.22
0.007	0.044	285	107.28
0.007	0.044	285	106.17
0.007	0.044	285	103.81

0.007	0.044	285	105.14
0.01	0.046	285	106.40
0.01	0.046	285	106.47
0.01	0.046	285	100.36
0.01	0.046	285	102.80
0.007	0.039	280	102.59
0.007	0.039	280	102.43
0.008	0.046	281	101.65
0.008	0.046	281	102.19
0.008	0.046	281	101.06
0.008	0.046	281	102.19
0.007	0.046	281	104.59
0.007	0.046	281	104.27
0.007	0.046	281	102.73
0.007	0.046	281	102.46
0.007	0.046	289	113.23
0.007	0.046	289	115.94
0.007	0.045	289	107.76
0.007	0.045	289	107.56
0.007	0.045	289	107.56
0.007	0.045	289	107.35
0.008	0.053	276	108.54
0.008	0.053	276	107.18
0.008	0.053	276	97.84
0.008	0.053	276	106.60
0.006	0.049	287	100.88
0.006	0.049	287	103.05
0.007	0.054	290	107.38
0.007	0.054	290	109.32
0.007	0.054	290	100.39
0.007	0.054	290	101.54
0.007	0.056	288	101.18
0.007	0.056	288	102.62
0.006	0.05	282	103.96
0.006	0.05	282	103.76
0.01	0.052	290	98.94
0.01	0.052	290	99.22
0.01	0.052	290	100.87
0.01	0.052	290	100.64

0.01	0.052	290	99.29
0.01	0.052	290	99.54
0.018	0.057	290	100.35
0.018	0.057	290	100.35
0.018	0.057	290	98.93
0.018	0.057	290	99.22
0.01	0.052	290	100.34
0.01	0.052	290	100.54
0.008	0.047	294	111.72
0.008	0.047	294	112.38
0.007	0.04	294	98.35
0.007	0.04	294	98.38
0.007	0.04	291	102.43
0.007	0.04	291	101.05
0.007	0.04	291	101.11
0.007	0.04	291	99.80
0.008	0.046	291	110.70
0.008	0.046	291	110.70
0.01	0.042	303	98.78
0.01	0.042	303	100.54
0.0326	0.0739	285	105.03
0.011	0.04	298	107.59
0.011	0.04	298	105.40
0.0326	0.0739	285	105.52
0.0326	0.0739	286	115.60
0.0326	0.0739	287	115.23
0.0326	0.0739	288	107.55
0.0326	0.0739	289	106.73
0.0098	0.0465	290	107.55
0.0098	0.0465	291	106.73
0.0098	0.0465	292	105.03
0.0098	0.0465	293	105.52
0.0076	0.0499	294	115.60
0.0076	0.0499	295	115.23
0.0079	0.0544	298	104.84
0.0079	0.0544	304	103.57
0.0146	0.0562	293	110.17
0.0066	0.0462	304	104.70
0.0066	0.0462	304	105.34

0.007	0.0492	304	102.17
0.0068	0.0489	304	104.62
0.0068	0.0489	304	106.60
0.0082	0.0459	304	103.51
0.0074	0.042	304	98.34
0.008	0.046	309	105.34

A.2 The new training set after heuristic elimination of rows that are not good for training ANN with 39 historical data (charge data) for 27 independent input variables and dependent output variable Tensile strength (R_m)

Table A.5: The new training set after heuristic elimination of rows that are not good for training ANN with 39 historical data (charge data) for 27 independent input variables and dependent output variable Tensile strength (R_m) – part 1

Charge	Width (mm)	Outside diameter (mm)	Al (wt%)	Si (wt%)	Fe (wt%)	Cu (wt%)	Mn (wt%)
92926	290.0	1,000.0	98.52	0.578	0.828	0.001	0.005
93321	292.0	600.0	98.479	0.583	0.862	0.001	0.006
93323	290.0	550.0	98.536	0.559	0.836	0.001	0.004
93326	290.0	1,000.0	98.482	0.58	0.869	0.001	0.004
93336	450.0	550.0	98.467	0.58	0.873	0.001	0.005
93336	326.0	550.0	98.467	0.58	0.873	0.001	0.005
93347	292.0	600.0	98.474	0.595	0.856	0.001	0.006
93761	450.0	550.0	98.534	0.57	0.807	0.002	0.006
93761	326.0	550.0	98.534	0.57	0.807	0.002	0.006
93763	300.0	900.0	98.493	0.584	0.837	0.002	0.005
93765	300.0	900.0	98.493	0.584	0.837	0.002	0.005
93982	450.0	600.0	98.446	0.613	0.849	0.002	0.006
94289	290.0	900.0	98.497	0.576	0.836	0.002	0.005
94298	290.0	1,000.0	98.437	0.59	0.876	0.002	0.006
94299	290.0	1,000.0	98.4	0.642	0.874	0.001	0.005
94334	290.0	550.0	98.466	0.57	0.865	0.002	0.008
94337	450.0	550.0	98.466	0.57	0.865	0.002	0.008

94337	450.0	550.0	98.408	0.625	0.868	0.003	0.016
94337	290.0	550.0	98.408	0.625	0.868	0.003	0.016
94337	450.0	550.0	98.466	0.57	0.865	0.002	0.008
94338	290.0	1,000.0	98.434	0.582	0.895	0.002	0.006
94481	290.0	1,000.0	98.435	0.613	0.875	0.002	0.005
94482	290.0	1,000.0	98.526	0.575	0.822	0.002	0.005
94483	290.0	550.0	98.434	0.585	0.896	0.003	0.006
94603	290.0	700.0	98.467	0.612	0.84	0.003	0.008
94755	450.0	550.0	98.3962	0.601	0.881	0.0039	0.0306
94755	292.0	750.0	98.523	0.572	0.828	0.003	0.008
94984	292.0	750.0	98.523	0.572	0.828	0.003	0.008
94984	450.0	550.0	98.3962	0.601	0.881	0.0039	0.0306
94990	450.0	550.0	98.4548	0.609	0.851	0.0022	0.0084
94995	300.0	600.0	98.479	0.586	0.837	0.002	0.0065
94997	290.0	700.0	98.4456	0.608	0.848	0.0026	0.0131
95334	300.0	600.0	98.4341	0.596	0.89	0.0014	0.0052
95334	290.0	900.0	98.4341	0.596	0.89	0.0014	0.0052
95335	280.0	850.0	98.4264	0.612	0.876	0.0014	0.0055
95337	300.0	600.0	98.451	0.605	0.8545	0.0056	0.0054
95343	300.0	600.0	98.451	0.605	0.8545	0.0056	0.0054
95345	280.0	600.0	98.4729	0.602	0.8397	0.003	0.0065
95680	280.0	600.0	98.4651	0.619	0.837	0.0029	0.0059

Table A.6: The new training set after heuristic elimination of rows that are not good for training ANN with 39 historical data (charge data) for 27 independent input variables and dependent output variable Tensile strength (Rm) – part 2

B (wt%)	Zn (wt%)	Pb (wt%)	Bi (wt%)	Mg (wt%)	In (wt%)	Ti (wt%)	Hg (wt%)
0.002	0.004	0.001	0	0.003	0	0.025	0.002
0.003	0.006	0.001	0	0.002	0.001	0.029	0.003
0.003	0.006	0.001	0	0.002	0	0.025	0.002
0.003	0.006	0.001	0	0.002	0	0.025	0.002
0.004	0.007	0.001	0	0.003	0	0.034	0.002
0.004	0.007	0.001	0	0.003	0	0.034	0.002
0.004	0.006	0.001	0	0.003	0	0.028	0.002
0.002	0.006	0.001	0.001	0.007	0	0.031	0.002
0.002	0.006	0.001	0.001	0.007	0	0.031	0.002
0.003	0.006	0.001	0.001	0.005	0	0.03	0.002

0.003	0.006	0.001	0.001	0.005	0	0.03	0.002
0.003	0.005	0.001	0	0.006	0	0.033	0.002
0.005	0.005	0.001	0	0.002	0	0.034	0.002
0.005	0.005	0.001	0	0.005	0	0.033	0.002
0.002	0.004	0.001	0	0.004	0	0.028	0.002
0.006	0.006	0.001	0.001	0.01	0	0.036	0.002
0.006	0.006	0.001	0.001	0.01	0	0.036	0.002
0.003	0.005	0.001	0.001	0.007	0	0.031	0.002
0.003	0.005	0.001	0.001	0.007	0	0.031	0.002
0.006	0.006	0.001	0.001	0.01	0	0.036	0.002
0.005	0.005	0.001	0	0.007	0	0.034	0.002
0.002	0.005	0.001	0	0.005	0	0.028	0.002
0.002	0.005	0.001	0	0.005	0	0.029	0.002
0.003	0.005	0.001	0	0.005	0	0.032	0.002
0.002	0.004	0.001	0.001	0.007	0	0.028	0.002
0.0061	0.005	0.001	0.0003	0.011	0.0002	0.036	0.002
0.002	0.005	0.001	0	0.005	0	0.025	0.002
0.002	0.005	0.001	0	0.005	0	0.025	0.002
0.0061	0.005	0.001	0.0003	0.011	0.0002	0.036	0.002
0.0027	0.0039	0.001	0.0005	0.005	0.0001	0.027	0.002
0.0046	0.0043	0.001	0.005	0.003	0.0001	0.035	0.002
0.0027	0.0046	0.001	0.0006	0.008	0.0001	0.029	0.002
0.0018	0.0037	0.001	0.0003	0.002	0	0.032	0.002
0.0018	0.0037	0.001	0.0003	0.002	0	0.032	0.002
0.0024	0.0041	0.001	0.0004	0.003	0.0001	0.034	0.002
0.002	0.0024	0.001	0.0007	0.003	0.0002	0.034	0.002
0.002	0.0024	0.001	0.0007	0.003	0.0002	0.034	0.002
0.0016	0.0046	0.00009	0.003	0.005	0	0.031	0.002
0.0023	0.0033	0.001	0.0005	0.004	0.0001	0.028	0.002

Table A.7: The new training set after heuristic elimination of rows that are not good for training ANN with 39 historical data (charge data) for 27 independent input variables and dependent output variable Tensile strength (R_m) – part 3

Ni (wt%)	Sn (wt%)	Ca (wt%)	V (wt%)	Cr (wt%)	Sb (wt%)	Ga (wt%)	Sum Hg Cd Pb (wt%)
0.002	0.001	0.001	0.008	0.002	0.004	0.011	0.002
0.002	0	0.001	0.005	0.002	0.004	0.011	0.004
0.002	0.001	0.001	0.004	0.002	0.004	0.01	0.003
0.002	0.001	0.001	0.004	0.002	0.004	0.01	0.003
0.002	0.001	0.001	0.003	0.002	0.004	0.01	0.003
0.002	0.001	0.001	0.003	0.002	0.004	0.01	0.003
0.002	0.001	0.001	0.004	0.002	0.004	0.01	0.002
0.002	0.001	0.001	0.007	0.002	0.004	0.012	0.003
0.002	0.001	0.001	0.007	0.002	0.004	0.012	0.003
0.002	0.001	0.001	0.008	0.002	0.004	0.011	0.003
0.002	0.001	0.001	0.008	0.002	0.004	0.011	0.003
0.002	0.001	0.001	0.012	0.002	0.004	0.011	0.003
0.002	0.001	0.001	0.014	0.002	0.004	0.011	0.003
0.002	0.001	0.001	0.016	0.002	0.004	0.011	0.003
0.002	0.001	0	0.017	0.001	0.004	0.011	0.003
0.002	0.001	0.001	0.006	0.002	0.004	0.011	0.003
0.002	0.001	0.001	0.006	0.002	0.004	0.011	0.003
0.002	0.001	0.001	0.008	0.002	0.004	0.011	0.003
0.002	0.001	0.001	0.008	0.002	0.004	0.011	0.003
0.002	0.001	0.001	0.006	0.002	0.004	0.011	0.003
0.002	0.001	0.001	0.005	0.002	0.004	0.01	0.003
0.002	0.001	0.001	0.005	0.002	0.004	0.011	0.003
0.002	0.001	0.001	0.005	0.002	0.004	0.01	0.002
0.002	0.001	0.001	0.006	0.002	0.004	0.011	0.003
0.002	0.001	0	0.004	0.002	0.004	0.01	0.003
0.0002	0.0009	0.0009	0.006	0.002	0.004	0.012	0.003
0.002	0.001	0.001	0.004	0.002	0.004	0.009	0.003
0.002	0.001	0.001	0.004	0.002	0.004	0.009	0.003
0.0002	0.0009	0.0009	0.006	0.002	0.004	0.012	0.003
0.0024	0.0011	0.0004	0.01	0.001	0.004	0.013	0.003
0.0024	0.001	0.0008	0.012	0.001	0.004	0.012	0.0029
0.0024	0.001	0.0003	0.013	0.002	0.004	0.012	0.0031
0.0021	0.0008	0.0005	0.008	0.001	0.004	0.013	0.0028

0.0021	0.0008	0.0005	0.008	0.001	0.004	0.013	0.0028
0.0022	0.001	0.0006	0.008	0.002	0.004	0.013	0.0029
0.0024	0.001	0.0007	0.008	0.001	0.005	0.014	0.003
0.0024	0.001	0.0007	0.008	0.001	0.005	0.014	0.003
0.0021	0.0007	0.0009	0.007	0.002	0.004	0.011	0.0025
0.0021	0.0009	0.0009	0.006	0.002	0.005	0.012	0.0028

Table A.8: The new training set after heuristic elimination of rows that are not good for training ANN with 39 historical data (charge data) for 27 independent input variables and dependent output variable Tensile strength (R_m) – part 4

Sum Ti Zr (wt%)	Sum Mn Zr (wt%)	Sum Mn Cr Ti V (wt%)	T (°C)	Rm (Mpa)
0.026	0.008	0.041	281	107.69
0.029	0.007	0.04	288	100.12
0.026	0.006	0.035	288	95.96
0.026	0.006	0.035	288	111.06
0.035	0.007	0.044	285	106.73
0.035	0.007	0.044	285	104.48
0.029	0.007	0.039	280	102.51
0.032	0.008	0.046	281	101.92
0.032	0.008	0.046	281	101.63
0.03	0.007	0.045	289	107.66
0.03	0.007	0.045	289	107.46
0.034	0.008	0.053	276	107.44
0.034	0.007	0.054	290	108.35
0.034	0.007	0.056	288	101.90
0.028	0.006	0.05	282	103.86
0.037	0.01	0.052	290	99.25
0.037	0.01	0.052	290	100.76
0.032	0.018	0.057	290	100.35
0.032	0.018	0.057	290	99.08
0.037	0.01	0.052	290	100.44
0.035	0.008	0.047	294	112.05
0.029	0.007	0.04	294	98.37
0.03	0.007	0.04	291	101.53
0.033	0.008	0.046	291	110.70
0.029	0.01	0.042	303	99.66
0.037	0.0326	0.0739	285	105.03

0.026	0.011	0.04	298	107.59
0.026	0.011	0.04	298	105.40
0.037	0.0326	0.0739	285	105.52
0.0282	0.0098	0.0465	293	105.28
0.0354	0.0079	0.0544	304	104.21
0.0299	0.0146	0.0562	293	110.17
0.0327	0.0066	0.0462	304	104.70
0.0327	0.0066	0.0462	304	105.34
0.0352	0.007	0.0492	304	102.17
0.0352	0.0068	0.0489	304	104.62
0.0352	0.0068	0.0489	304	106.60
0.0316	0.0082	0.0459	304	103.51
0.0292	0.0074	0.042	304	98.34

A.3 Input data for training ANN with 109 historical data (charge data) for 27 independent input variables and dependent output variable Elongation (A)

Table A.9: Input data for training ANN with 109 historical data (charge data) for 27 independent input variables and dependent output variable Elongation (A) – part 1

Charge	Width (mm)	Outside diameter (mm)	Al (wt%)	Si (wt%)	Fe (wt%)	Cu (wt%)	Mn (wt%)
92929	290.0	900.0	98.489	0.587	0.847	0.001	0.005
92929	290.0	900.0	98.489	0.587	0.847	0.001	0.005
92926	290.0	1,000.0	98.52	0.578	0.828	0.001	0.005
92926	290.0	1,000.0	98.52	0.578	0.828	0.001	0.005
92926	290.0	1,000.0	98.52	0.578	0.828	0.001	0.005
92926	290.0	1,000.0	98.52	0.578	0.828	0.001	0.005
93321	292.0	600.0	98.479	0.583	0.862	0.001	0.006
93321	292.0	600.0	98.479	0.583	0.862	0.001	0.006
93327	290.0	550.0	98.536	0.559	0.836	0.001	0.004
93327	290.0	550.0	98.536	0.559	0.836	0.001	0.004
93323	290.0	1,000.0	98.429	0.626	0.875	0.001	0.005
93323	290.0	1,000.0	98.429	0.626	0.875	0.001	0.005
93323	290.0	1,000.0	98.429	0.626	0.875	0.001	0.005

93323	290.0	1,000.0	98.429	0.626	0.875	0.001	0.005
93328	290.0	1,000.0	98.482	0.58	0.869	0.001	0.004
93328	290.0	1,000.0	98.482	0.58	0.869	0.001	0.004
93326	290.0	600.0	98.472	0.595	0.844	0.001	0.004
93326	290.0	600.0	98.472	0.595	0.844	0.001	0.004
93326	290.0	600.0	98.472	0.595	0.844	0.001	0.004
93326	290.0	600.0	98.472	0.595	0.844	0.001	0.004
93325	290.0	600.0	98.51	0.595	0.828	0.001	0.004
93325	290.0	600.0	98.51	0.595	0.828	0.001	0.004
93339	450.0	550.0	98.467	0.58	0.873	0.001	0.005
93339	450.0	550.0	98.467	0.58	0.873	0.001	0.005
93339	326.0	550.0	98.467	0.58	0.873	0.001	0.005
93339	326.0	550.0	98.467	0.58	0.873	0.001	0.005
93336	290.0	1,000.0	98.448	0.577	0.889	0.002	0.008
93336	290.0	1,000.0	98.448	0.577	0.889	0.002	0.008
93336	290.0	1,000.0	98.448	0.577	0.889	0.002	0.008
93336	290.0	1,000.0	98.448	0.577	0.889	0.002	0.008
93347	292.0	600.0	98.474	0.595	0.856	0.001	0.006
93347	292.0	600.0	98.474	0.595	0.856	0.001	0.006
93761	450.0	550.0	98.534	0.57	0.807	0.002	0.006
93761	450.0	550.0	98.534	0.57	0.807	0.002	0.006
93761	326.0	550.0	98.534	0.57	0.807	0.002	0.006
93761	326.0	550.0	98.534	0.57	0.807	0.002	0.006
93762	290.0	600.0	98.484	0.593	0.836	0.002	0.006
93762	290.0	600.0	98.484	0.593	0.836	0.002	0.006
93762	290.0	600.0	98.484	0.593	0.836	0.002	0.006
93762	290.0	600.0	98.484	0.593	0.836	0.002	0.006
93765	295.0	600.0	98.471	0.592	0.852	0.001	0.005
93765	295.0	600.0	98.471	0.592	0.852	0.001	0.005
93763	300.0	900.0	98.493	0.584	0.837	0.002	0.005
93763	300.0	900.0	98.493	0.584	0.837	0.002	0.005
93763	300.0	900.0	98.493	0.584	0.837	0.002	0.005
93763	300.0	900.0	98.493	0.584	0.837	0.002	0.005
93982	300.0	600.0	98.446	0.613	0.849	0.002	0.006
93982	300.0	600.0	98.446	0.613	0.849	0.002	0.006
93982	450.0	600.0	98.446	0.613	0.849	0.002	0.006
93982	450.0	600.0	98.446	0.613	0.849	0.002	0.006
94237	280.0	530.0	98.472	0.564	0.88	0.002	0.004
94237	280.0	530.0	98.472	0.564	0.88	0.002	0.004

94289	290.0	900.0	98.497	0.576	0.836	0.002	0.005
94289	290.0	900.0	98.497	0.576	0.836	0.002	0.005
94289	290.0	900.0	98.497	0.576	0.836	0.002	0.005
94289	290.0	900.0	98.497	0.576	0.836	0.002	0.005
94298	290.0	1,000.0	98.437	0.59	0.876	0.002	0.006
94298	290.0	1,000.0	98.437	0.59	0.876	0.002	0.006
94299	290.0	1,000.0	98.4	0.642	0.874	0.001	0.005
94299	290.0	1,000.0	98.4	0.642	0.874	0.001	0.005
94337	290.0	550.0	98.466	0.57	0.865	0.002	0.008
94337	290.0	550.0	98.466	0.57	0.865	0.002	0.008
94337	290.0	550.0	98.466	0.57	0.865	0.002	0.008
94337	290.0	550.0	98.466	0.57	0.865	0.002	0.008
94337	450.0	550.0	98.466	0.57	0.865	0.002	0.008
94337	450.0	550.0	98.466	0.57	0.865	0.002	0.008
94334	450.0	550.0	98.408	0.625	0.868	0.003	0.016
94334	450.0	550.0	98.408	0.625	0.868	0.003	0.016
94334	290.0	550.0	98.408	0.625	0.868	0.003	0.016
94334	290.0	550.0	98.408	0.625	0.868	0.003	0.016
94337	450.0	550.0	98.466	0.57	0.865	0.002	0.008
94337	450.0	550.0	98.466	0.57	0.865	0.002	0.008
94338	290.0	1,000.0	98.434	0.582	0.895	0.002	0.006
94338	290.0	1,000.0	98.434	0.582	0.895	0.002	0.006
94482	290.0	1,000.0	98.435	0.613	0.875	0.002	0.005
94482	290.0	1,000.0	98.435	0.613	0.875	0.002	0.005
94482	290.0	1,000.0	98.435	0.613	0.875	0.002	0.005
94482	290.0	1,000.0	98.435	0.613	0.875	0.002	0.005
94483	290.0	1,000.0	98.526	0.575	0.822	0.002	0.005
94483	290.0	1,000.0	98.526	0.575	0.822	0.002	0.005
94481	290.0	550.0	98.434	0.585	0.896	0.003	0.006
94481	290.0	550.0	98.434	0.585	0.896	0.003	0.006
94603	290.0	700.0	98.467	0.612	0.84	0.003	0.008
94603	290.0	700.0	98.467	0.612	0.84	0.003	0.008
94984	450.0	550.0	98.3962	0.601	0.881	0.0039	0.0306
94755	292.0	750.0	98.523	0.572	0.828	0.003	0.008
94755	292.0	750.0	98.523	0.572	0.828	0.003	0.008
94984	450.0	550.0	98.3962	0.601	0.881	0.0039	0.0306
94984	290.0	550.0	98.3962	0.601	0.881	0.0039	0.0306
94984	290.0	550.0	98.3962	0.601	0.881	0.0039	0.0306
94984	326.0	550.0	98.3962	0.601	0.881	0.0039	0.0306

94984	326.0	550.0	98.3962	0.601	0.881	0.0039	0.0306
94990	326.0	550.0	98.4548	0.609	0.851	0.0022	0.0084
94990	326.0	550.0	98.4548	0.609	0.851	0.0022	0.0084
94990	450.0	550.0	98.4548	0.609	0.851	0.0022	0.0084
94990	450.0	550.0	98.4548	0.609	0.851	0.0022	0.0084
94994	290.0	550.0	98.4313	0.613	0.8655	0.0018	0.0061
94994	290.0	550.0	98.4313	0.613	0.8655	0.0018	0.0061
94995	300.0	600.0	98.479	0.586	0.837	0.002	0.0065
94995	300.0	600.0	98.479	0.586	0.837	0.002	0.0065
94997	290.0	700.0	98.4456	0.608	0.848	0.0026	0.0131
95334	300.0	600.0	98.4341	0.596	0.89	0.0014	0.0052
95334	290.0	900.0	98.4341	0.596	0.89	0.0014	0.0052
95335	280.0	850.0	98.4264	0.612	0.876	0.0014	0.0055
95337	300.0	600.0	98.451	0.605	0.8545	0.0056	0.0054
95337	294.0	800.0	98.451	0.605	0.8545	0.0056	0.0054
95343	300.0	600.0	98.4729	0.602	0.8397	0.003	0.0065
95345	280.0	600.0	98.4651	0.619	0.837	0.0029	0.0059
95680	280.0	600.0	98.512	0.586	0.821	0.001	0.007

Table A.10: Input data for training ANN with 109 historical data (charge data) for 27 independent input variables and dependent output variable Elongation (A) – part 2

B (wt%)	Zn (wt%)	Pb (wt%)	Bi (wt%)	Mg (wt%)	In (wt%)	Ti (wt%)	Hg (wt%)
0.002	0.004	0.001	0	0.002	0	0.03	0.002
0.002	0.004	0.001	0	0.002	0	0.03	0.002
0.002	0.004	0.001	0	0.003	0	0.025	0.002
0.002	0.004	0.001	0	0.003	0	0.025	0.002
0.002	0.004	0.001	0	0.003	0	0.025	0.002
0.002	0.004	0.001	0	0.003	0	0.025	0.002
0.003	0.006	0.001	0	0.002	0.001	0.029	0.003
0.003	0.006	0.001	0	0.002	0.001	0.029	0.003
0.003	0.006	0.001	0	0.002	0	0.025	0.002
0.003	0.006	0.001	0	0.002	0	0.025	0.002
0.002	0.006	0.001	0	0.002	0	0.026	0.002
0.002	0.006	0.001	0	0.002	0	0.026	0.002
0.002	0.006	0.001	0	0.002	0	0.026	0.002
0.002	0.006	0.001	0	0.002	0	0.026	0.002

0.003	0.006	0.001	0	0.002	0	0.025	0.002
0.003	0.006	0.001	0	0.002	0	0.025	0.002
0.009	0.005	0.001	0	0.002	0	0.038	0.002
0.009	0.005	0.001	0	0.002	0	0.038	0.002
0.009	0.005	0.001	0	0.002	0	0.038	0.002
0.009	0.005	0.001	0	0.002	0	0.038	0.002
0.002	0.005	0.001	0	0.001	0	0.025	0.002
0.002	0.005	0.001	0	0.001	0	0.025	0.002
0.004	0.007	0.001	0	0.003	0	0.034	0.002
0.004	0.007	0.001	0	0.003	0	0.034	0.002
0.004	0.007	0.001	0	0.003	0	0.034	0.002
0.004	0.007	0.001	0	0.003	0	0.034	0.002
0.003	0.006	0.001	0.001	0.004	0	0.032	0.002
0.003	0.006	0.001	0.001	0.004	0	0.032	0.002
0.003	0.006	0.001	0.001	0.004	0	0.032	0.002
0.003	0.006	0.001	0.001	0.004	0	0.032	0.002
0.004	0.006	0.001	0	0.003	0	0.028	0.002
0.004	0.006	0.001	0	0.003	0	0.028	0.002
0.002	0.006	0.001	0.001	0.007	0	0.031	0.002
0.002	0.006	0.001	0.001	0.007	0	0.031	0.002
0.002	0.006	0.001	0.001	0.007	0	0.031	0.002
0.002	0.006	0.001	0.001	0.007	0	0.031	0.002
0.002	0.007	0.001	0	0.006	0	0.031	0.002
0.002	0.007	0.001	0	0.006	0	0.031	0.002
0.002	0.007	0.001	0	0.006	0	0.031	0.002
0.002	0.007	0.001	0	0.006	0	0.031	0.002
0.004	0.007	0.001	0.001	0.004	0	0.031	0.002
0.004	0.007	0.001	0.001	0.004	0	0.031	0.002
0.003	0.006	0.001	0.001	0.005	0	0.03	0.002
0.003	0.006	0.001	0.001	0.005	0	0.03	0.002
0.003	0.006	0.001	0.001	0.005	0	0.03	0.002
0.003	0.006	0.001	0.001	0.005	0	0.03	0.002
0.003	0.005	0.001	0	0.006	0	0.033	0.002
0.003	0.005	0.001	0	0.006	0	0.033	0.002
0.003	0.005	0.001	0	0.006	0	0.033	0.002
0.003	0.005	0.001	0	0.006	0	0.033	0.002
0.003	0.005	0.001	0.001	0.002	0	0.028	0.002
0.003	0.005	0.001	0.001	0.002	0	0.028	0.002
0.005	0.005	0.001	0	0.002	0	0.034	0.002

0.005	0.005	0.001	0	0.002	0	0.034	0.002
0.005	0.005	0.001	0	0.002	0	0.034	0.002
0.005	0.005	0.001	0	0.002	0	0.034	0.002
0.005	0.005	0.001	0	0.005	0	0.033	0.002
0.005	0.005	0.001	0	0.005	0	0.033	0.002
0.002	0.004	0.001	0	0.004	0	0.028	0.002
0.002	0.004	0.001	0	0.004	0	0.028	0.002
0.006	0.006	0.001	0.001	0.01	0	0.036	0.002
0.006	0.006	0.001	0.001	0.01	0	0.036	0.002
0.006	0.006	0.001	0.001	0.01	0	0.036	0.002
0.006	0.006	0.001	0.001	0.01	0	0.036	0.002
0.006	0.006	0.001	0.001	0.01	0	0.036	0.002
0.006	0.006	0.001	0.001	0.01	0	0.036	0.002
0.003	0.005	0.001	0.001	0.007	0	0.031	0.002
0.003	0.005	0.001	0.001	0.007	0	0.031	0.002
0.003	0.005	0.001	0.001	0.007	0	0.031	0.002
0.003	0.005	0.001	0.001	0.007	0	0.031	0.002
0.006	0.006	0.001	0.001	0.01	0	0.036	0.002
0.006	0.006	0.001	0.001	0.01	0	0.036	0.002
0.005	0.005	0.001	0	0.007	0	0.034	0.002
0.005	0.005	0.001	0	0.007	0	0.034	0.002
0.002	0.005	0.001	0	0.005	0	0.028	0.002
0.002	0.005	0.001	0	0.005	0	0.028	0.002
0.002	0.005	0.001	0	0.005	0	0.028	0.002
0.002	0.005	0.001	0	0.005	0	0.028	0.002
0.002	0.005	0.001	0	0.005	0	0.029	0.002
0.002	0.005	0.001	0	0.005	0	0.029	0.002
0.003	0.005	0.001	0	0.005	0	0.032	0.002
0.003	0.005	0.001	0	0.005	0	0.032	0.002
0.002	0.004	0.001	0.001	0.007	0	0.028	0.002
0.002	0.004	0.001	0.001	0.007	0	0.028	0.002
0.0061	0.005	0.0014	0.0003	0.011	0.0002	0.036	0.002
0.002	0.005	0.001	0	0.005	0	0.025	0.002
0.002	0.005	0.001	0	0.005	0	0.025	0.002
0.0061	0.005	0.0014	0.0003	0.011	0.0002	0.036	0.002
0.0061	0.005	0.0014	0.0003	0.011	0.0002	0.036	0.002
0.0061	0.005	0.0014	0.0003	0.011	0.0002	0.036	0.002
0.0061	0.005	0.0014	0.0003	0.011	0.0002	0.036	0.002
0.0061	0.005	0.0014	0.0003	0.011	0.0002	0.036	0.002

0.0027	0.0039	0.0013	0.0005	0.005	0.0001	0.027	0.002
0.0027	0.0039	0.0013	0.0005	0.005	0.0001	0.027	0.002
0.0027	0.0039	0.0013	0.0005	0.005	0.0001	0.027	0.002
0.0027	0.0039	0.0013	0.0005	0.005	0.0001	0.027	0.002
0.0039	0.0044	0.0013	0.0007	0.003	0.0002	0.03	0.002
0.0039	0.0044	0.0013	0.0007	0.003	0.0002	0.03	0.002
0.0046	0.0043	0.0012	0.005	0.003	0.0001	0.035	0.002
0.0046	0.0043	0.0012	0.005	0.003	0.0001	0.035	0.002
0.0027	0.0046	0.0014	0.0006	0.008	0.0001	0.029	0.002
0.0018	0.0037	0.001	0.0003	0.002	0	0.032	0.002
0.0018	0.0037	0.001	0.0003	0.002	0	0.032	0.002
0.0024	0.0041	0.0011	0.0004	0.003	0.0001	0.034	0.002
0.002	0.0024	0.0011	0.0007	0.003	0.0002	0.034	0.002
0.002	0.0024	0.0011	0.0007	0.003	0.0002	0.034	0.002
0.0016	0.0046	0.0009	0.003	0.005	0	0.031	0.002
0.0023	0.0033	0.001	0.0005	0.004	0.0001	0.028	0.002
0.002	0.005	0.001	0	0.003	0	0.026	0.002

Table A.11: Input data for training ANN with 109 historical data (charge data) for 27 independent input variables and dependent output variable Elongation (A) – part 3

Ni (wt%)	Sn (wt%)	Ca (wt%)	V (wt%)	Cr (wt%)	Sb (wt%)	Ga (wt%)
0.002	0.001	0.001	0.006	0.002	0.005	0.011
0.002	0.001	0.001	0.006	0.002	0.005	0.011
0.002	0.001	0.001	0.008	0.002	0.004	0.011
0.002	0.001	0.001	0.008	0.002	0.004	0.011
0.002	0.001	0.001	0.008	0.002	0.004	0.011
0.002	0	0.001	0.005	0.002	0.004	0.011
0.002	0	0.001	0.005	0.002	0.004	0.011
0.002	0.001	0.001	0.004	0.002	0.004	0.01
0.002	0.001	0.001	0.004	0.002	0.004	0.01
0.002	0.001	0.001	0.004	0.002	0.004	0.011
0.002	0.001	0.001	0.004	0.002	0.004	0.011
0.002	0.001	0.001	0.004	0.002	0.004	0.011
0.002	0.001	0.001	0.004	0.002	0.004	0.011
0.002	0.001	0.001	0.004	0.002	0.004	0.01

0.002	0.001	0.001	0.014	0.002	0.004	0.011
0.002	0.001	0.001	0.014	0.002	0.004	0.011
0.002	0.001	0.001	0.016	0.002	0.004	0.011
0.002	0.001	0.001	0.016	0.002	0.004	0.011
0.002	0.001	0	0.017	0.001	0.004	0.011
0.002	0.001	0	0.017	0.001	0.004	0.011
0.002	0.001	0.001	0.006	0.002	0.004	0.011
0.002	0.001	0.001	0.006	0.002	0.004	0.011
0.002	0.001	0.001	0.006	0.002	0.004	0.011
0.002	0.001	0.001	0.006	0.002	0.004	0.011
0.002	0.001	0.001	0.006	0.002	0.004	0.011
0.002	0.001	0.001	0.006	0.002	0.004	0.011
0.002	0.001	0.001	0.008	0.002	0.004	0.011
0.002	0.001	0.001	0.008	0.002	0.004	0.011
0.002	0.001	0.001	0.008	0.002	0.004	0.011
0.002	0.001	0.001	0.006	0.002	0.004	0.011
0.002	0.001	0.001	0.006	0.002	0.004	0.011
0.002	0.001	0.001	0.005	0.002	0.004	0.01
0.002	0.001	0.001	0.005	0.002	0.004	0.01
0.002	0.001	0.001	0.005	0.002	0.004	0.011
0.002	0.001	0.001	0.005	0.002	0.004	0.011
0.002	0.001	0.001	0.005	0.002	0.004	0.011
0.002	0.001	0.001	0.005	0.002	0.004	0.01
0.002	0.001	0.001	0.005	0.002	0.004	0.01
0.002	0.001	0.001	0.005	0.002	0.004	0.01
0.002	0.001	0.001	0.006	0.002	0.004	0.011
0.002	0.001	0.001	0.006	0.002	0.004	0.011
0.002	0.001	0	0.004	0.002	0.004	0.01
0.002	0.001	0	0.004	0.002	0.004	0.01
0.0002	0.0009	0.0009	0.006	0.002	0.004	0.012
0.002	0.001	0.001	0.004	0.002	0.004	0.009
0.002	0.001	0.001	0.004	0.002	0.004	0.009
0.0002	0.0009	0.0009	0.006	0.002	0.004	0.012
0.0002	0.0009	0.0009	0.006	0.002	0.004	0.012
0.0002	0.0009	0.0009	0.006	0.002	0.004	0.012
0.0002	0.0009	0.0009	0.006	0.002	0.004	0.012
0.0002	0.0009	0.0009	0.006	0.002	0.004	0.012
0.0024	0.0011	0.0004	0.01	0.001	0.004	0.013

0.0024	0.0011	0.0004	0.01	0.001	0.004	0.013
0.0024	0.0011	0.0004	0.01	0.001	0.004	0.013
0.0024	0.0011	0.0004	0.01	0.001	0.004	0.013
0.0025	0.0012	0.0009	0.012	0.002	0.005	0.013
0.0025	0.0012	0.0009	0.012	0.002	0.005	0.013
0.0024	0.001	0.0008	0.012	0.001	0.004	0.012
0.0024	0.001	0.0008	0.012	0.001	0.004	0.012
0.0024	0.001	0.0003	0.013	0.002	0.004	0.012
0.0021	0.0008	0.0005	0.008	0.001	0.004	0.013
0.0021	0.0008	0.0005	0.008	0.001	0.004	0.013
0.0022	0.001	0.0006	0.008	0.002	0.004	0.013
0.0024	0.001	0.0007	0.008	0.001	0.005	0.014
0.0024	0.001	0.0007	0.008	0.001	0.005	0.014
0.0021	0.0007	0.0009	0.007	0.002	0.004	0.011
0.0021	0.0009	0.0009	0.006	0.002	0.005	0.012
0.002	0.001	0.001	0.012	0.002	0.004	0.012

Table A.12: Input data for training ANN with 109 historical data (charge data) for 27 independent input variables and dependent output variable Elongation (A) – part 4

Sum Hg Cd Pb (wt%)	Sum Ti Zr (wt%)	Sum Mn Zr (wt%)	Sum Mn Cr Ti V (wt%)	T (°C)	A (wt%)
0.003	0.03	0.007	0.043	290	2.80
0.003	0.03	0.007	0.043	290	2.52
0.002	0.026	0.008	0.041	281	0.97
0.002	0.026	0.008	0.041	281	0.99
0.002	0.026	0.008	0.041	281	0.97
0.002	0.026	0.008	0.041	281	0.99
0.004	0.029	0.007	0.04	288	1.88
0.004	0.029	0.007	0.04	288	1.85
0.003	0.026	0.006	0.035	288	2.18
0.003	0.026	0.006	0.035	288	1.69
0.003	0.026	0.007	0.036	288	1.59
0.003	0.026	0.007	0.036	288	1.30
0.003	0.026	0.007	0.036	288	2.35
0.003	0.026	0.007	0.036	288	2.19
0.003	0.026	0.006	0.035	288	2.35
0.003	0.026	0.006	0.035	288	2.19

0.003	0.039	0.006	0.049	288	1.98
0.003	0.039	0.006	0.049	288	2.76
0.003	0.039	0.006	0.049	288	2.18
0.003	0.039	0.006	0.049	288	1.69
0.003	0.026	0.006	0.035	288	1.98
0.003	0.026	0.006	0.035	288	2.76
0.003	0.035	0.007	0.044	285	2.51
0.003	0.035	0.007	0.044	285	2.21
0.003	0.035	0.007	0.044	285	2.30
0.003	0.035	0.007	0.044	285	2.55
0.003	0.033	0.01	0.046	285	1.64
0.003	0.033	0.01	0.046	285	1.57
0.003	0.033	0.01	0.046	285	1.05
0.003	0.033	0.01	0.046	285	1.00
0.002	0.029	0.007	0.039	280	2.07
0.002	0.029	0.007	0.039	280	2.35
0.003	0.032	0.008	0.046	281	1.43
0.003	0.032	0.008	0.046	281	1.54
0.003	0.032	0.008	0.046	281	1.61
0.003	0.032	0.008	0.046	281	1.84
0.003	0.032	0.007	0.046	281	1.48
0.003	0.032	0.007	0.046	281	1.39
0.003	0.032	0.007	0.046	281	1.48
0.003	0.032	0.007	0.046	281	1.39
0.003	0.032	0.007	0.046	289	2.57
0.003	0.032	0.007	0.046	289	2.74
0.003	0.03	0.007	0.045	289	2.52
0.003	0.03	0.007	0.045	289	2.20
0.003	0.03	0.007	0.045	289	2.52
0.003	0.03	0.007	0.045	289	2.20
0.003	0.034	0.008	0.053	276	2.48
0.003	0.034	0.008	0.053	276	2.32
0.003	0.034	0.008	0.053	276	2.01
0.003	0.034	0.008	0.053	276	2.28
0.003	0.028	0.006	0.049	287	1.57
0.003	0.028	0.006	0.049	287	1.97
0.003	0.034	0.007	0.054	290	1.86
0.003	0.034	0.007	0.054	290	2.14
0.003	0.034	0.007	0.054	290	1.54

0.003	0.034	0.007	0.054	290	1.61
0.003	0.034	0.007	0.056	288	1.63
0.003	0.034	0.007	0.056	288	1.79
0.003	0.028	0.006	0.05	282	1.37
0.003	0.028	0.006	0.05	282	1.38
0.003	0.037	0.01	0.052	290	0.56
0.003	0.037	0.01	0.052	290	0.57
0.003	0.037	0.01	0.052	290	0.83
0.003	0.037	0.01	0.052	290	0.77
0.003	0.037	0.01	0.052	290	0.56
0.003	0.037	0.01	0.052	290	0.57
0.003	0.032	0.018	0.057	290	0.83
0.003	0.032	0.018	0.057	290	0.77
0.003	0.032	0.018	0.057	290	0.56
0.003	0.032	0.018	0.057	290	0.57
0.003	0.037	0.01	0.052	290	0.77
0.003	0.037	0.01	0.052	290	0.83
0.003	0.035	0.008	0.047	294	1.67
0.003	0.035	0.008	0.047	294	1.75
0.003	0.029	0.007	0.04	294	1.53
0.003	0.029	0.007	0.04	294	1.59
0.003	0.029	0.007	0.04	291	1.54
0.003	0.029	0.007	0.04	291	1.30
0.002	0.03	0.007	0.04	291	1.54
0.002	0.03	0.007	0.04	291	1.30
0.003	0.033	0.008	0.046	291	1.71
0.003	0.033	0.008	0.046	291	1.83
0.003	0.029	0.01	0.042	303	1.51
0.003	0.029	0.01	0.042	303	1.57
0.003	0.037	0.0326	0.0739	285	1.32
0.003	0.026	0.011	0.04	298	1.69
0.003	0.026	0.011	0.04	298	1.48
0.003	0.037	0.0326	0.0739	285	1.44
0.003	0.037	0.0326	0.0739	286	1.71
0.003	0.037	0.0326	0.0739	287	1.42
0.003	0.037	0.0326	0.0739	288	1.96
0.003	0.037	0.0326	0.0739	289	1.84
0.003	0.0282	0.0098	0.0465	290	1.96
0.003	0.0282	0.0098	0.0465	291	1.84

0.003	0.0282	0.0098	0.0465	292	1.32
0.003	0.0282	0.0098	0.0465	293	1.44
0.0032	0.0314	0.0076	0.0499	294	1.71
0.0032	0.0314	0.0076	0.0499	295	1.42
0.0029	0.0354	0.0079	0.0544	298	2.46
0.0029	0.0354	0.0079	0.0544	304	2.13
0.0031	0.0299	0.0146	0.0562	293	2.24
0.0028	0.0327	0.0066	0.0462	304	1.73
0.0028	0.0327	0.0066	0.0462	304	1.75
0.0029	0.0352	0.007	0.0492	304	1.42
0.003	0.0352	0.0068	0.0489	304	2.14
0.003	0.0352	0.0068	0.0489	304	1.69
0.0025	0.0316	0.0082	0.0459	304	1.87
0.0028	0.0292	0.0074	0.042	304	1.41
0.003	0.027	0.008	0.046	309	2.53

A.4 The new training set after heuristic elimination of rows that are not good for training ANN with 26 historical data (charge data) for 27 independent input variables and dependent output variable Elongation (A)

Table A.13: The new training set after heuristic elimination of rows that are not good for training ANN with 26 historical data (charge data) for 27 independent input variables and dependent output variable Elongation (A) – part 1

Charge	Width (mm)	Outside diameter (mm)	Al (wt%)	Si (wt%)	Fe (wt%)	Cu (wt%)	Mn (wt%)
93323	290.0	550.0	98.536	0.559	0.836	0.001	0.004
93326	290.0	1,000.0	98.482	0.58	0.869	0.001	0.004
93336	450.0	550.0	98.467	0.58	0.873	0.001	0.005
93336	326.0	550.0	98.467	0.58	0.873	0.001	0.005
93347	292.0	600.0	98.474	0.595	0.856	0.001	0.006
93761	450.0	550.0	98.534	0.57	0.807	0.002	0.006
93761	326.0	550.0	98.534	0.57	0.807	0.002	0.006
93763	300.0	900.0	98.493	0.584	0.837	0.002	0.005
93765	300.0	900.0	98.493	0.584	0.837	0.002	0.005

94289	290.0	900.0	98.497	0.576	0.836	0.002	0.005
94334	290.0	550.0	98.466	0.57	0.865	0.002	0.008
94337	450.0	550.0	98.466	0.57	0.865	0.002	0.008
94337	290.0	550.0	98.408	0.625	0.868	0.003	0.016
94337	450.0	550.0	98.466	0.57	0.865	0.002	0.008
94338	290.0	1,000.0	98.434	0.582	0.895	0.002	0.006
94481	290.0	1,000.0	98.435	0.613	0.875	0.002	0.005
94482	290.0	1,000.0	98.526	0.575	0.822	0.002	0.005
94483	290.0	550.0	98.434	0.585	0.896	0.003	0.006
94755	450.0	550.0	98.3962	0.601	0.881	0.0039	0.0306
94995	300.0	600.0	98.479	0.586	0.837	0.002	0.0065
94997	290.0	700.0	98.4456	0.608	0.848	0.0026	0.0131
95334	300.0	600.0	98.4341	0.596	0.89	0.0014	0.0052
95334	290.0	900.0	98.4341	0.596	0.89	0.0014	0.0052
95335	280.0	850.0	98.4264	0.612	0.876	0.0014	0.0055
95345	280.0	600.0	98.4729	0.602	0.8397	0.003	0.0065
95680	280.0	600.0	98.4651	0.619	0.837	0.0029	0.0059

Table A.14: The new training set after heuristic elimination of rows that are not good for training ANN with 26 historical data (charge data) for 27 independent input variables and dependent output variable Elongation (*A*) – part 2

B (wt%)	Zn (wt%)	Pb (wt%)	Bi (wt%)	Mg (wt%)	In (wt%)	Ti (wt%)	Hg (wt%)	Ni (wt%)
0.003	0.006	0.001	0	0.002	0	0.025	0.002	0.002
0.003	0.006	0.001	0	0.002	0	0.025	0.002	0.002
0.004	0.007	0.001	0	0.003	0	0.034	0.002	0.002
0.004	0.007	0.001	0	0.003	0	0.034	0.002	0.002
0.004	0.006	0.001	0	0.003	0	0.028	0.002	0.002
0.002	0.006	0.001	0.001	0.007	0	0.031	0.002	0.002
0.002	0.006	0.001	0.001	0.007	0	0.031	0.002	0.002
0.003	0.006	0.001	0.001	0.005	0	0.03	0.002	0.002
0.003	0.006	0.001	0.001	0.005	0	0.03	0.002	0.002
0.005	0.005	0.001	0	0.002	0	0.034	0.002	0.002
0.006	0.006	0.001	0.001	0.01	0	0.036	0.002	0.002
0.006	0.006	0.001	0.001	0.01	0	0.036	0.002	0.002
0.003	0.005	0.001	0.001	0.007	0	0.031	0.002	0.002
0.006	0.006	0.001	0.001	0.01	0	0.036	0.002	0.002
0.005	0.005	0.001	0	0.007	0	0.034	0.002	0.002

0.002	0.005	0.001	0	0.005	0	0.028	0.002	0.002
0.002	0.005	0.001	0	0.005	0	0.029	0.002	0.002
0.003	0.005	0.001	0	0.005	0	0.032	0.002	0.002
0.0061	0.005	0.0014	0.0003	0.0105	0.0002	0.0358	0.0016	0.0002
0.0046	0.0043	0.0012	0.005	0.0032	0.0001	0.0345	0.0017	0.0024
0.0027	0.0046	0.0014	0.0006	0.0077	0.0001	0.029	0.0017	0.0024
0.0018	0.0037	0.001	0.0003	0.0024	0	0.0318	0.0018	0.0021
0.0018	0.0037	0.001	0.0003	0.0024	0	0.0318	0.0018	0.0021
0.0024	0.0041	0.0011	0.0004	0.0028	0.0001	0.0343	0.0018	0.0022
0.0016	0.0046	0.0009	0.003	0.0051	0	0.0306	0.0016	0.0021
0.0023	0.0033	0.001	0.0005	0.0038	0.0001	0.0282	0.0018	0.0021

Table A.15: The new training set after heuristic elimination of rows that are not good for training ANN with 26 historical data (charge data) for 27 independent input variables and dependent output variable Elongation (A) – part 3

Sn (wt%)	Ca (wt%)	V (wt%)	Cr (wt%)	Sb (wt%)	Ga (wt%)	Sum Hg Cd Pb (wt%)
0.001	0.001	0.004	0.002	0.004	0.01	0.003
0.001	0.001	0.004	0.002	0.004	0.01	0.003
0.001	0.001	0.003	0.002	0.004	0.01	0.003
0.001	0.001	0.003	0.002	0.004	0.01	0.003
0.001	0.001	0.004	0.002	0.004	0.01	0.002
0.001	0.001	0.007	0.002	0.004	0.012	0.003
0.001	0.001	0.007	0.002	0.004	0.012	0.003
0.001	0.001	0.008	0.002	0.004	0.011	0.003
0.001	0.001	0.008	0.002	0.004	0.011	0.003
0.001	0.001	0.014	0.002	0.004	0.011	0.003
0.001	0.001	0.006	0.002	0.004	0.011	0.003
0.001	0.001	0.006	0.002	0.004	0.011	0.003
0.001	0.001	0.008	0.002	0.004	0.011	0.003
0.001	0.001	0.006	0.002	0.004	0.011	0.003
0.001	0.001	0.005	0.002	0.004	0.01	0.003
0.001	0.001	0.005	0.002	0.004	0.011	0.003
0.001	0.001	0.005	0.002	0.004	0.01	0.002
0.001	0.001	0.006	0.002	0.004	0.011	0.003
0.0009	0.0009	0.0055	0.002	0.004	0.0115	0.003
0.001	0.0008	0.012	0.0014	0.0043	0.012	0.0029
0.001	0.0003	0.0126	0.0015	0.0043	0.0118	0.0031

0.0008	0.0005	0.0078	0.0014	0.0042	0.0127	0.0028
0.0008	0.0005	0.0078	0.0014	0.0042	0.0127	0.0028
0.001	0.0006	0.0079	0.0015	0.0044	0.0132	0.0029
0.0007	0.0009	0.0071	0.0017	0.0039	0.011	0.0025
0.0009	0.0009	0.0064	0.0015	0.0047	0.0115	0.0028

Table A.16: The new training set after heuristic elimination of rows that are not good for training ANN with 26 historical data (charge data) for 27 independent input variables and dependent output variable Elongation (A) – part 4

Sum Ti Zr (wt%)	Sum Mn Zr (wt%)	Sum Mn Cr Ti V (wt%)	T (°C)	A (wt%)
0.026	0.006	0.035	288	1.94
0.026	0.006	0.035	288	2.27
0.035	0.007	0.044	285	2.36
0.035	0.007	0.044	285	2.43
0.029	0.007	0.039	280	2.21
0.032	0.008	0.046	281	1.49
0.032	0.008	0.046	281	1.73
0.03	0.007	0.045	289	2.36
0.03	0.007	0.045	289	2.36
0.034	0.007	0.054	290	2.00
0.037	0.01	0.052	290	0.57
0.037	0.01	0.052	290	0.80
0.032	0.018	0.057	290	0.57
0.037	0.01	0.052	290	0.80
0.035	0.008	0.047	294	1.71
0.029	0.007	0.04	294	1.56
0.03	0.007	0.04	291	1.46
0.033	0.008	0.046	291	1.77
0.037	0.0326	0.0739	285	1.32
0.0354	0.0079	0.0544	304	2.30
0.0299	0.0146	0.0562	293	2.24
0.0327	0.0066	0.0462	304	1.73
0.0327	0.0066	0.0462	304	1.75
0.0352	0.007	0.0492	304	1.42
0.0316	0.0082	0.0459	304	1.87
0.0292	0.0074	0.042	304	1.41